
# ADDIS ABABA INSTITUTE OF TECHNOLOGY

# SCHOOL OF CIVIL AND ENVIRONMENTAL ENGINEERING

## Assessment of Degradation and Performance Improvement of Railway Ballast with Geosynthetics - A Case Study of National Railway Network

By

Kedir Abdu

**A Thesis Submitted To School Of Graduate Studies of Addis Ababa University in Partial Fulfillment of the Requirements for the Degree of Master of Science in Civil Engineering**

Advisors

Dr.- Ing. Henok Fikre

Mr. Matias Kabtamu (MSc)

May, 2015

# ABSTRACT

The increasing demands of higher axle loads, speeds and usage means understanding the ballast behavior and its interaction with the infrastructure remains a critical element to the design and successful operation of ballasted railway track, Therefore it is important to study the degradation of ballast to increase and predict ballast life on the track, reduce waste track, keep good track quality and minimize the frequency and cost of ballast replacement.

The primary objectives of this thesis are to identify the major source of ballast degradation, minimizing the ballast degradation, improve the performance of the ballast as well as the track, to avoid repeated maintenance by minimizing the ballast degradation and finally minimizing ballast degradation of railway line mainly using geosynthetics materials namely Geocells and Geogrids.

Literatures have been thoroughly reviewed and the preliminary analysis were performed prior to the Finite Element Method (FEM) analysis with the software ANSYS. The analysis is comprised of typical unreinforced and geocell and geogrid reinforced ballast section of National Railway Network; track settlement, subgrade stress and subgrade stress - strain have been observed. Assessments have been made and promising results are obtained.

The result of the finite element analysis (FEA) shows that ballast embankment reinforced with geocell have reduced the track settlement and the subgrade stress beside this the intrusion of geocell in the ballast provides a more linear stress-strain distribution.

Ballast embankment reinforced with geogrid was also analyzed; the ballast was reinforced at the ballast-subballast interface and within the ballast. The reinforcement at the ballast-subballast interface have reduced the track settlement and the subgrade stress much better than geogrid reinforcement within the ballast and in both cases a linear stress-strain distribution is obtained.

Finally conclusions were made that show geocell and geogrid improved the performance of weak degraded ballast and fresh good quality ballast. Also using reinforced ballast embankment on soft subgrade reduced and distributes stress more evenly as well as reduced the track settlement.

# ACKNOWLEDGEMENTS

It is my deepest gratitude and respect to my advisors Dr.- Ing. Henok Fikre and Mr. Matias Kabtamu for their valuable advice, sincerity, very humble way of approach which is never been forgotten throughout my life for the successful completion of this thesis. I also would like to extend my respect and appreciation to all staff of Addis Ababa Institute of Technology, School of Civil and Environmental Engineering, Librarians and Administrative workers of the institute: without their support, this thesis would not have been possible.

Kedir Abdu

# LIST OF CONTENTS

ABSTRACT I
ACKNOWLEDGEMENTS II
LIST OF CONENTS III
LIST OF FIGURES VI
LIST OF TABLES X
NOTATION XI

**1. Introduction** 1

1.1. Background 1
1.2. Statement of the Problem 2
1.3. Objectives 3
1.4. Methodology 3
1.5. Thesis Outline 4

**2. Literature Review** 6

2.1. Introduction 6
2.2. Track Components And Functions 7
2.2.1. Track Components and Functions 8
2.2.2. Track Forces 10
2.3. Ballast 11
2.3.1. Ballast Properties 12
2.3.1.1. Effect of Particle Shape on Ballast Functions 12
2.3.1.2. Ballast Gradation 13
2.3.2. Mechanical Behavior of Ballast 14
2.3.2.1. Resilient Behavior of Granular Material 14
2.3.2.2. Permanent Strain Behavior of Granular Material 16
2.4. Ballast Degradation 19

2.4.1. Driving Forces of Degradation 21
2.4.2. Ballast Settlement 23
2.4.3. Ballast Fouling 25
2.5. Ballast and Geosynthetics 29
2.5.1. Ballast and Geocell 30
2.5.2. Ballast and Geogrid 36
2.6. Summary 44

**3. Finite Element Modeling and Analysis** 45

3.1. Introduction 45
3.2. Preliminary Analysis 46
3.2.1. Project Description 46
3.2.2. Loading 50
3.2.3. Beam on Elastic Foundation Rail Analysis 50
3.2.4. Sleeper Stress Analysis 59
3.2.5. Ballast Analysis 67
3.3. Finite element analysis 72
3.3.1. Assumptions 72
3.3.2. Symmetry 72
3.3.3. Geometry and Cross-Section 73
3.3.4. Idealization of Three-Dimensional Railway Substructure 81
3.3.5. Elements 82
3.3.6. Meshing 82
3.3.6.1. Unreinforced 82
3.3.6.2. Reinforced with Geocell 84
3.3.6.3. Reinforced with Geogrid 85
3.3.7. Contact 87
3.3.8. Boundary Conditions 87
3.3.9. Analysis 88

3.3.10. Material Properties 89
3.3.11. Loading 91
3.4. Discussion of Results 91

**4. Parametric Study** 100
4.1. Unreinforced versus Reinforced with Geocell 100
4.2. Unreinforced versus Reinforced with Geogrid 103

**5. Conclusions and Recommendation** 106
5.1. Conclusions 106
5.2. Recommendations 107

**References** 109

# LIST OF FIGURES


| | | |
|---|---|---|
| Figure 2.1 | Superstructure and substructure components of a railway line, (a) lateral view, and (b) longitudinal view | 8 |
| Figure 2.2 | Uplift of rails | 11 |
| Figure 2.3 | Strains in granular material during one cycle of load application | 15 |
| Figure 2.4 | Effect of stress ratio on permanent strain | 17 |
| Figure 2.5 | Effect of repeated load applications | 18 |
| Figure 2.6 | Influence of Drainage on Permanent Deformation Development | 19 |
| Figure 2.7 | Degradation process of railways infrastructure | 20 |
| Figure 2.8 | Degradation process of railway track with load dependent wearing | 21 |
| Figure 2.9: | Schematic representation of source of ballast fouling | 26 |
| Figure 2.10 | Effect of degree of fouling and type of fouling material on Ballast settlement | 28 |
| Figure 2.11 | Typical Geocell Section, Expanded Plan View | 31 |
| Figure 2.12 | Railway geometry with absence of grovels. b. Railway geometry with geocell confinement. c. Mesh of embedded geocell | 34 |
| Figure 2.13 | a. Subgrade stress distribution below geocell-reinforced embankment. b. Subgrade stress distribution below unreinforced embankment | 35 |
| Figure 2.14 | the Mechanism of Interlock | 37 |
| Figure 2.15 | Geogrids at the bottom of, or within the ballast | 38 |
| Figure 2.16 | Geogrids at the bottom of the sub-ballast, directly on the existing or prepared subgrade | 38 |
| Figure 2.17 | Reinforcing effect of geogrid | 40 |

| | | |
|---|---|---|
| Figure 2.18 | Variation of permanent deflection with commutative axle tones for CBR=∞ and CBR=39. | 42 |
| Figure 2.19 | Variation of permanent deflection with cumulative axle tones for CBR=1 | 42 |
| Figure 2.20 | Variation of permanent deflection with cumulative axle tones for Dr = 100 mm | 43 |
| Figure 3.1 | HXD1C High Power AC Drive Six-Axle (7200kw) Freight Electric Locomotive | 47 |
| Figure 3.2 | Flow chart for conventional ballasted track structure design | 49 |
| Figure 3.3 | Schematic representation of beam on elastic foundation model of three axle bogie | 51 |
| Figure 3.4 | Bending moment diagram of beam on elastic foundation model | 54 |
| Figure 3.5 | Deflection diagram of beam on elastic foundation model | 54 |
| Figure 3.6 | Uniform Distribution of wheel-rail contact stress | 56 |
| Figure 3.7 | Schematic of typical rail – fastening system | 59 |
| Figure 3.8 | Typical Section of Track Substructure | 70 |
| Figure 3.9 | Geometry of Track Section | 71 |
| Figure 3.10 | Symmetry of the line considered for FEA | 71 |
| Figure 3.11 | Railway track 3D model | 73 |
| Figure 3.12 | Model of rail profile UIC54 | 74 |
| Figure 3.13 | 3D Model of pre-stressed concrete sleeper | 75 |
| Figure 3.14 | Railway geometry without geocell (ballast removed for illustration) | 80 |
| Figure 3.15 | Railway geometry without geogrid (ballast removed for illustration) | 80 |
| Figure 3.16 | Rail deflection and stress distribution profile | 81 |

| | | |
|---|---|---|
| Figure 3.17 | Assumed ballast-tie reaction from wheel load | 81 |
| Figure 3.18 | Mesh of ballasted railway track and foundation | 83 |
| Figure 3.19 | Mesh of rail, sleeper and foundation (ballast removed for illustration). | 83 |
| Figure 3.20 | Mesh of ballasted railway track reinforced with geocell and foundation | 84 |
| Figure 3.21 | Mesh of rail, sleeper, geocell and foundation | 84 |
| Figure 3.22 | Mesh of embedded geocell | 85 |
| Figure 3.23 | Mesh of ballasted railway track reinforced with geogrid and foundation | 86 |
| Figure 3.24 | Mesh of rail, sleeper, geogrid and foundation | 86 |
| Figure 3.25 | Boundary conditions of the FE model | 88 |
| Figure 3.26 | Deformation/track settlement of unreinforced ballast embankment | 92 |
| Figure 3.27 | Subgrade stress versus track depth of unreinforced ballast | 93 |
| Figure 3.28 | Subgrade stress versus strain of unreinforced ballast | 94 |
| Figure 3.29 | Deformation /track settlement of geocell reinforced ballast Embankment | 95 |
| Figure 3.30 | Subgrade stress versus track depth of geocell reinforced ballast | 96 |
| Figure 3.31 | Subgrade stress versus strain of geocell reinforced ballast | 97 |
| Figure 3.32 | Track settlement of geogrid reinforced ballast embankment | 97 |
| Figure 3.33 | Subgrade stress versus track depth of geogrid reinforced ballast | 98 |
| Figure 3.34 | Subgrade stress versus strain of geocell reinforced ballast | 99 |
| Figure 4.1 | Track settlement of unreinforced and geocell reinforced ballast Embankment | 100 |

Figure 4.2 Subgrade stress of unreinforced and geocell reinforced ballast embankment 101

Figure 4.3 Subgrade stress-strain of unreinforced and geocell reinforced ballast embankment 102

Figure 4.4 Track settlement of unreinforced and geogrid reinforced ballast embankment 103

Figure 4.5 Subgrade stress of reinforced and geogrid reinforced ballast embankment 104

Figure 4.6 Subgrade stress-strain of unreinforced and geogrid reinforced ballast embankment 105

# LIST OF TABLES


| | | |
|---|---|---|
| Table 2.1 | Recommended Ballast Gradations | 14 |
| Table 2.2 | Parameters influencing track degradation | 22 |
| Table 2.3 | Deterioration process of different superstructure components | 23 |
| Table 2.4 | Source of ballast fouling | 27 |
| Table 2.5 | Classification of ballast based on fouling index | 28 |
| Table 2.6 | Functions of Geosynthetics | 29 |
| Table 2.7 | Polyethylene and Geocell Cellular Confinement System Properties | 33 |
| Table 2.8 | Physical Properties for Geogrids used in Track Stabilization | 49 |
| Table 3.1 | Adopted rail profile section properties | 51 |
| Table 3.2 | Acceptable Rail Stress for Continuous Welded Rail | 55 |
| Table 3.3 | Selected sleeper dimensions | 60 |
| Table 3.4 | Polyethylene and Geocell Cellular Confinement System Properties | 76 |
| Table 3.5 | Physical Properties for Geogrids used in Track Stabilization | 78 |
| Table 3.6 | Stress and internal friction angle values of geogrid | 78 |
| Table 4.1: | Summary of finite element analysis for ballast reinforced with geocell | 102 |
| Table 4.2: | Summary of finite element analysis for ballast reinforced with geogrid | 105 |

# NOTATION

| | |
|---|---|
| $\beta$ | Characteristics length |
| $\phi$ | Dynamic impact factor |
| $\sigma_{all}$ | Allowable rail bending stress |
| $\tau_{all}$ | Allowable rail shear stress |
| $\sigma_b$ | Rail bending stress |
| $\tau_{max}$ | Maximum rail shear stress |
| $\sigma_{mean}$ | Mean rail contact stress |
| $\sigma_t$ | Rail temperature stress |
| $\sigma_{ult}$ | Ultimate tensile strength of rail |
| $\sigma_y$ | Rail yield stress |
| $\sigma_z$ | Subgrade vertical pressure |
| $f_s'$ | Yield strength of prestressing tendons |
| *a* | Constant related to thickness of the particle or breadth of rail contact area |
| *AREMA* | American Railway Engineering and Maintenance-of-way Association |
| *b* | Constant related to width of the particle or width of rail contact area |
| *BOEF* | Beam on Elastic Foundation |
| *CAD* | Computer-Aided Design |
| *CBR* | California Bearing Ratio |
| *D* | Wheel diameter |
| *DF* | Distribution factor |
| $D_r$ | Depth of reinforcement below the tie |
| *ERC* | Ethiopian Railways Corporation |

| | |
|---|---|
| *FEA* | Finite Element Analysis |
| *FEM* | Finite Element Method |
| $F_I$ | Fouling index |
| $F_{normal}$ | Finite normal contact force |
| $g$ | Distance between rail centers |
| *HDPE* | High Density Polyethylene |
| $k$ | Track modulus |
| $k_{normal}$ | Contact stiffness |
| $l$ | Total sleeper length |
| $M_c$ | Maximum negative sleeper bending moment at the rail center |
| $M_m$ | Maximum rail bending moment |
| $M_r$ | Maximum positive sleeper bending moment at the rail seat |
| $P$ | Flakiness ratio of a particle |
| *PSD* | Particle size distribution |
| $p_a$ | Average ballast pressure |
| $P^D$ | Design wheel load |
| $p_i$ | Initial prestressing force |
| $P_s$ | Static wheel load |
| $Q_{centrifugal}$ | Increase in wheel due to centrifugal force |
| $Q_{dynamic}$ | Dynamic wheel load component |
| $q_r$ | Vertical rail seat load |
| $Q_{static}$ | Static wheel load |
| $Q_{wind}$ | Increase in wheel due to wind |

| | |
|---|---|
| *RCF* | Rolling contact fatigue |
| $R_w$ | Wheel radius |
| *S* | Sleeper spacing |
| *UIC* | International Union of Railways |
| *USACE* | United States Army Corps of Engineers |
| *V* | Design speed |
| *w* | Uniformly distribution sleeper load |
| *x* | Distance from reference wheel |
| $x_{penetration}$ | Element penetration |
| *y* | Rail deflection |
| $z_{min}$ | Minimum ballast depth |
| $Z_t$ , $Z_b$ | Section modulus of the rail |

# CHAPTER ONE

# 1. INTRODUCTION

## 1.1. Background

The railway track system plays an important role in providing a good transportation system in a country. A very large portion of the annual budget to sustain the railway track system goes into track maintenance. In the past, most attention has been given to the track superstructure consisting of the rails, the fasteners and the sleepers, and less attention has been given to the substructure consisting of the ballast, the sub ballast and the subgrade. Even though the substructure components have a major influence on the cost of track maintenance, less attention has been given to the substructure because the properties of the substructure are more variable and difficult to define than those of the superstructure [1].

Good quality track ballast is made of crushed natural rock with particles between 28 mm and 50 mm in diameter. A high proportion of particles finer than this will reduce its drainage properties, and a high proportion of larger particles result in the load on the ties being distributed improperly. Angular stones are preferable to naturally rounded ones, as angular stones interlock with each other, inhibiting track movement. Soft materials such as limestone are not particularly suitable, as they tend to degrade under load when wet, causing deterioration of the line; granite, although expensive, is one of the best materials in this regard [2].

Track ballast forms the track bed upon which railway sleepers or railroad ties are laid. It is packed between, below, and around the ties. The principal purpose of the ballast section is to anchor the track and provide resistance against lateral, longitudinal and vertical movement of ties and rail, i.e., stability. Additionally, the ballast section bears and distributes the applied load with diminished unit pressure to the subgrade beneath, gives immediate drainage to the track, facilitates maintenance, and provides a necessary degree of elasticity and resilience [3].

Ballast should be strong, hard-wearing, stable, drainable, easy to clean, workable, resistant to deformation, easily available, and reasonably cheap to purchase. Ballast materials forming part of railway structures are subjected to cyclic loads. As a result of these loads, ballast

densification, aggregate degradation, and lateral spread of the ballast material underneath the ties takes place inducing permanent deformations on the railways.

After long term service, ballast becomes damaged and contaminated and its gradation changes. As a result, its performance reduces. This process is called “degradation”. The major causes of ballast degradation are ballast fouling and ballast settlement.

Ballast fouling is the presence of more fines in the ballast and the major causes of ballast fouling. They are; ballast breakdown, infiltration from ballast surface, sleeper wear, infiltration from underlying granular layers and subgrade infiltration

Ballast settlement occurs in two major phases [4]; directly after tamping and the second phase of settlement is slower and there is a more or less linear relationship between settlement and time (or load).

This thesis concentrates on minimizing ballast degradation or improving the performance of railway ballast by intrusion of geocell and geogrid. Preliminary analysis was performed for typical section of national railway network prior to Finite Element Method (FEM) modeling. The modeling were performed for ballast embankment reinforced with geocell, geogrid at two different locations and unreinforced section for the purpose of comparing or control, finally results were compared to show the level/degree of improvement and recommendations are presented.

## 1.2. Statement of the Problem

The major problem related to the construction of conventional ballasted track is the degradation of the ballast material. Over time, ballast is crushed or moved by the weight of traffic load passing over it, periodically requiring re-leveling ("tamping") and eventually to be cleaned or replaced. If this is not done, the tracks may become uneven causing swaying, rough riding and possibly derailments.

Ballast degradation fills voids progressively with fine particles (fouled); the effect on the volume change due to fouling from ballast particle breakage will result in settlement as the ballast particles migrate downwards.

The major problems caused by poor ballasted track are:-

- the track quality (track shift, cross-level, alignment, profile, twist) will be greatly affected
- poor damping of impact loading
- increase the rate of settlement
- cause uneven stress distribution hence failure
- repeated maintenances which will affect economy of the country

Therefore, to satisfy track requirements (durable, rigid and smooth) it is important to control ballast degradation and quality and investigate potential methods to improve the performance of ballast for the effective functioning of a railway line.

## 1.3. Objectives

The main objectives of this research are:-

- identifying the possible causes of railway ballast degradation
- improving the performance of the rail ballast by incorporating geosynthetics namely geogrid and geocell
- performing a quasi-static analysis for a typical section of the National Railway Network from Addis Ababa/Sebeta to Djibouti line
- assessing the performance of the railway ballast reinforced with geocell, geogrid and unreinforced section for typical section of national railway network based on the result of Finite Element Analysis (FEA).

## 1.4. Methodology

Literatures regarding ballast degradation and main causes of ballast degradation are thoroughly studied and reviewed. Technical papers, manuals, journals and publications regarding the current trends of using geosynthetics in the railway industry were reviewed. The data and data sources are from Ethiopian Railways Corporation (ERC), American Railway Engineering and Maintenance of Way Association (AREMA) manual and other acknowledged publications.

A preliminary analysis based on Beam on Elastic Foundation (BOEF) theory, where the rail is assumed to be laid on continuous elastic foundation were performed for that purpose to determine the input variables for the Finite Element Analysis (FEA), and hence the entire procedure is summarized step by step below:

- Data collection and summarizing
- Preliminary analysis based on BOEF for typical section of the National Railway Network
- Modeling of the track with and without geogrid/geocell using a software package SolidWorks
- Finite Element Analysis (FEA) of the track with and without geogrid/geocell using a software package called ANSYS
- Assessing the result of finite element analysis of the track section unreinforced, reinforced with geocell and geogrid.

## 1.5. Thesis Outline

This thesis is divided into five chapters. A brief outline of this thesis is given below:

Chapter 1 is the introductory containing the general background, statement of the problem, objectives of the research, methodology and structure of the thesis.

Chapter 2 is the literature review which includes: general description of various track components and its function, properties of ballast, gradation and mechanical behavior of ballast, details about ballast degradation and deriving forces of degradation, ballast settlement and ballast fouling. And finally, ballast and geosynthetics, which covers: the use and significance, material requirement, application location and reinforcement principles are reviewed.

Chapter 3 is finite element modeling and analysis and is divided into three subtopics; introduction, preliminary analysis and finite element analysis of railway substructure. The analysis gives introduction about the general methods and procedures used. preliminary analysis has been performed which includes, general description of the project, loading, beam on elastic foundation analysis, sleeper stress analysis and ballast analysis. The last sub topic is finite

element analysis of the track section unreinforced, reinforced with geocell and geogrid and finally presents the finite element analysis result.

Chapters 4 is a parametric study on some selected parameters that needs due consideration: track settlement, subgrade stress and subgrade stress-strain and categorized into two subtopics: track substructure unreinforced and reinforced with geocell and geogrid. Comparisons between reinforced and unreinforced section have been made.

The Last chapter, Chapter 5 summarizes the main findings of this research study; conclusions have been made based on the result of the FEM analysis. Finally, recommendations have been made for further research. This chapter is followed by a list of references.

# CHAPTER TWO

# 2. LITERATURE REVIEW

## 2.1. Introduction

The railway is an integral part of the transport network as it has a large capacity and is financially viable. However, traditional railway foundations or substructures have become increasingly overloaded in recent years, owing to the rapidly increasing number of faster and heavier trains. Two significant problems arising from increasing axle loads are track deformation and ballast degradation. The maintenance cycles are becoming more frequent and increasingly expensive as a result of these problems. To achieve optimum performance of the rail maintenance and minimize the maintenance cost, it is necessary to understand the behavior of railway ballast and the solutions of maintenance work [1].

A very large portion of the annual budget to sustain the railway track system goes into track maintenance. In the past, most attention has been given to the track superstructure consisting of the rails, the fasteners and the sleepers, and less attention has been given to the substructure consisting of the ballast, the sub ballast and the subgrade. Even though the substructure components have a major influence on the cost of track maintenance, less attention has been given to the substructure because the properties of the substructure are more variable and difficult to define than those of the superstructure [1].

Track ballast forms the track bed upon which railway sleepers or railroad ties are laid. It is packed between, below, and around the ties. It is used to bear the load from the railroad ties, to facilitate drainage of water, and also to keep down vegetation that might interfere with the track structure. This also serves to hold the track in place as the trains roll by. It is typically made of crushed stone, although ballast sometimes consists of other less suitable materials. Ballast should be strong, hard-wearing, stable, drainable, easy to clean, workable, resistant to deformation, easily available, and reasonably cheap to purchase. Ballast materials forming part of railway structures are subjected to cyclic loads. As a result of these loads, ballast densification, aggregate degradation, and lateral spread of the ballast material underneath the ties takes place inducing permanent deformations on the railways [1].

In conventional track design, ballast degradation and associated plastic deformation are not taken into account directly. Consequently, frequent remedial actions and expensive track maintenance are required. To some extent, this problem is due to a poor understanding of ballast behavior in railway track. In this literature, the current state of research pertaining to the behavior of railway ballast degradation and performance improvement using geosynthetics is reviewed.

## 2.2. Track components and functions

Railway track is designed to provide an economical and safe transportation system for passenger and freight traffic. This requires a track stable enough in alignment under various speeds and axle loadings. A traditional ballasted railway track system consists of a superstructure on top of a substructure. The superstructure comprises the following components: rail, fastening system, sleepers and ties. The substructure is composed of ballast, sub-ballast, and subgrade. During a train passage, the wheel loads from the train spread from the superstructure to the substructure through the sleeper-ballast interface [1]. The functions and characteristics of every component in both the superstructure and the substructure will be further discussed.

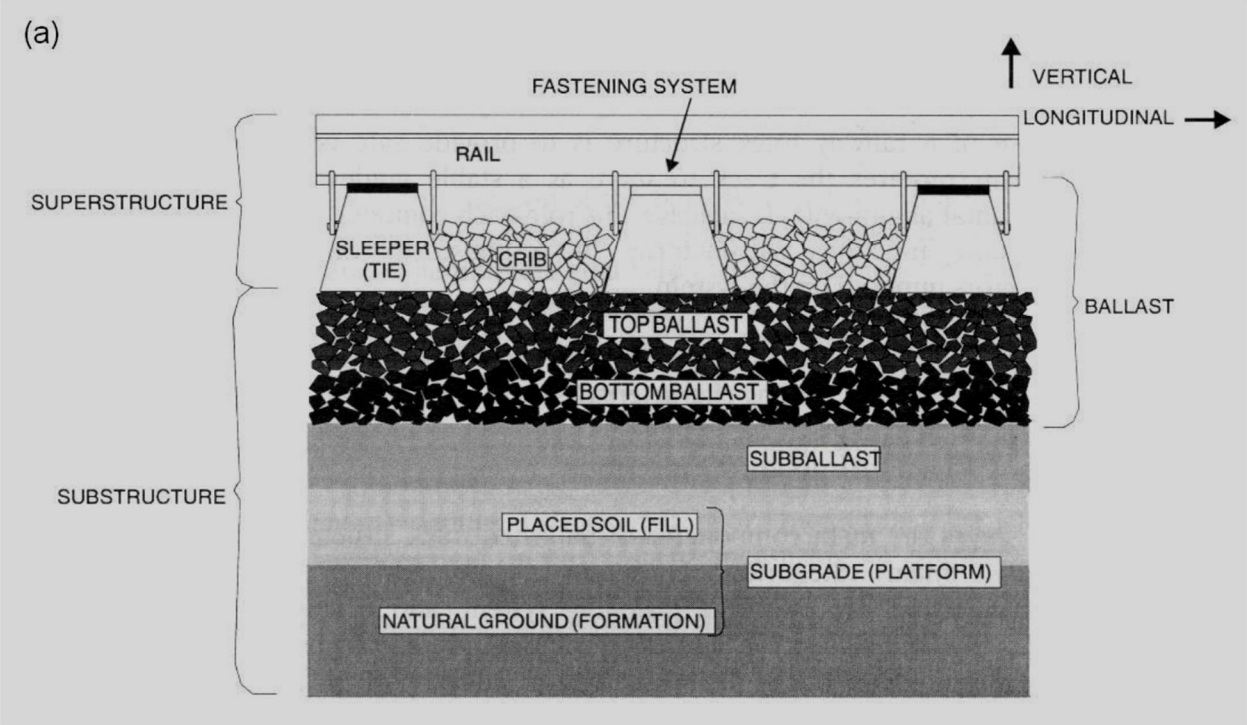


Figure 2.1a: Superstructure and substructure components of a railway line, lateral view [1]

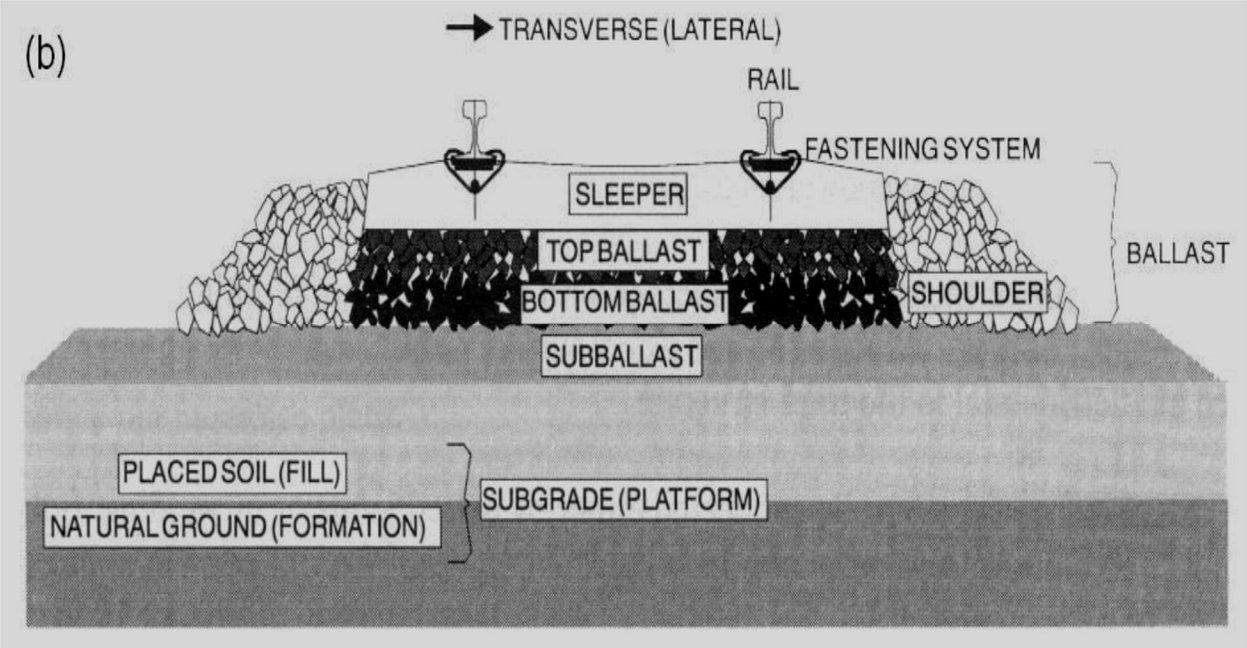


Figure 2.1b: Superstructure and substructure components of a railway line, longitudinal view [1]

## 2.2.1. Track Components

Rails are longitudinal steel members to direct train wheels; the only parts of the track component that come into direct contact with the train. Therefore, the rails transfer concentrated wheel loads to the supporting sleepers. The rails must be stiff enough to carry the wheel loads with minimum deflection between sleeper supports. The vertical and lateral profile of the rails must be coupled with the profile of the wheels, as any defect on the rail or wheel surface might cause a significant magnitude of dynamic load which is detrimental to the railway track structure. Rail sections may be connected by bolted joints or welding, and these joints may lead to large impact loads from trains that affect the track components below [1].

The fastening system is used to hold the rails onto the sleepers, to ensure fixing of the rails. Depending on the type of the sleeper and geometry of the rail, various kinds of fastening systems are utilized. In some situations, rail pads are used on top of the sleepers to absorb the energy generated by the traffic movements. Besides resisting vertical, lateral, longitudinal and overturning movements of the rail, the fastening system can aid in damping traffic vibrations, and prevent or reduce rail/sleeper attrition.

The main functions of sleepers are to provide a solid, even and flat platform for the rails, and support the rail fastening system. They are laid on the top of a compacted ballast layer. Sleepers receive the rail loads and distribute them over a wider ballast area to decrease the stress to an acceptable level. In addition, the sleepers can be used to resist lateral, longitudinal as well as vertical rail movement through anchorage of the superstructure into the ballast. Sleepers can be made of wood, concrete or steel. Currently, timber and concrete sleepers are the most common types of sleepers, which are used worldwide. Steel sleepers are expensive so this type is only used in special situations [5].

Railway ballast can be defined as granular coarse aggregate. Traditionally, angular, crushed hard stones and rocks, uniformly graded, free of dust and dirt and not prone to cementing action have been considered good ballast materials. Ballast is a granular material with high bearing capacity that is placed above sub-ballast or subgrade to act as a platform, to support the track superstructure. Its main function is to spread the high loads of passing axles to the subgrade. In doing this, there are high stresses transmitted through the ballast. Moreover, ballast provides a certain amount of resiliency as well as energy absorption for the railway track. The source of ballast varies between different areas, depending on the quality and availability of the material. Ballast index characteristics include particle size, shape, gradation, surface roughness, particle density, bulk density, strength, durability, hardness, toughness, resistance to attrition and weathering [1].

Sub-ballast is composed of well-graded crushed rock or sand gravel mixtures, and it sits between the ballast and the subgrade material. The sub-ballast layer transmits and distributes stress from the ballast layer to the subgrade over a larger area to reduce the magnitude of resultant stress. Furthermore, another important function is to prevent interpenetration between the ballast and subgrade layer. Sub-ballast acts as a filter to stop upward migration of subgrade particles into the ballast and penetration of coarse ballast into subgrade. In particular, some of the functions of the sub-ballast may be achieved through the use of sand or geosynthetic materials like membrane and filter fabrics [5].

Subgrade provides the foundation on which the track is constructed. It can be existing natural soil or placed soil. The subgrade must be stiff and have enough bearing strength and stability to

avoid excessive settlement. Lack of the required quality will result in an unacceptable disturbance of the track system, and even ballast and sub-ballast will not stay in very good condition.

### 2.2.2. Track forces

In order to design an adequate railway track substructure and understand how ballast works on a railway track, it is necessary to know the type and magnitude of forces that are imposed on the railway track during its lifetime. Generally, these loads are exerted by the sleepers on the ballast layer through wheel-rail-sleeper interactions. There are two main forces acting on the ballast: the vertical force of the moving train and the squeezing action of tamping during maintenance work. The vertical force consists of static and dynamic components. The static load is due to the dead weight of the superstructure and train, whereas the dynamic load is a function of the speed of the train and the track conditions.

The vertical downward force at the rail-wheel contact point, as shown in Figure 2.2, tends to lift up the rail and sleeper some distance away from the contact point. With the advancing wheel, the uplifted sleeper will be forced down creating a high impact load onto the ballast particles and the track structure as a whole. As previously mentioned, the impact force is very much dependent on the train speed and load. Meanwhile, this movement can cause a pumping action in the ballast, which can cause deterioration of track structure components and increase the ballast settlement by exerting a higher force on the ballast and pumping up fouling materials from sub-layers [5].

According to [3], the vertical wheel force consists of a static component, equal to the weight of the train divided by the number of wheels, in addition to a dynamic variance. Furthermore, they stated that vertical dynamic variation, such as bounce and forces caused by wheel flats or wheel/rail defects, could cause huge impacts and vibrations.

[15] Concluded that the total vertical wheel load on the rail could be classified into two groups: quasi-static load and dynamic load, the quasi-static load is composed of the following components [5]:

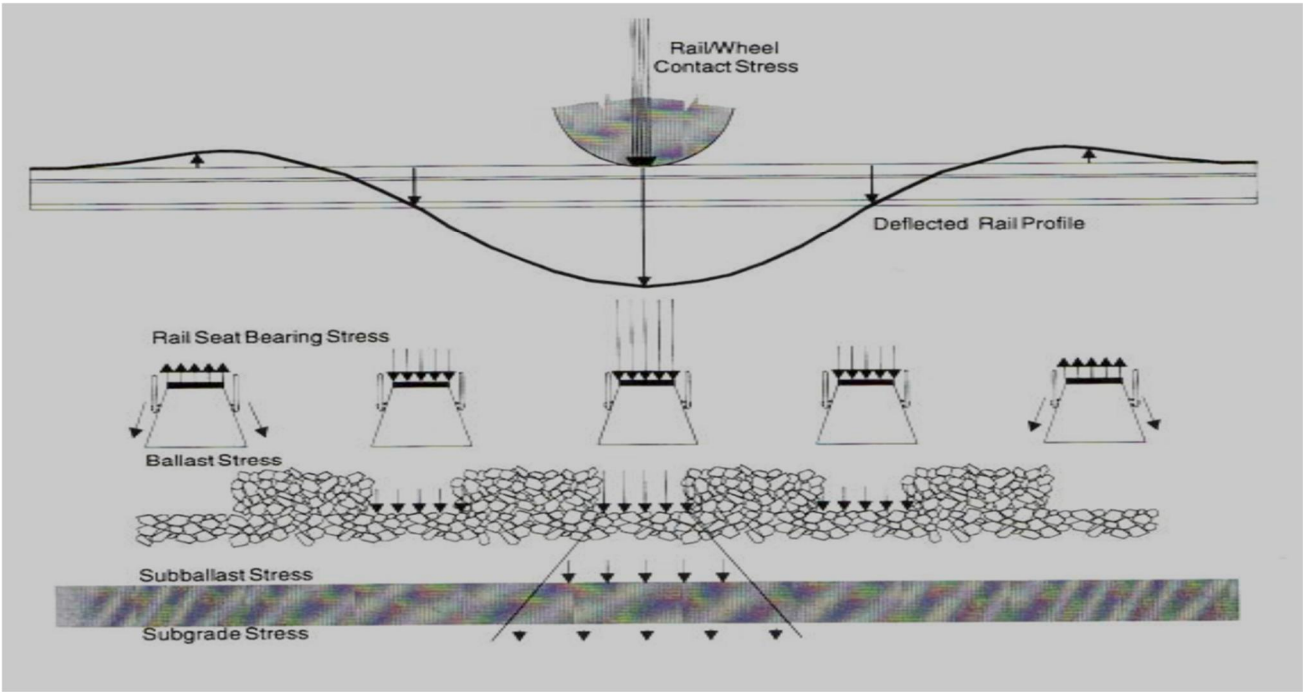


Figure 2.2: Uplift of rails [1]

$$Q_{total}=Q_{quasi-static}+Q_{dynamic} \quad \text{.....2.1}$$

$$Q_{quasi-static}=Q_{static}+Q_{centrifugal}+Q_{wind} \quad \text{.....2.2}$$

The other main force acting on railway track is maintenance tamping, which has been recognized as the most effective method to correct and restore track geometry. It is a very common railway maintenance technique used at present. Track force on the ballast is achieved through squeezing the ballast, and this high squeezing force causes ballast breakage which significantly increases ballast deterioration.

## 2.3. Ballast

Traditionally, the main factors in the choice of ballast materials are availability and economic reasons. Ideal ballast materials are angular, crushed, hard stones and rocks, uniformly graded, free of dust and dirt, and not prone to cementing action. However, there has not been universal standard on the specification. The ability of ballast to perform its functions depends on the particle characteristics (e.g. particle size, shape, angularity, hardness, surface texture and durability) together with the in-situ physical state (e.g. grain structure and density) [7].

## 2.3.1. Ballast Properties

### 2.3.1.1. Effect of Particle Shape on Ballast Functions

Particle shape influences not only the physical state of the assembly (grain structure and porosity) but also the particle interactions (inter particle friction and contact force). In the past, various attempts have been made to characterize the particle shape of railway ballast. However, due to the complexity and irregularity of the shape of particle, universally accepted effective parameters on shape characteristic have not been established so far. In the railway industry, various shape characteristics (i.e. flakiness, elongation, sphericity, angularity and surface texture) are used.

a. Flakiness or flatness

A flat particle is defined as one in which the ratio of thickness to width of its circumscribing rectangular prism is less than a specified value. This ratio is called the flakiness ratio of a particle P and can be expressed as [7]:

$$P = \frac{a}{b} (0 < p \leq 1.0) \text{.....2.3}$$

Where a = thickness of the particle, b = width of the particle.

After having conducted a set of triaxial ballast tests to investigate the ballast shape on ballast performance, according to [4] randomly placed flaky material had a higher mobilized friction angle than did no flaky material at the same void ratio. However, when the flaky particles became oriented, their behavior was highly anisotropic. When they are oriented at the angle of the shear plane they had significantly lower deviator stress and angle of internal friction than no flaky particles. When the flaky particles were oriented perpendicular to the direction of applied stress, they had a much higher deviator stress and angle of internal friction than no flaky materials [7].

From the ballast maintenance point of view, increasing the percentage of the flaky particles could increase the ballast degradation rate and the degree of fouling and thus will increase the ballast maintenance work. Furthermore, better particle interlocking due to the existence of a substantial portion of flaky particles in a ballast sample will make the ballast maintenance work

more difficult. So, it is reasonable to assume that the ballast maintenance work increases with the percentage of the flaky particles in a ballast.

b. Angularity or roundness

Angularity, or its inverse, roundness, is a measure of the sharpness of the edges and corners of an individual particle. Roundness defined as the ratio of the average radius of curvature of the corners and edges of a particle to the radius of the maximum inscribed circle.

Ballast fouling capacity and drainage ability mainly depend on the ballast voids ratio. Because an angular ballast can produce better particle interlocking, it generally has looser initial and final particle skeletons than a rounded ballast, Therefore, an angular ballast usually has a relatively larger voids ratio than does a rounded ballast, which means that an angular ballast has a better ballast fouling resistance capacity and drainage ability. However, from the ballast maintenance point of view, angular ballast may need more ballast maintenance work because it is easily degraded and deformed under the repeated loading of trains. Moreover, better particle interlocking could make the ballast maintenance more difficult [7].

c. Surface texture

Surface texture is believed to have an important effect on ballast performance. A rough particle surface is critical to form a high inter-particle friction force, which will increase the shear strength of the ballast and the track stability. On the contrary, a smooth surface will create a low inter-particle friction force which will result in an easy rearrangement of particles and cause more ballast-related track deformation. To quantify the ballast particle surface texture, a visual estimate of particle surface roughness is recommended. Particle surface roughness is divided into four group categories in the visual method. They are rough, medium rough, medium smooth and smooth.

### 2.3.1.2. Ballast Gradation

The selection of the particle size distribution of ballast layer has a great effect on both in-situ performance and the economic evaluation of track design. It is widely accepted that a narrow gradation would best meet the requirements for railway ballast. Sufficient voids are formed

within the railway ballast with a narrow gradation and, therefore, it provides efficient drainage of water from the ballast track bed.

The AREMA (2.4.5) manual provides recommended values of ballast gradation size as shown in the table 2.1 below:

Table 2.1: Recommended Ballast Gradations [3]

| Size No. (See Note 1) | Nominal Size Square Opening | Percent Passing | | | | | | | | | |
|---|---|---|---|---|---|---|---|---|---|---|---|
| | | 3″ | 2½″ | 2″ | 1½″ | 1″ | ¾″ | ½″ | d″ | No.4 | No. 8 |
| 24 | 2½″- ¾″ | 100 | 90-100 | | 25-60 | | 0-10 | 0-5 | – | – | – |
| 25 | 2½″ - d″ | 100 | 80-100 | 60-85 | 50-70 | 25-50 | – | 5-20 | 0-10 | 0-3 | – |
| 3 | 2″ - 1″ | – | 100 | 95-100 | 35-70 | 0-15 | – | 0-5 | – | – | – |
| 4A | 2″ - ¾″ | – | 100 | 90-100 | 60-90 | 10-35 | 0-10 | – | 0-3 | – | – |
| 4 | 1½″ - ¾″ | – | – | 100 | 90-100 | 20-55 | 0-15 | – | 0-5 | – | – |
| 5 | 1″ - d″ | – | – | – | 100 | 90-100 | 40-75 | 15-35 | 0-15 | 0-5 | – |
| 57 | 1″ - No. 4 | – | – | – | 100 | 95-100 | – | 25-60 | – | 0-10 | 0-5 |
| Note 1: Gradation Numbers 24, 25, 3, 4A and 4 are main line ballast materials. Gradation Numbers 5 and 57 are yard ballast materials. | | | | | | | | | | | |

## 2.3.2. Mechanical Behavior of Ballast

The understanding of the behavior of granular material plays a very important role in the modern railway system. The deformation response of granular material under repeated loading is commonly characterized by a residual (permanent) deformation as well as a recoverable (resilient) deformation. The behavior of a granular material under repeated loading is non-linear and is stress dependent. The magnitude of plastic strain per cycle generally decreases with the number of load cycles and the difference between the maximum strain under peak load and the permanent strain after unloading for each cycle is known as the resilient strain. It is important to understand the nonlinearity behavior of granular material as it affects the stress condition and ultimately settlement behavior [8].

### 2.3.2.1. Resilient Behavior of Granular Material

The resilient modulus as defined by the repeated deviator stress divided by the recoverable (resilient) axial strain during unloading in a triaxial test. It is vital to have a good understanding

of the resilient behavior of the track bed material as this is known to have an effect on the degradation and rate of settlement of the rail track. Figure 2.3 illustrates the typical strain in a granular material [8].

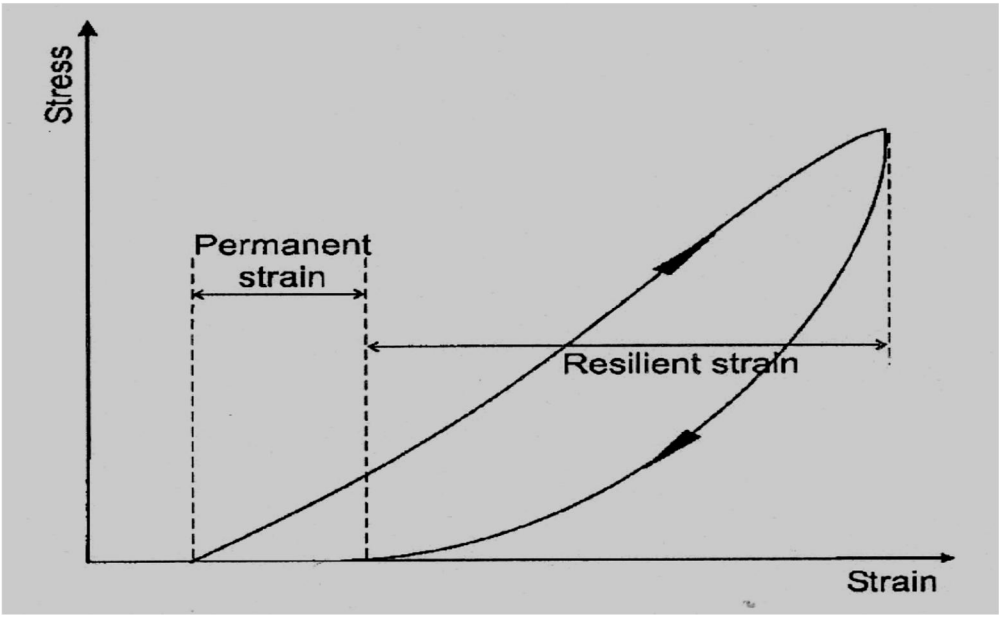


Figure 2.3: Strains in granular material during one cycle of load application [8]

a. Effect of Stress

Researches show the sizable influence of confining pressure and the sum of principal stresses on the resilient behavior of granular material and they stated that a change from 20 to 200kPa in the confining pressure would result in an increase of 500% in the resilient modulus.

b. Effect of Aggregate Type and Particle Shape

[8] Claimed that gravel, when compared to crushed limestone exhibits a higher resilient modulus. Researchers reported that crushed aggregate, with its increased angularity, demonstrates better load spreading capability and a higher resilient modulus than uncrushed gravel with its rather characteristically rounded aggregate. Researches showed tested various types of granular material with the same grading and found a 50% increase in resilient modulus of angular material at low mean normal stress condition compared to that of rounded gravel. In addition, under repeated load triaxial tests on different granular materials they found that at low

strain, the resilient modulus of granular material may be influenced by particle texture and that a correlation exists between elastic stiffness and surface friction of a material.

c. Effect of Stress History and Number of Load Cycles

It is widely reported in literature that stress or loading history exerts a certain degree of influence over the resilient behavior of granular material. For example a series of repeated load triaxial tests on samples of well-graded crushed limestone of the same compaction and density characteristics in a dry state, the results indicated that the material was subjected to effects of stress history that could be reduced by a preloading regime. And concluded that the effect of stress history could be nearly eliminated and a constant resilient response could be achieved after a 100- cycle application of the same stress amplitude [8].

d. Effect of Aggregate Type and Particle Shape

The general view regarding the effect of aggregate type is that crushed aggregate with its angular shape compared to rounded aggregate has a higher resilient modulus with a better load spreading capability. The resilient modulus of rough, angular crushed material compared to that of rounded gravel, with the same grading, was found to be higher by a factor of 50% at low mean normal stress and about 25% at high mean normal stress. However, it is important to note that the effect of aggregate type is only apparent when other parameters such as grading, density and applied stresses are kept constant.

e. Effect of Load Duration and Load Sequence

There is widespread agreement among researchers that load duration and frequency has little or no impact on the resilient behavior of granular material. For instant the resilient modulus of sand showed a modest increase from 160 to 190 MPa when the loading duration was decreased dramatically from 20 minutes to 0.3 seconds [8].

### 2.3.2.2. Permanent Strain Behavior of Granular Material

The irrecoverable strain of granular material as shown in Figure 2.4 is often a trigger for maintenance activities on a rail track. On a rail track, the accumulation of such permanent strain is due to the rearrangement of particles as well as particle breakage.

f. Effect of Stress

It is evident that stress level is one of the most important factors governing the development of permanent deformation in granular materials. Researchers reported that the accumulation of axial permanent deformation is related to deviator stress and inversely linked to confining pressure. the permanent strain accumulated over a certain number of load cycles is directly related to the stress ratio, defined as the ratio of deviator stress q to confining stress $\sigma_3$. According to their report, increasing the stress ratio $q / \sigma_3$ will result in the increase in permanent strain as shown in Figure 2.4. The figure also shows that for the same stress ratio, (i.e. 20/5 and 60/15) increasing the stress path length will increase the amount of permanent strain [8].

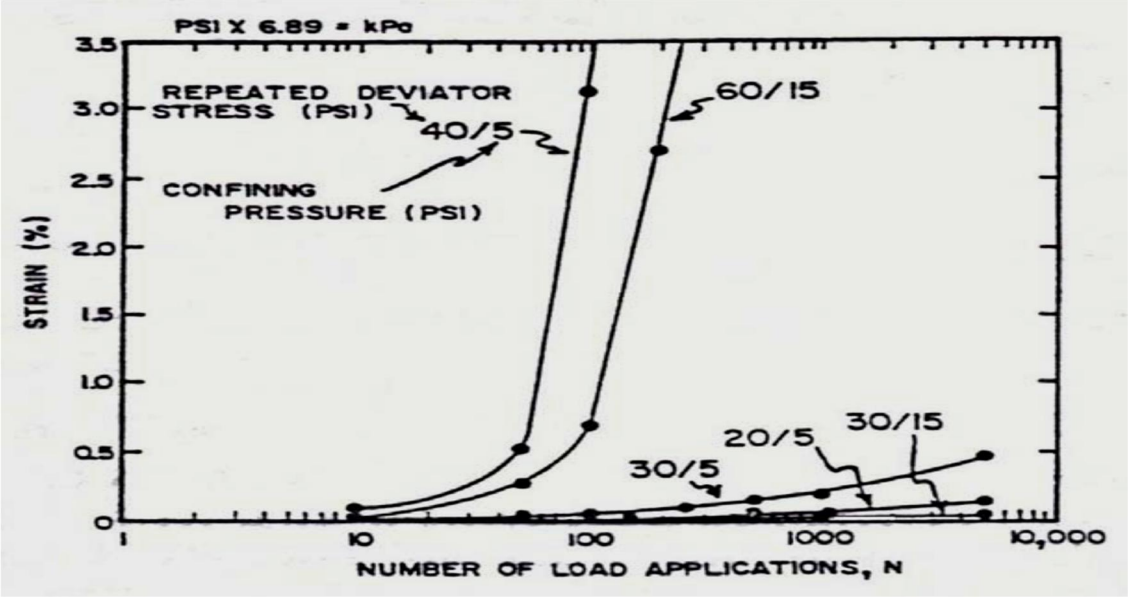


Figure 2.4: Effect of stress ratio on permanent strain [8]

g. Effect of Number of Load Applications

The increase in the permanent deformation in granular material is a gradual process with each load application contributing to an increment of strain. In the context of a railway line, each passing axle of the train acts as a load that will in turn induce strain causing permanent deformation. With reference to the literature, the significance of the number of load cycles is well documented by many prominent researchers, with many varying observations. Several researchers have indicated continuously increasing permanent strain under repeated loading (see Figure 2.5) [8].

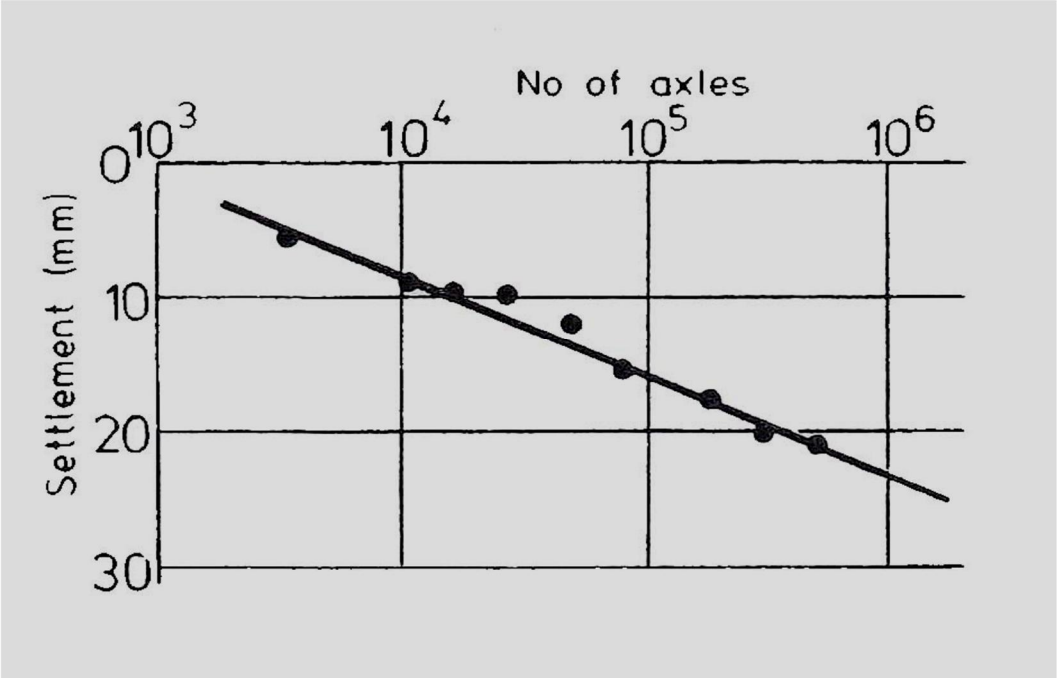


Figure 2.5: Effect of repeated load applications [8]

h. Effect of Moisture Content

The presence of moisture in granular material has both merit and disadvantage. On the one hand, an adequate amount of water may produce negative pore water pressure that in turn increases the stiffness and strength of unbound granular material. On the other hand, as saturation approaches, excessive pore water pressure reduces the effective stress and results in a poorer permanent deformation resistance.

i. Effect of Stress History

Permanent deformation behavior of granular material is related to its stress history (order of the application of loads). Permanent deformation in a granular material is much higher when full load is applied immediately rather than when it is increased in successions. The effect of stress history appears as a result of gradual material stiffening by each load application, causing a reduction in the proportion of permanent to resilient strains during subsequent loading cycles. The effect of stress history has not been well explored even though it is well documented in the literature. More work has to be done to quantify this effect [8].

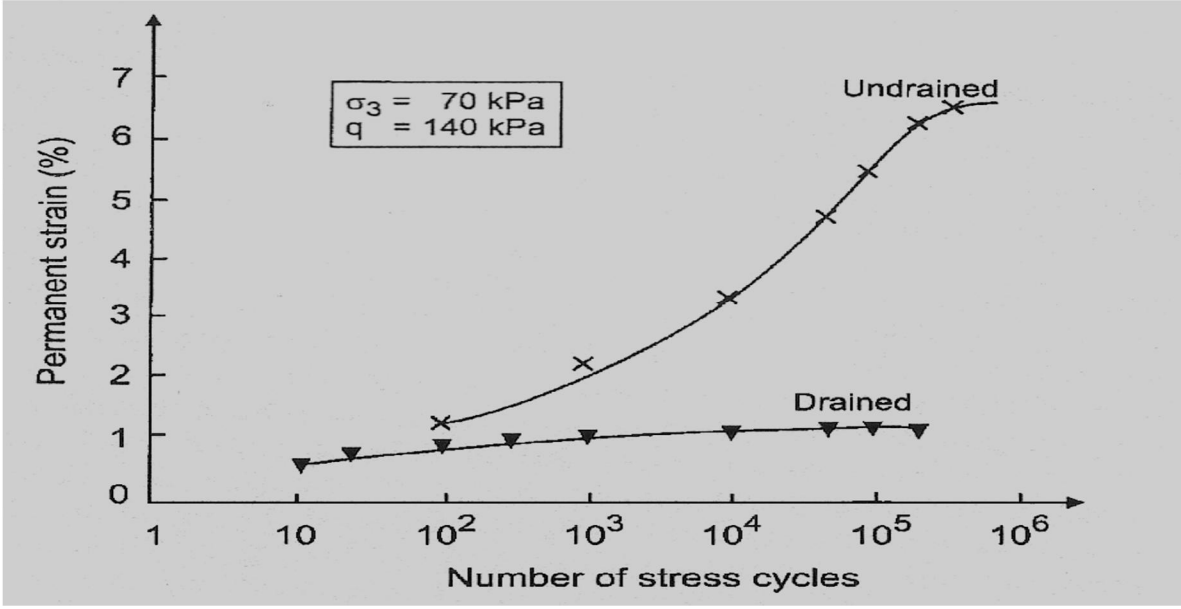


Figure 2.6: Influence of Drainage on Permanent Deformation Development [8]

j. Effect of Density

The effect of density, often described in conjunction with the degree of compaction in a material, is reported by many sources as a very important factor for the long term behavior of granular material. Resistance to permanent deformation under repeated loading is improved with increased density. 80% and 22% reduction in permanent strain, in crushed limestone and gravel respectively, when the material density was increased from Proctor to modified Proctor density (90% – 92% of modified Procter density is equivalent to the specified 95% standard Procter density except for fine sand where the difference is bigger). The effect of density on permanent strain is particularly apparent in angular material if there is no accompanying transient pore pressure during loading. In the case of rounded particles, e.g. gravel, the effect is deemed to be less significant due to the fact of its initially higher relative density for the same compaction effort [8].

## 2.4. Ballast Degradation

Degradation or deterioration is the reduction of the original quality due to various influences. By far the most significant factor contributing to the deterioration is the dynamic load. The dynamic load is directly related to the axle load and track geometry.

The main processes of track deterioration are [6]:

- Wear
- Fatigue and
- Settlement.

The mechanism of the track faults creation can be presented briefly and simplified as follows (Figure 2.7):

- Track irregularities (track geometry or running surface) ❶ lead to increase of the dynamic forces, which accelerates the rail wear. Through the fasteners ❷, the consequences are transferred to the sleepers ❸ and the ballast ❹ and finally to the substructure ❺ [6].

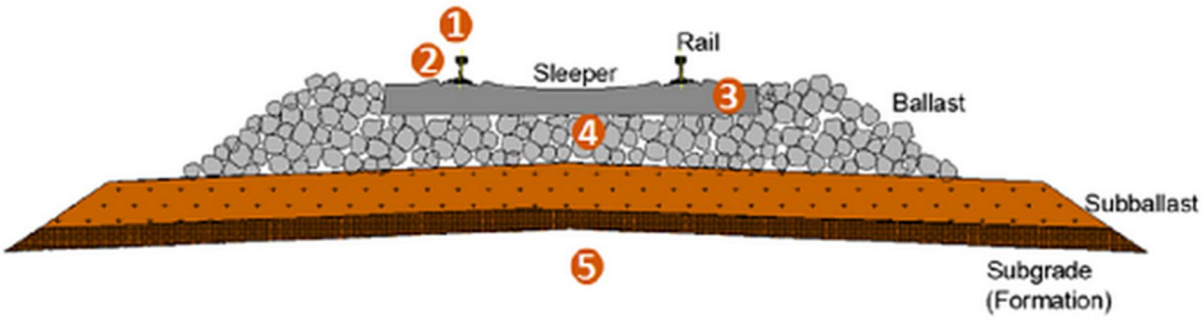


Figure 2.7: Degradation process of railways infrastructure

- As a consequence, fine material from the subgrade goes up to the ballast
- The existence or entrance of water to the ballast bed accelerates the deterioration procedure of the track.

Three main groups of factors may be distinguished that contribute to the degradation of railway infrastructure:

- **Use:** wear by physical contact and dynamic load
- **Environment:** climatic influence, water
- **Failures:** faulty components, bad construction

In most of the cases it is not just one of these factors that causes degradation, but a combination of them.

The bad state or quality of track components contributes significantly to the degradation of the track geometry. Bad track geometry produces higher dynamic loads on the track components, which accelerates their degradation. The degradation curve of a generic railway track component is shown by the figure below [6].

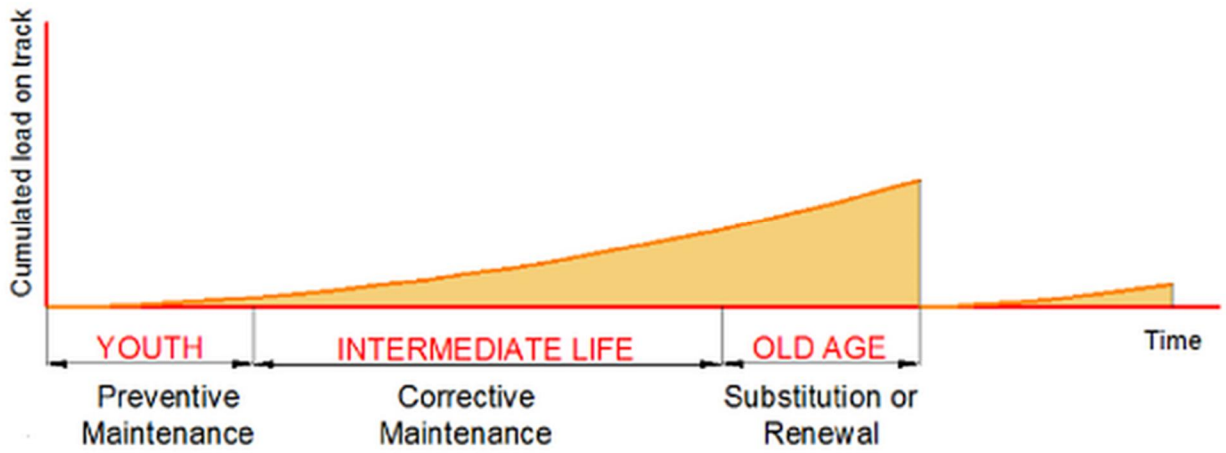


Figure 2.8: Degradation process of railway track with load dependent wearing [6]

### 2.4.1. Driving Forces of Degradation

In some cases, the track can degrade without any traffic (e.g. the soil may settle due to weight of the embankment, especially in the early years after construction). In most cases running trains is the driving force of deterioration.

A railway track is designed to distribute the load from trains down to the soil/ground. This distribution through super- and substructure depends on original tracks design and current track condition. Stiffness of different components in the track structure, as well as the resulting (global) track stiffness will partly determine how the loads are distributed.

The static quasi-static and dynamic forces are all important for track degradation. Some aspect determining forces and thereby influence degradation is listed (table 2.2) [6]:

Table 2.2: Parameters influencing track degradation [6]

| Subsystem | Characteristics | Influence of the Subsystem |
|---|---|---|
| **Vehicle** | • Speed<br>• Axle load<br>• Unsprang mass<br>• Suspension<br>• Wheel profile<br>• Axle spacing etc. | • Static<br>• Quasi-static and<br>• Dynamic forces |
| | • Wheel (current condition such as wheel flat and wheel corrugation) | • Dynamic force |
| **Track** | • Track design geometry (Curves etc.) | • Static and<br>• Quasi-static forces |
| | • Track geometry quality | • Dynamic forces |
| | • corrugation | • high-frequency forces |
| | • rail imperfections such as joints or poor welds | • impact forces |

The forces stated above influence the functions of the basic components in the track which in turn affect degradation and the failure process. The failure of each component has an effect on the function of other components in the track system.

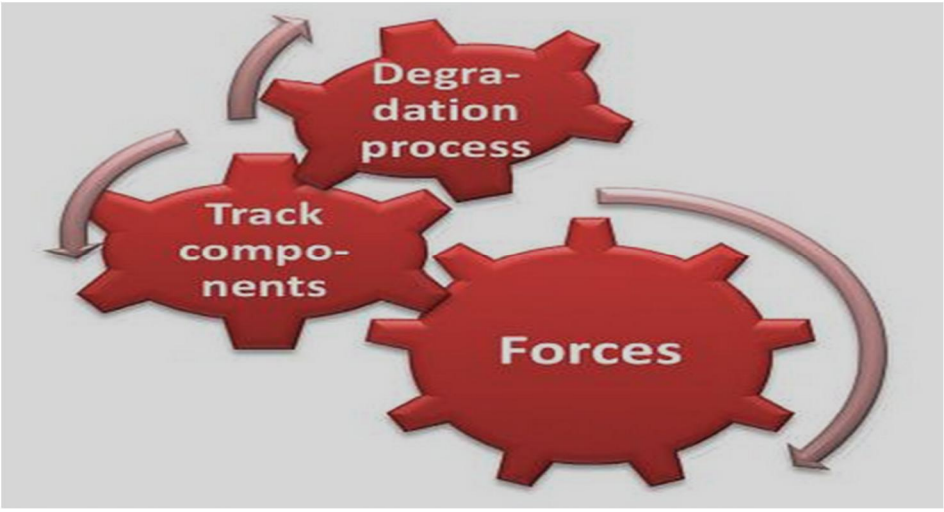

In order to be able to measure the defects and failures and to prevent catastrophic failures, it is important to analyses the characteristics of each component which are significant for deterioration process. The deterioration process of the different superstructure components is described in table 2.3 [6]:

Table 2.3: deterioration process of different superstructure components [6]

| **Track components** | **Deterioration process** |
|---|---|
| The rails | The rail experiences wear and fatigue.<br>Rail deterioration is often complicated relation between<br>• Vehicle characteristics,<br>• Creepage in the wheel-rail contact and<br>• Other factors.<br>Deterioration by Rolling Contact Fatigue (RCF) is in many cases significant and also safety-related (RCF initiates cracks that will grow by time and traffic, what can lead to a rail break). |
| The fastener, rail pads, sleepers | The fastener, rail pads and sleepers have all their own deterioration processes, which are dependent of the forces, bending moment's etc. acting on them. |
| The ballast and sub-ballast | Due to stone reorientation the ballast and sub-ballast layers get differential settlement. This leads to wear of the ballast stones.<br>Fines produced by this wear together with possible other material (ballast fouling), are causing decreased drainage conditions.<br>The subgrade may be exposed to settlement. Varying settlement along the track (resulting in differential settlements), are directly visible as track geometry quality variations. |

## 2.4.2. Ballast Settlement

As mentioned, the factors that control the performance of the ballast are poorly understood. The long-term behavior of the railroad track, including the ballast behavior and the damage

mechanisms underlying the ballast settlement, is stated that there do not exist any generally accepted damage and settlement equations, and hardly any material equations for the ballast itself. Only different suggestions to describe the ballast settlement from a phenomenological point of view are available; the settlement then being a function of number of loading cycles and/or magnitude of the loading.

Railway track will settle (change its position) as a result of permanent deformation in the ballast and underlying soil. After having been used some time, the track will not be so straight and at so good level as it was when it was new. The settlement is caused by the repeated traffic loading and the severity of the settlement depends on the quality and the behavior of the ballast, the sub-ballast, and the subgrade.

Ballast settlement occurs in two major phases [9]:

- Directly after tamping, when the track position has been adjusted to a straight level, the settlement is relatively fast until the gaps between the ballast particles have been reduced and the ballast is consolidated,
- The second phase of settlement is slower and there is a more or less linear relationship between settlement and time (or load).

The second phase of settlement is caused by several basic mechanisms of ballast and subgrade behavior:

- continued (after the first phase) volume reduction, i.e. densification of the ballast and sub ground, caused by particle rearrangement produced by repeated train loading,
- sub-ballast and/or subgrade penetration into ballast voids. This causes the ballast to sink into the sub-ballast and subgrade and the track level will change accordingly,
- volume reduction caused by particle breakdown from train loading or environmental factors; i.e. ballast particles may fracture (divide into two or more pieces) due to the loading,
- volume reduction caused by abrasive wear. A particle may diminish in volume due to abrasive wear at points in contact with other particles, i.e. originally cornered stones become rounded, thus occupying less space,

- inelastic recovery on unloading. Due to micro-slip between ballast particles at loading, all deformations will not be fully recovered upon unloading the track. In this case the permanent deformation is a function of both stress history and stress state,
- movement of ballast and subgrade particles away from under the sleepers. This causes the sleepers to sink into the ballast and subgrade,
- lateral, and possibly also longitudinal (in the rail direction), movement of sleepers causing the ballast beneath the sleepers to be "pushed away", and the sleepers will sink deeper into the ballast.

The first four items concern densification of ballast and subgrade, whereas the three last-mentioned items concern inelastic behavior of the ballast and subgrade materials.

Concerning the volume reduction or densification caused by particle rearrangement produced by repeated train loading, it could be mentioned that the train load also may have an opposite effect. Due to the elastic foundation, the train load will lift the track (rails and sleepers) in front of and behind the loading point, thus reducing or eliminating the preload (the dead load) caused by the rails and sleepers on the ballast. At the same time, due to the dynamic high-frequency train-track interaction forces, waves will propagate from the wheel-rail contact patches, either through the ballast and subgrade or through the track structure, to the region with the unloaded ballast. These waves will normally propagate faster than the train, giving vibrations in the unloaded ballast. This, in turn, may cause a rearrangement of the ballast particles so that the density decreases. As a result, this may cause a lift, at least temporarily, of the track.

### 2.4.3. Ballast Fouling

Ballast fouling is the presence of more fines in the ballast material from crushed aggregate, sleeper wear, fine particles from sub-grade or external ("surface spillage") fines from freight and coal fouling, which causes soft and deformable ballast structure [11].

[1] Describe railway ballast fouling as generated by particles smaller than 4.76 mm diameter that are situated within the void spaces of the ballast particles. When the ballast is made up of greater than 20% of fouled material by weight, the ballast layer can be considered highly fouled because the ballast to ballast contact is compromised by the fine grained materials.

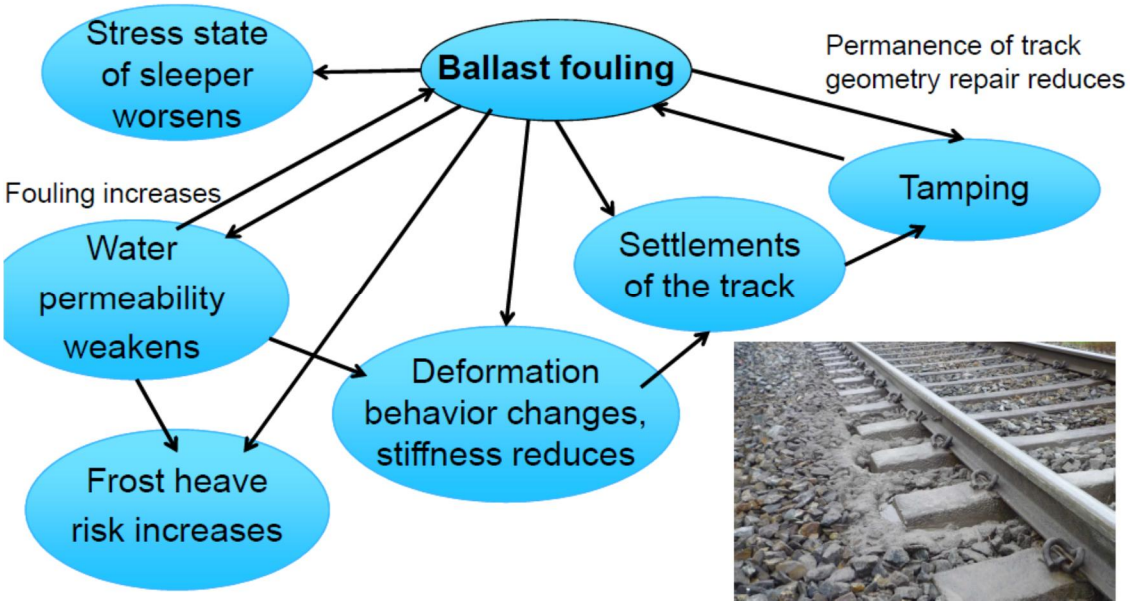


Figure 2.9: schematic representation of source of ballast fouling [11]

a. Mechanisms of Ballast Fouling

Based on an extensive literature review and observations, [1] found that ballast fouling was caused through five primary modes. These sources of ballast fouling are as follows [11]:

- Abrasion and breakdown of ballast due to rail loading, tamping, and freeze/thaw
- Degradation of rail ties
- Migration of subgrade material into the ballast layer
- Migration of sub-ballast or subgrade material into the ballast layer
- Migration of environmental material into the surface of the ballast

b. Effect of fouling material on ballast behavior

Fouling materials can have a beneficial or adverse effect on fouled ballast. The effect depends on the types of fouling material present, the degree of fouling and the water content. [1] Conducted box tests to investigate the effect of fouling materials on ballast settlement. Figure 2.10 shows the effect of different degrees of fouling and fouling materials on ballast settlement. It can be seen that ballast settlement increases with increasing degree of fouling for all fouling materials. [1] Noted that if the fouling material was moist silt, the ballast settled less than if moist clay was

the fouling material, provided the degree of fouling was less than 20%. However, the reverse behavior was observed if the degree of fouling was more than 20%.

Table 2.4: source of ballast fouling [11]

| ***Category*** | ***Source of ballast fouling*** | ***Amount (% by weight)*** |
|---|---|---|
| Ballast breakdown | from handling (at quarry, from dumping, transportation), Tamping<br>Traffic damage (repeated loading, vibration)<br>Chemical weathering, Thermal stress (desert)<br>Freezing of water in particles | 76 |
| Ballast surface infiltration | Delivered with ballast<br>Dropped from trains<br>Wind blown<br>Water borne<br>Splashing from adjacent wet spots | 7 |
| Sleeper wear | Sleeper-ballast interaction | 1 |
| Underlying granular layer infiltration | Old track bed breakdown<br>Sub-ballast particle migration from inadequate gradation | 13 |
| Subgrade infiltration | Infiltration from subgrade into ballast | 3 |

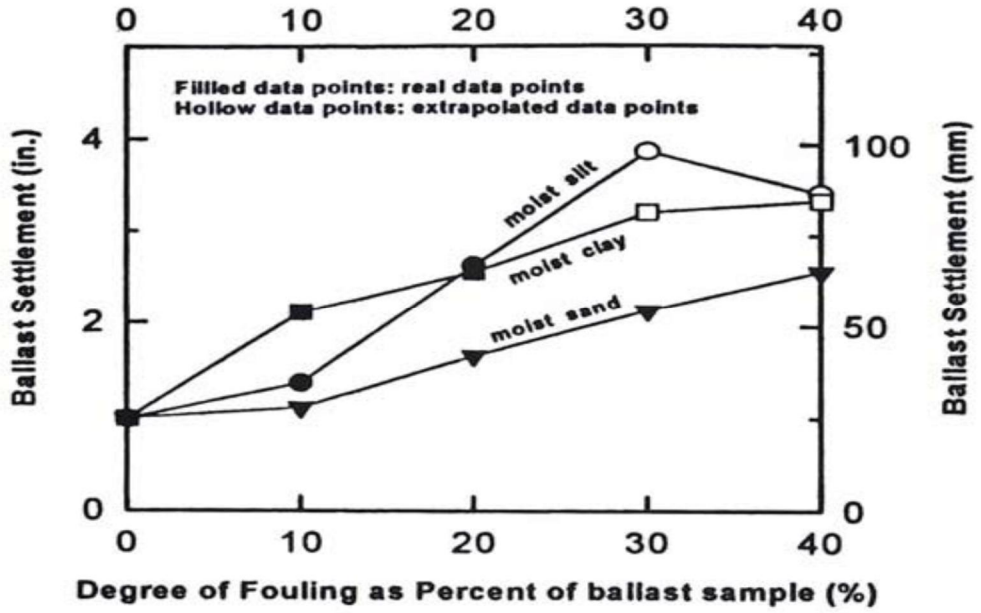


Figure 2.10: Effect of degree of fouling and type of fouling material on ballast settlement [1]

Fouling index $F_I$: measure of fine particles content

$$P_I = P_4 + P_{200} \quad \text{.....2.4}$$

Where $P_4 =$ % pass at 4.75mm sieve

$P_{200}$ = % *pass at* 0.075*mm sieve*

A clean and good ballast material should have a value of $F_I < 1$

Table 2.5: classification of ballast based on fouling index [1]

| Classification | Fouling index |
|---|---|
| Clean | < 1 |
| Moderately clean | 1 to < 10 |
| Moderately fouled | 10 to < 20 |
| Fouled | 20 to < 40 |
| Highly fouled | ≥ 40 |

## 2.5. Ballast and Geosynthetics

Geosynthetics may perform the following functions in new track construction or rehabilitation: separation of materials with different particle size distributions, filtration, and drainage and soil reinforcement. In railroad construction, geosynthetics may be installed within or beneath the ballast or sub ballast layers.

Table 2.6: Functions of Geosynthetics

| Type of Geosynthetic | Functions |
|---|---|
| Geotextiles<br>• Woven<br>• Non-woven | Reinforcement<br>Filtration<br>Separation<br>Transmission of fluids |
| Geogrids | Reinforcement |
| Geomesh | Reinforcement<br>Filtration |
| Geonets | Transmission of fluids |
| Geomats | Reinforcement |
| Geocells | Reinforcement<br>Confinement |
| Geocomposite | Reinforcement<br>Separation<br>Filtration<br>Transmission of fluids |
| Geomembranes | Isolation<br>Separation<br>Reinforcement |

In order to meet the demand of increasing number of rail commuters, railways face the challenge of increasing the competitiveness and attractiveness of rail transport in terms of speed, increased tonnages, higher frequency and reliability. This in turn necessitates enhanced quality of track that depends on the better functioning of ballast, an important component of rail track. However, there have been numerous track problems caused by the densification, degradation and lateral spreading of ballast. Therefore, it is important to inhibit the lateral spreading of ballast to optimize the track performance and reduce the maintenance costs.

One of the promising approaches to improve the track performance is to reinforce the ballast with geosynthetics. Once in place, the geosynthetic-reinforcement offers the following major benefits to the rail industry [12]

(i) it holds the ballast in place by restraining its lateral movement thereby preventing the track settlement and rail misalignment

(ii) it increases the confining pressure on ballast thereby reducing particle degradation that helps maintaining the ballast angularity and track shear strength.

With regards to the position of reinforcement, several researchers have argued that the beneficial effects of reinforcement in the form of reduction in track settlement could be enhanced considerably by placing within the ballast. However, the effectiveness of reinforcement in providing the aforementioned benefits depends on the level of interaction between ballast and geosynthetics.

Geosynthetics reinforcement (geogrids and geocells) installed over unstable subgrades may eliminate the necessity to replace this soil, increasing the load bearing capacity of the system due to better stress distribution. When installed within the ballast or sub ballast layers, geosynthetics may help to reduce settlements associated with the lateral spreading of the ballast and sub ballast materials. The main geosynthetic characteristics that must be considered for this function are the interaction between geosynthetic-soil/ballast, resistance to mechanical damage.

### 2.5.1. Ballast and Geocell

A cellular confinement system is a three-dimensional honeycomb-shaped structure of interconnected individual geocell units. Geocells are typically formed from high-density polyethylene sheet strips connected in series, using full-depth ultrasonic welded seams, aligned perpendicular to the longitudinal axis of the strips. When expanded, the interconnected strips form the walls of the flexible, three-dimensional structure Figure 2.11. Cohesionless granular material is then added to the structure and compacted. When compacted, it produces an interaction structure, resulting in an increase in bearing capacity over that of the unconfined granular material [3].

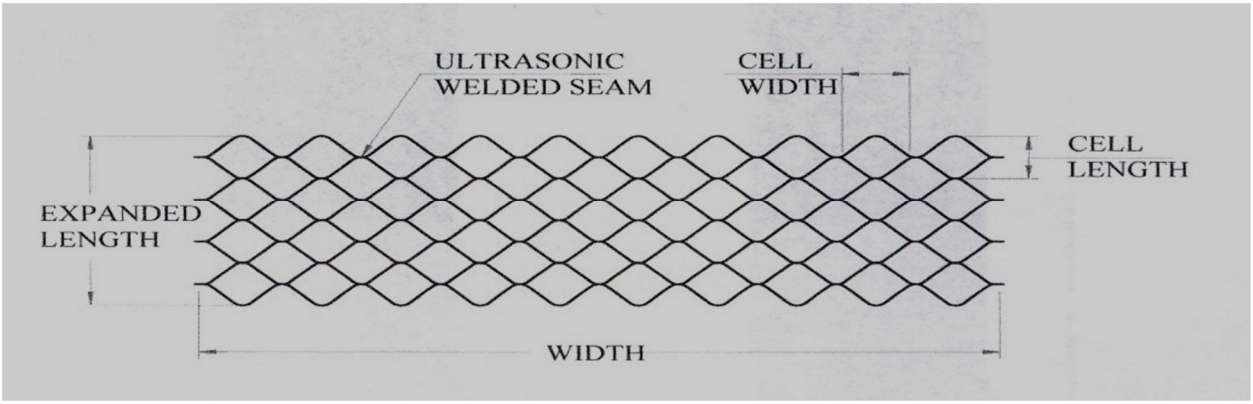


Figure 2.11: Typical Geocell Section, Expanded Plan View

Three required components of the Cellular Confining System are [3]:

- The geocell cellular confinement sections.
- The granular infill material.
- The geotextile separation layer, if required

a. Significance and Use [3]:

*Load Support* - The interaction structure produced by the cellular confinement system functions as a layer that distributes loads to a pressure that the underlying soils will satisfactorily support. The system may be used under track roadbeds (below the ballast section), vehicle roadbeds or other railroad facilities, which are constructed, or will be constructed over soils with lower than acceptable bearing capacities that cannot be economically removed due to schedule or excess material excavation and replacement costs. When bearing capacities of the supporting soils are of a magnitude that will not support the existing or proposed loads, the cellular confinement system may be considered as a load support alternative. The minimum cell depth for load support should be 8 inches (200 mm), unless otherwise designated by the Engineer.

*Slope and Channel Protection* - The interaction of the structure with a well graded, granular infill material can provide a slope covering that will allow drainage of the groundwater through the system, while protecting the slope from erosion. Infill material for channel protection should be sized according to the site-specific channel soil and flow conditions. The minimum cell depth for Slope and Channel Protection should be 6 inches (150 mm).

*Earth Retention* - In cases where steep, non-load bearing earth fill is required to allow for signal installations, signs, and other minor items, geocells can be used to retain earth materials in place without excessive compaction efforts, and where subsidence is tolerable. The minimum cell depth for Earth Retention should be 4 inches (100 mm).

b. Material Requirements

The geocell cellular confinement sections shall have the minimum chemical and physical properties as shown in Table 2.7. The surface of the geocells may be smooth or textured. Surface texturing can take the form of indentations or perforations. Texture features should be in horizontal rows, with each row staggered and separated from the adjacent row. No texture feature should be located within 1.5 inches (38 mm) of a cell weld [3].

c. Infill Material

For structural applications, the infill material shall be a dry, granular, cohesionless material, having filtering characteristics compatible with the subgrade below and the ballast section above, as specified by the engineer. The material shall be a well-graded crushed stone with a maximum particle size of 1.5 inches (37.5 mm), with no greater than 10% passing the #200 sieve. The coarse fraction of the material shall have a Los Angeles Abrasion test wear of no greater than 50%.

[13] Observe the effect of reinforcement material on overall performance. Conclusions made from numerical modeling of geocell applied to a railroad scenario include:

- the confinement of the ballast using geocell was quite effective in reducing vertical deformations, especially when low-quality material was used. Higher shear strength of the ballast reduces the need for reinforcement, reducing the need for substructure improvement. This is promising when considering the possibility for using weaker ballast materials like recycled ballast or well-graded particles, or allow for longer maintenance cycles when the ballast loses shear strength.

Table 2.7: Polyethylene and Geocell Cellular Confinement System Properties

| Property | Unit | Value | Test Method |
|---|---|---|---|
| Polyethylene Content | $lb/ft^3$ ($g/cm^3$) | 59.0 - 60.2 (0.945 - 0.965) | ASTM D1505 |
| Carbon Black | % | 1.5 - 2.0 | ASTM D4218 |
| Sheet Thickness | (mil) mm | 50 ±5% (1.25) | ASTM D3767 |
| Minimum ESCR[1] | Hr | 3000 | ASTM D1693 |
| Seam Peel Strength | lb (N) | 450 (2000) | USACOE Tech Report GL-86-19, Appendix A |
| Cell Area (Maximum) | $in^2$ ($cm^2$) | 44.8 (289)<br>71.3 (460)<br>187.0 (1206) | Load Support and Severe Slope Protection Applications<br>Load Support, Slope and Channel Protection, Earth Retention Applications<br>Channel Protection and Earth Retention Applications |
| Seam Hang Strength-Test | A 4" (102 mm) wide seam sample shall support a 160 lb (72.5 kg) load for 7 days minimum in a temperature controlled environment undergoing a temperature change on a 1 hour cycle from ambient[2] room to 130°F (54°C). | | |
| Alternative Seam Hang Strength-Test | A 4" (102 mm) wide seam sample shall support a 160 lb (72.5 kg) load for 30 days minimum in an ambient[2] room temperature environment. | | |
| [1] ESCR - Environmental Stress Crack Resistance<br>[2] Ambient room temperature is 74°F ±4° (23°C ±2°) | | | |

- the use of geocell confinement reduced the vertical settlement, although it was not as significant as expected. This is likely due to the large stresses transferred to the subgrade, with or without the geocell. The geocell, however, did assist in redistributing the stresses more evenly, possibly preventing development of high shear strains and failure, especially upon softer subgrades. Upon stiffer foundations, the geocell prevents vertical settlement by reducing lateral squeeze of the ballast due to high loading.

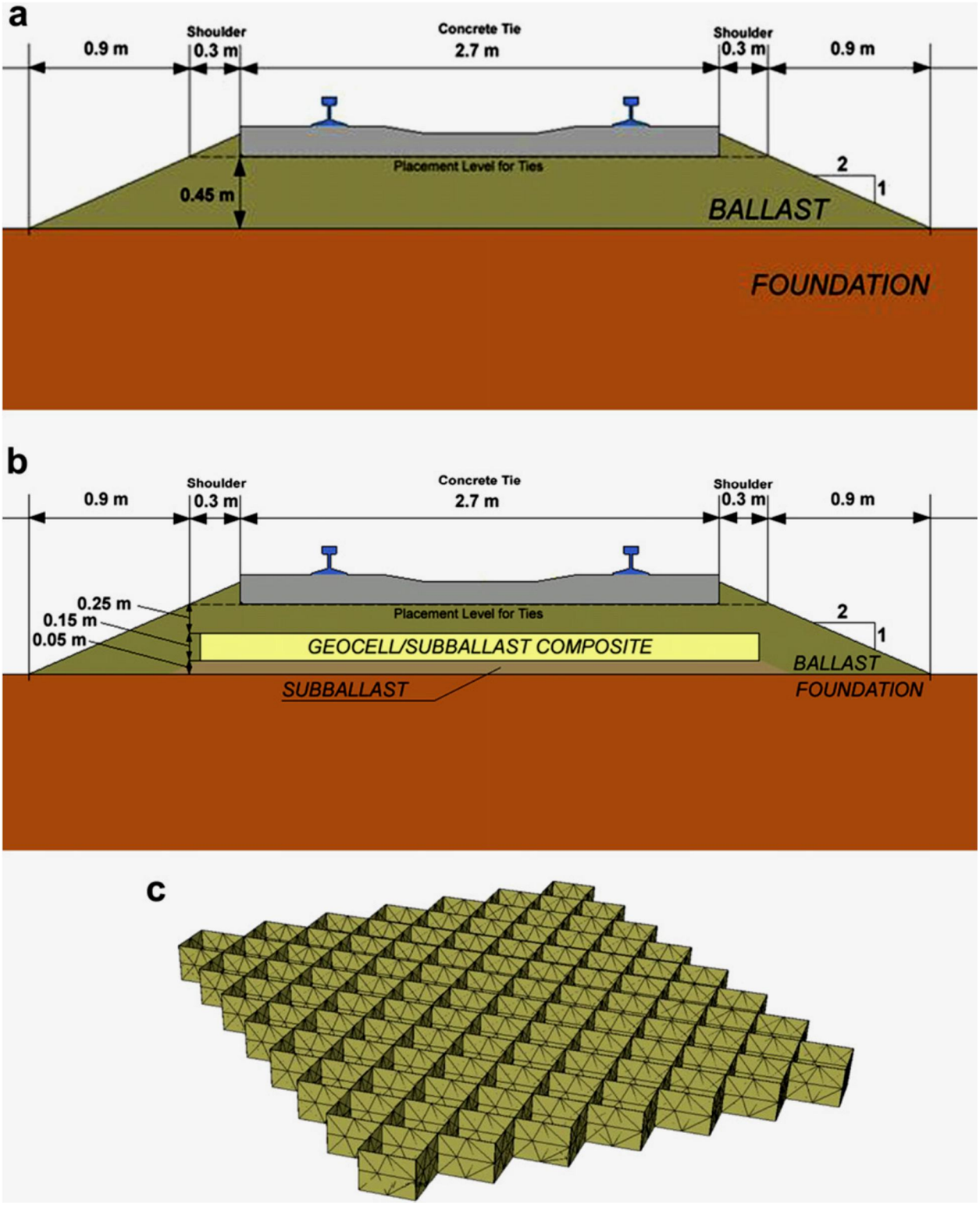


Figure 2.12: Railway geometry with absence of gravel. b. Railway geometry with geocell confinement. c. Mesh of embedded geocell [13]

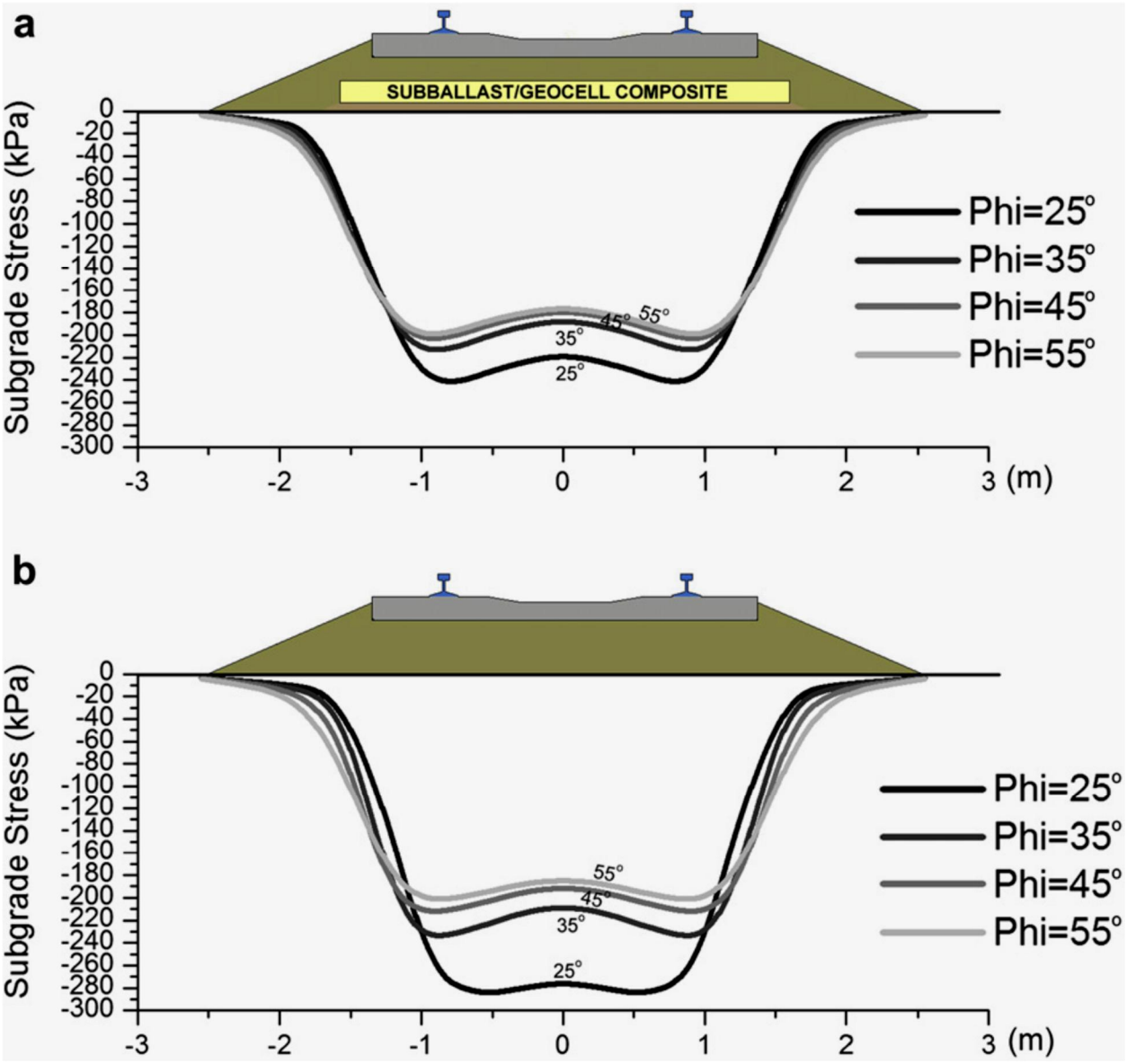


Figure 2.13: a. Subgrade stress distribution below geocell-reinforced embankment. b. Subgrade stress distribution below unreinforced embankment [13].

- lateral spreading along the slope of the railroad substructure was greatly reduced with application of confinement to the ballast. The prevention of lateral spreading is especially pronounced when the railroad substructure overlies softer subgrades and when weaker ballast materials are used. This was demonstrated by the significant reduction in horizontal displacements along the slope of the ballasted foundation, especially at or below the level of the confined layer. The use of the geocell confinement likely

contributes resistance to spreading above the reinforcement through frictional resistance of the composite mattress.

- The geocell allowed for a more uniform subgrade stress distribution. In addition to being more uniform, the magnitudes of stresses were reduced significantly in addition to distribution of stresses to a wider area, in turn, mobilizing more of the subgrade's shear strength and preventing shear failure. Not only did use of geocell distribute the stress more evenly; it reduced the magnitude of the subgrade stresses when placed over a very compressible foundation or in an embankment consisting of weak ballast.

- When using materials commonly used as geosynthetic reinforcements for geocell, the benefit of using superior geocell polymers in comparison to lower stiffness ones is not exceptionally pronounced, likely because the reinforcement material is still orders of magnitude stiffer than the ballast surrounding it.

### 2.5.2. Ballast and Geogrid

Geogrid is defined as a geosynthetic formed by a regular network of tensile elements with apertures of sufficient size to allow strike-through of surrounding soil, rock or other geotechnical materials. Geogrids are principally used for reinforcement purposes, but under some circumstances, they can also help to provide effective separation between two soil or granular fill layers [3].

a. Significance and Use

Significant performance benefits have been documented when geogrids are included within the ballast or subballast layers of a roadbed section. The effects of the reinforcement are particularly apparent where the roadbed is placed on soft or medium strength subgrades.

The reinforcement mechanism, often termed "mechanical stabilization", occurs when larger aggregate particles partially penetrate and interlock within the apertures of the geogrid. Subsequent compaction results in the aggregate and geogrid being "interlocked"; forming a semi rigid mat that helps to distribute train loads and thereby reducing stresses on the subgrade.

Some of the documented benefits in the use of geogrid reinforcement within the roadbed section include the following [3]:

- Increased ballast life (life cycle cost savings)
- Reduced roadbed thickness (initial cost savings)
- Reduced track deflection resulting in less wear and tear of the mechanical components of the rail track
- Maintenance of good drainage within the roadbed section
- Smoother transitions between areas with differing subgrade strengths

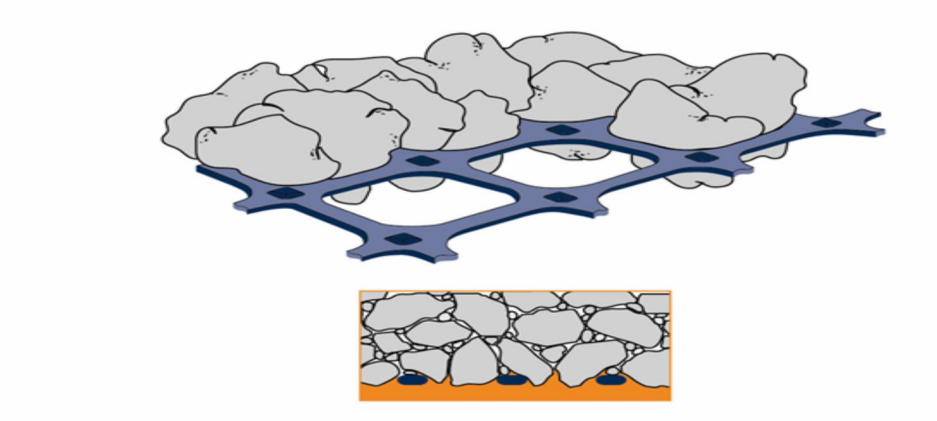

Figure 2.14: The Mechanism of Interlock [3]

b. Application Locations

Geogrids tend to be used in one or both of two main locations within the roadbed section [3]:

a. At the bottom of, or within the ballast (Figure 2.15) this provides direct ballast reinforcement and thereby reduces the rate of track settlement; it therefore increases the length of the maintenance cycle. This approach is generally favored when the roadbed is founded on a relatively firm subgrade.

b. At the bottom of the sub-ballast, directly on the existing or prepared subgrade (Figure 16) this is done in order to increase the bearing capacity of the track foundation. This approach is generally favored when the roadbed is founded on a relatively soft subgrade.

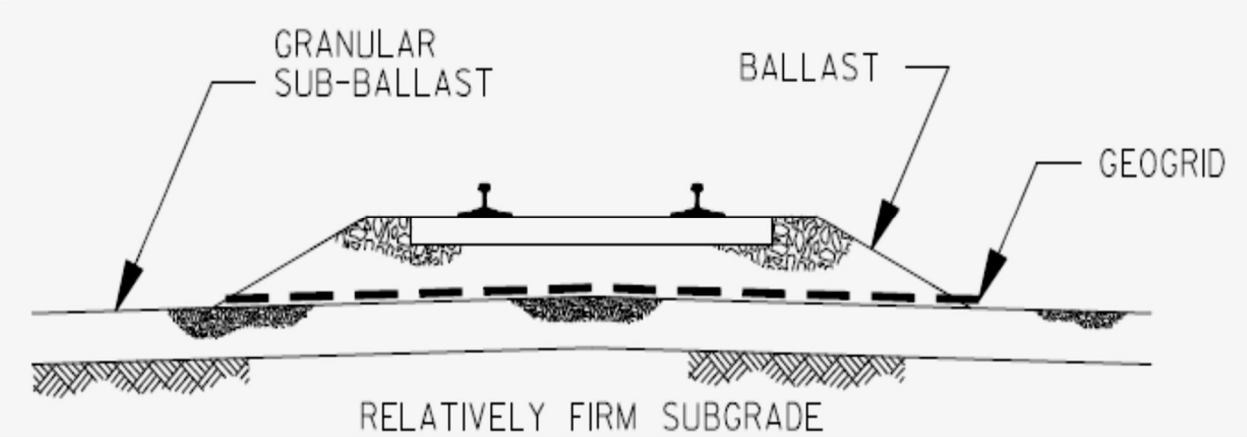


Figure 2.15: Geogrids at the bottom of, or within the ballast [3]

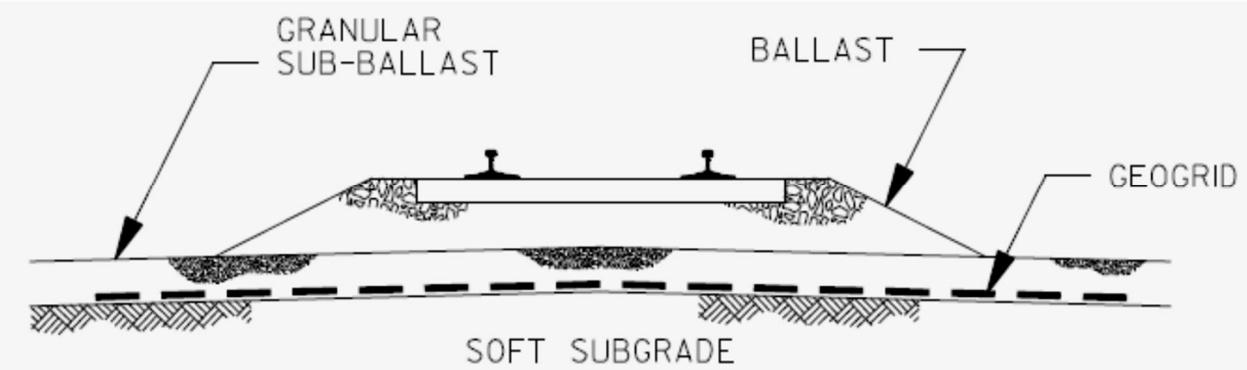


Figure 2.16: Geogrids at the bottom of the sub-ballast, directly on the existing or prepared subgrade [3]

c. Material Requirements

In order for a geogrid to perform effectively as a reinforcement layer, it is necessary that it be able to effectively transfer load through interaction with the surrounding aggregate. The material properties shown in Table 2.8 are recommended for geogrids used in ballast and sub-ballast reinforcement applications [3]:

Table 2.8: Physical Properties for Geogrids used in Track Stabilization [3]

| Property | Test Method | Units | Minimum Value (Sub-ballast reinforcement) | Minimum Value (Ballast reinforcement) |
|---|---|---|---|---|
| Aperture size (min. - max.) | Direct measurement | Inches (mm) | 0.70 - 1.60 (17.8 - 40.6) | 1.70 - 2.50 (43.2 x 63.5) |
| Open area | Direct measurement | % | 70 | 75 |
| Rib thickness | ASTM D1777 | Inches (mm) | 0.05 (1.27) | 0.05 (1.27) |
| Junction thickness | ASTM D1777 | Inches (mm) | 0.16 (4.0) | 0.17 (4.4) |
| Aperture stability modulus @ 20cm-kg | US Army Corps of Engineers 62 | lb-ft/deg (kg-cm/deg) | 0.470 (6.5) | 0.419 (5.8) |
| Flexural rigidity (Machine direction) | ASTM D1388 | (lb-ft) (mg-cm) | 0.0542 (750,000) | 0.0325 (450,000) |
| Tensile modulus @ 2% strain (machine x cross machine direction) | ASTM D6637-01 | lb/ft (kN/m) | 18,500 x 30,000 (270 x 437) | 19,000 x 32,500 (277 x 474) |
| Junction strength | GRI GG2-87 | lb/ft (kN/m) | 1080 (15.7) | 956 (13.9) |
| Junction efficiency | GRI GG2-87 | % | 90 | 90 |
| Carbon black | ASTM 4218 | % | 0.5 | 0.5 |

The application of geogrids to prevent the track deterioration has grown rapidly in the last few decades. The track deterioration is different from global failure of structures like landslides, because it is an accumulation of plastic deformations either in the ballast layer or in the subgrade layer. The deterioration especially in soft subgrade layer has serious influence on the safety and efficiency (speed restriction) of train operations. Many expensive, disruptive and frequent repair operations are often required to maintain the ballast characteristics due to the problem of settlement. Because of this, the use of geogrids has proved to be a simple and economical method of reinforcing track ballast. It provides an extremely cost-effective solution for the reinforcement of ballast over a soft subgrade [7].

d. Reinforcing principle

Several authors have studied the reinforcement mechanisms associated with the interaction of geogrids and unbound aggregate. Perkins (1999), it suggested that there are four separate

reinforcement mechanisms. These reinforcement mechanisms are shown in Figure 2.17 and are described below [14]:

- Confinement of the aggregate by the geogrid results in a reduction in the amount of lateral spreading.
- Confinement results in an increase in the lateral stress within the aggregate, thereby increasing its stiffness. This reduces the dynamic (recoverable) deformation for each load cycle.
- An increased modulus of the aggregate, results in an improved vertical stress distribution onto the underlying subgrade. The effect is that the surface deformation will be less and more uniform.
- A reduction in the shear stress within the subgrade leading to lower vertical strain.

It is widely agreed that an appropriate stiffness and an ability to interlock effectively with the material is vital to achieve the reinforcing effect of a polymer geogrid. The geogrid works on the premise that the ballast penetrates the apertures and interlocks with the grid. This interlock leads to a strong horizontal shear resistance and restrains the ballast from lateral movement even when dynamic loading is applied. In practice this means that the settlement rate is reduced.

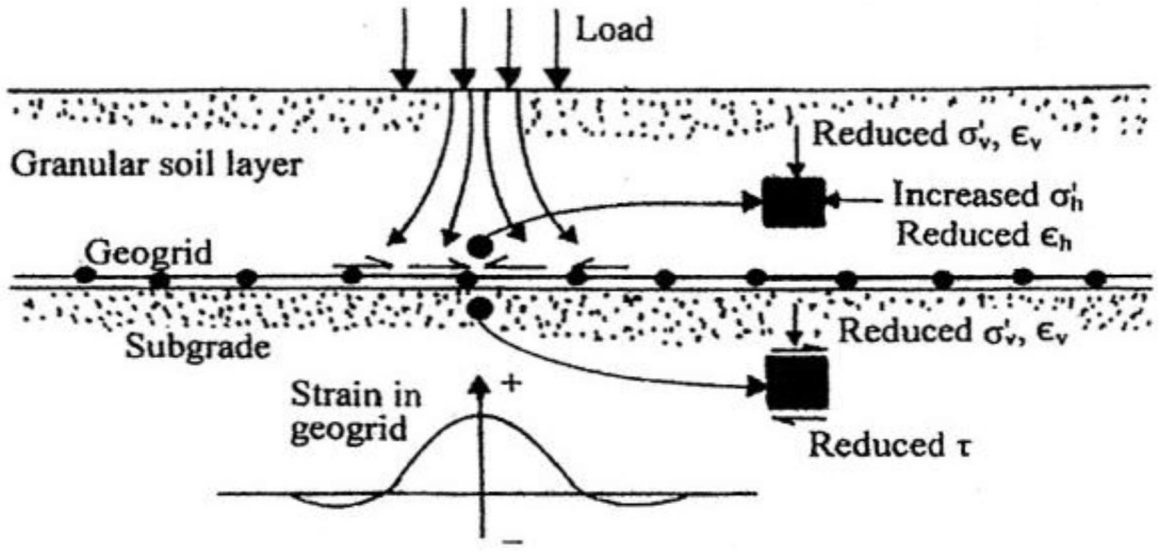


Figure 2.17: Reinforcing effect of geogrid [14]

An important factor to consider is the placement and installation of the geogrid. If this is not done according to required standards it could lead to rapid initial settlement until adequate interlock is achieved. Generally, there are two major application areas for the use of geogrids within the track substructure. Geogrid can be used to reduce the rate of track settlement and hence extend the maintenance cycle frequency with huge whole life cost benefits. Also geogrid can be used in the sub-ballast layer to increase the bearing capacity especially over soft subgrade, with significant thickness reductions and savings in both the capital and environmental costs [1].

[14] Reported results from a large-scale model test program comprising a single tie/ballast system constructed over an artificial subgrade with variable. The tie (width 250 mm x 150 mm deep) was laid on a ballast layer having a thickness of 450 mm. A biaxial geogrid was used for reinforcement of the ballast. The depth of reinforcement below the tie ($D_r$) ranged from 50 mm to 200 mm. Cyclic loads (peak load of 85 kN per rail tie) with frequencies varying from 0.5 to 3 Hz were applied to the tie. This provided a bearing pressure of 370 $kN/m^2$ which represents a typical magnitude of dynamic load felt by ballasts directly beneath the tie for track modulus between 14 and 84 MN/m/m of rail.

According to [14], Tests were subjected to a maximum number of load repetitions that were equivalent to 2 to 20 million cumulative axle tones in track. Figures 2.18 and 2.19 show the variation of permanent deformation with cumulative axle tones, respectively, for rigid subgrade support (CBR = $\infty$), flexible subgrade support (CBR = 39), and very flexible subgrade support (CBR = 1). It is obvious from these figures that the inclusion of geogrid in the ballast layer reduces the permanent deformation for any given cumulative axle tones. However, the effect becomes progressively pronounced with the decrease in CBR of the subgrade. This fact is also clearly demonstrated in Figure 2.20, which is for $D_r$ = 100 mm.

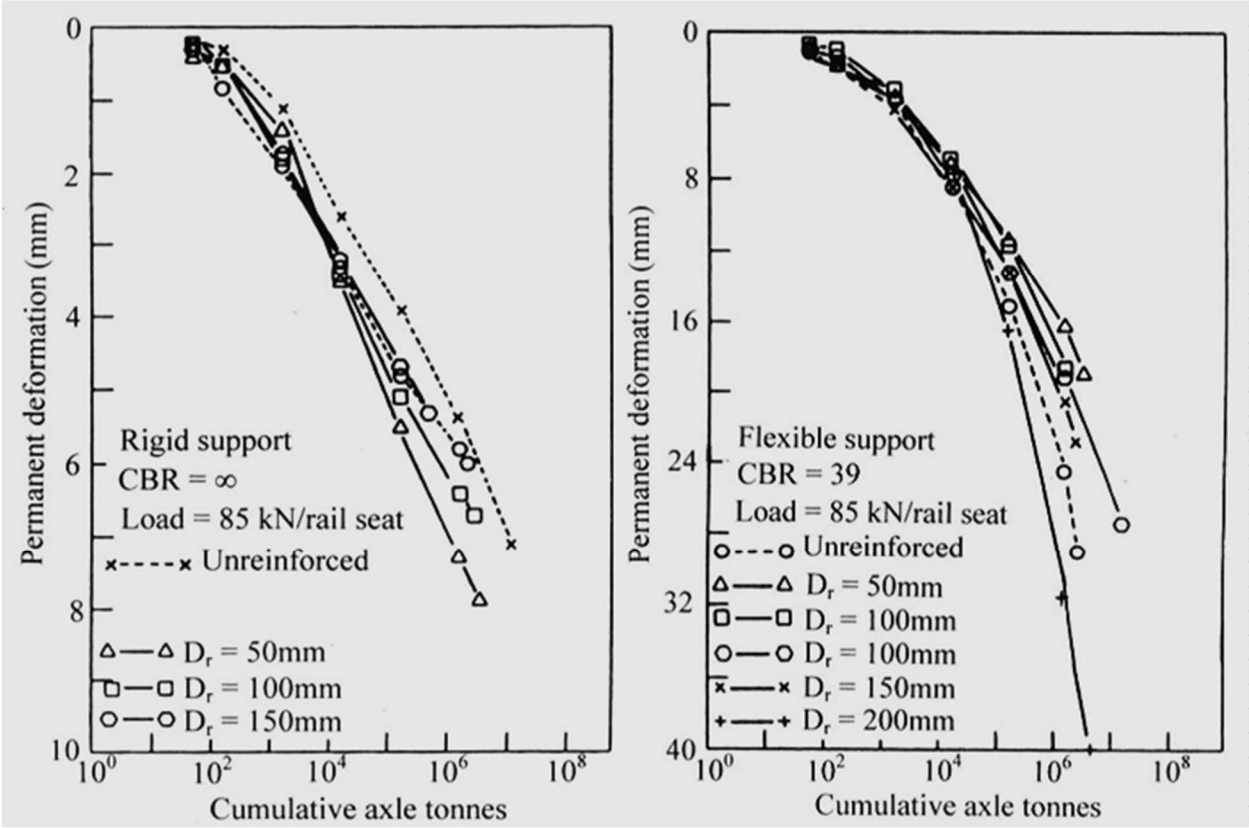


Figure 2.18: Variation of permanent deflection with commutative axle tonnes for CBR=∞ and CBR=39.[14]

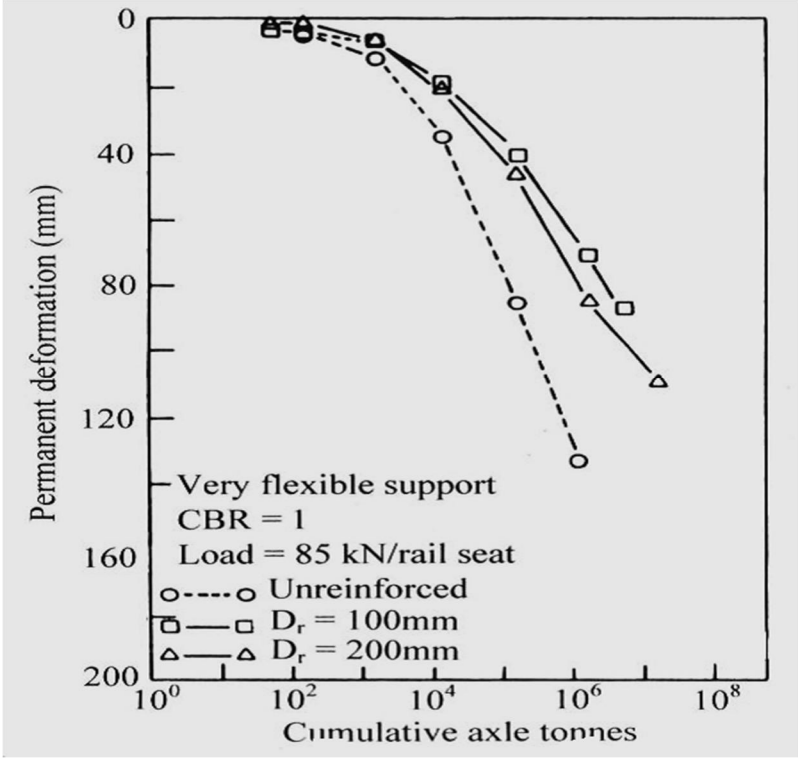


Figure 2.19: Variation of permanent deflection with cumulative axle tonnes for CBR=1[14]

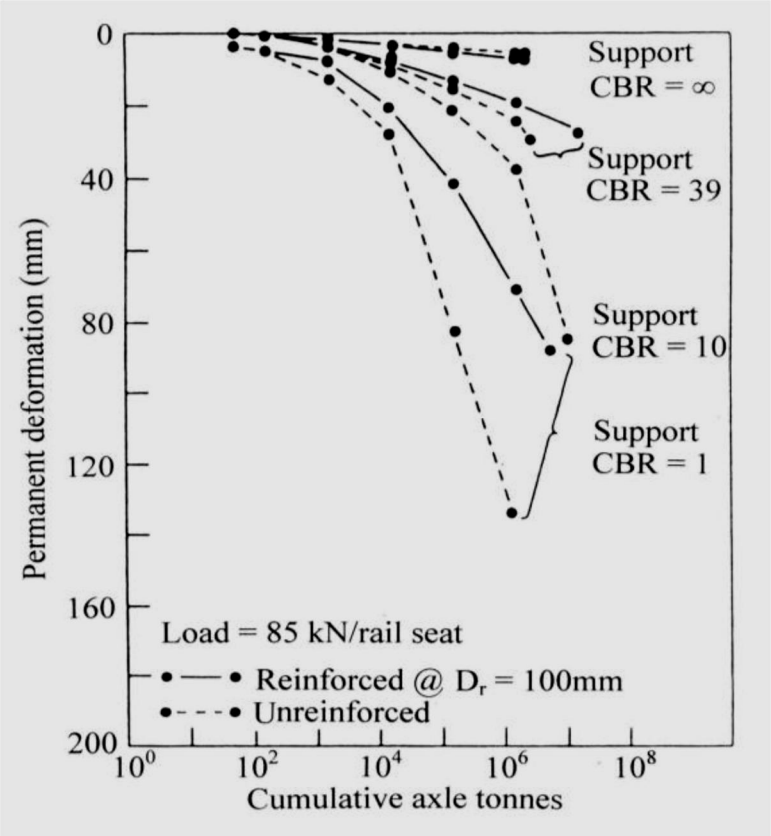


Figure 2.20: Variation of permanent deflection with cumulative axle tonnes for $D_r$ = 100 mm [14]

According to [14], the transfer to stress is a function of the location of the geogrid in relation to the bottom of the tie. Based on the plots shown above it appears that the optimum value of $D_r$ varies between 50 to 100 mm. However this depth may be unsatisfactory from practical considerations, that is, construction and maintenance. Hence, a value of $D_r \approx 200$ mm is probably more acceptable.

## 2.6. Summary

Track deterioration has a serious influence on the safety and efficiency (speed restriction) of train operations. Many expensive, disruptive and frequent repair operations are often required to maintain the ballast characteristics due to the problem of settlement. Because of this, a geosynthetic (geogrid/geocell) solution that has proved to be a simple and economical method of reinforcing track ballast is widely used.

The literature review presented in this chapter provided understanding and appreciation of how a conventional rail track functions with added focus on the ballast material. The ballast specifications and its typical characteristics were discussed.

The review also indicated good understanding on the subject regarding track component and track forces, the behavior of ballast (effect of particle shape, ballast gradation and the resilient behavior of granular materials and permanent strain behavior), Effect of stress, stress history and number of load cycles were among others reported to affect the behavior of granular material.

This literature also covers in depth ballast degradation, the process of ballast degradation, the influence of ballast degradation on the performance of track operation the driving forces of ballast gradation, ballast settlement, phases of ballast settlement and define ballast fouling, the mechanisms of ballast fouling and effect of ballast fouling on the performance of the rail track.

The functions of geosynthetics namely geocells and geogrids were discussed, their material characteristics and requirements, significance and use, application location and reinforcement principles are reviewed.

The remainder of this thesis will examine and discuss the result of the analysis and modeling of railway ballast reinforced with geogrid and geocell with the aid of FEA package ANSYS.

# CHAPTER THREE

# 3. FINITE ELEMENT MODELING AND ANALYSIS

## 3.1. Introduction

This chapter deals with modeling of the 3D geometry of the track unreinforced, reinforced with geocell and geogrid, selection of the material properties, loading of the track and Finite Element Analysis (FEA). A brief summary of the routines that have been used are presented.

The finite element method (FEM) is the dominant discretization technique in structural mechanics. The basic concept in the physical interpretation of FEM is the subdivision of the mathematical model into disjoint (non-overlapping) components of simple geometry called finite elements. The response of each element is expressed in terms of a finite number of degree of freedom characterized as the value of unknowns functions at a set of nodal points.

For the purpose of this thesis two commercial software have been used, SolidWorks and a finite element method (FEM) software *ANSYS*.

SolidWorks: is 3D solid modeling CAD (computer-aided design) software used to model any type of solid objects.

ANSYS: general multi-purpose software, used to simulate interactions of all disciplines of physics, structural, vibration, fluid dynamics, heat transfer and electromagnetic for engineers. ANSYS enables to simulate tests or working conditions, enables to test in virtual environment before manufacturing prototypes of products and uses FEM principles.

A preliminary analysis based on has been performed aiming to determine the input variables for the FEA.

The analysis includes:

- General project description under consideration
- Determination of the loading
- Beam on Elastic Foundation Analysis

- Rail stress analysis
- Sleeper stress analysis
- Ballast stress analysis, depth and gradation determination and
- Determination of the dimension of track geometry

Behavior or parameters observed during the numerical simulation includes vertical displacement (track settlement), subgrade vertical stress, subgrade stress and strain and lateral displacement. Comparison between railroad ballast reinforced with geocell and geogrid and that of unreinforced have been made.

## 3.2. Preliminary Analysis

### 3.2.1. Project Description

The Addis Ababa/Sebeta – Port of Djibouti railway line starts at the highlands of Ethiopia and traverses along the rift valley and terminates in the low lands of Djibouti. The land form and terrain condition varies from highland and plateau in Ethiopian to desert plain land in Djibouti. Except in a few undulating sections, most of the railway line can be considered flat terrain with acceptable altitude difference [17].

The strata along the railway line are largely covered with tertiary-quaternary basalt, trachyte, tuff, volcanic lava and Mesozoic sedimentary rocks and Paleozoic substratum are sparsely exposed. Covering soils are mainly hard plastic-like black cotton soil, silty clay, mollisol and soft soil with large thickness difference [17].

The railway line is to be built in areas of highland terrace, shallow hill and plain, with wide terrain and small undulating in some sections. There is basically no natural disaster and major unfavorable geological features such as landslide, collapse, debris flow, coal bed and gob along the whole line. Main engineering geological problems are seismic faults, expansive soils, loose rock and bedrock soft interlayer, unstable slope and soft soil [17]

i. Rolling Stocks Specifications [16]:

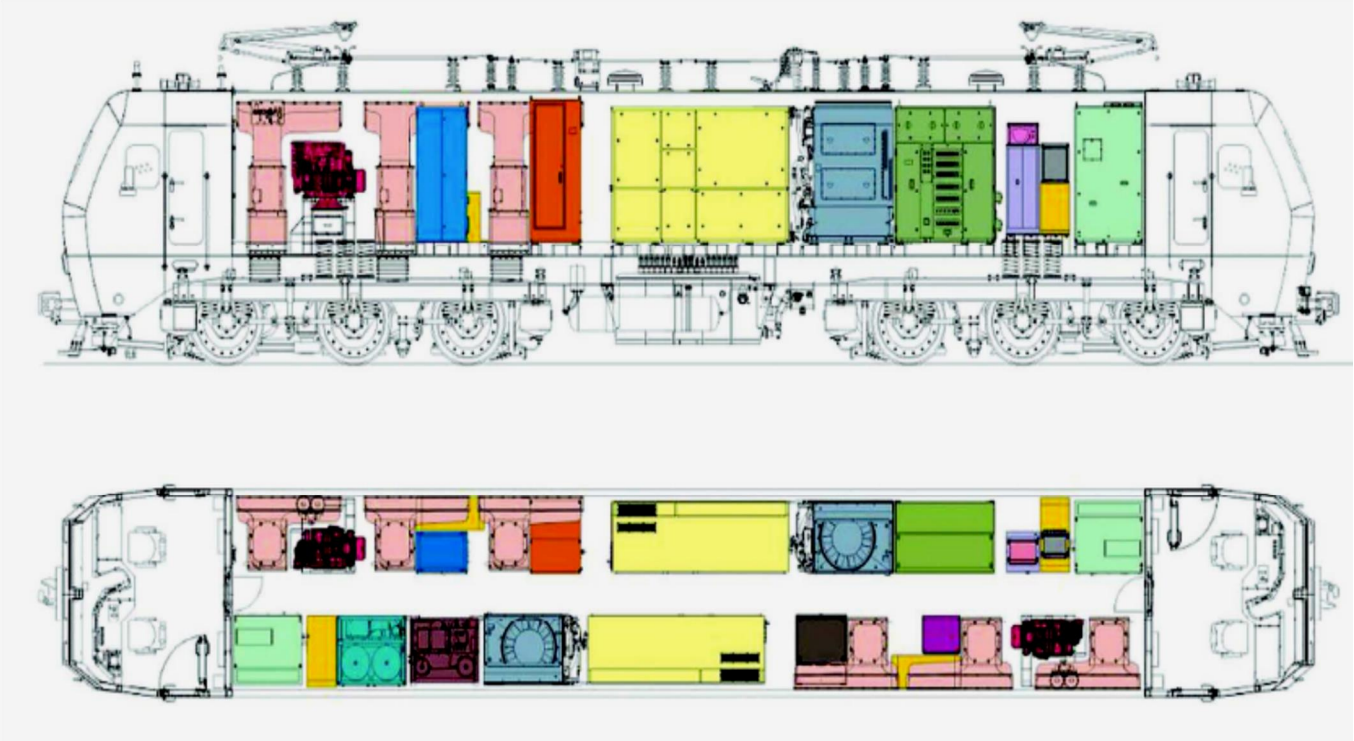

Figure 3.1: HXD1C High Power AC Drive Six-Axle (7200kw) Freight Electric Locomotive [16]

| | |
|---|---|
| Axle type | CO-CO |
| Locomotive total weight in working order | 150(+3)% t(25t axle load)<br>138(-1))% t(23t axle load) |
| Wheel rim power | 7200kw |
| Startup traction effort | 570kN(25t axle load)<br>520kN(23t axle load) |
| Continuous traction effort | 400kN(25t axle load)<br>370kN(23t axle load) |
| Continuous speed | 65 km/h(25t axle load)<br>70 km/h(23t axle load) |
| Max. electric braking effort | 400kN(25t axle load)<br>370kN(23t axle load) |

ii. Key Parameters and Dimensions [16]:

| | |
|---|---|
| Loading Capacity | 70t |
| Dead weight | ≤25t |
| Design Speed | 120km/h |

iii. Technical parameters of the bogie [16]:

| | |
|---|---|
| Fixed Wheel Base | 1830mm |
| Wheel Diameter | 840mm |
| Railway Gauge | 1435mm |
| Axle Load | 25t |
| Design speed | 120km/h |

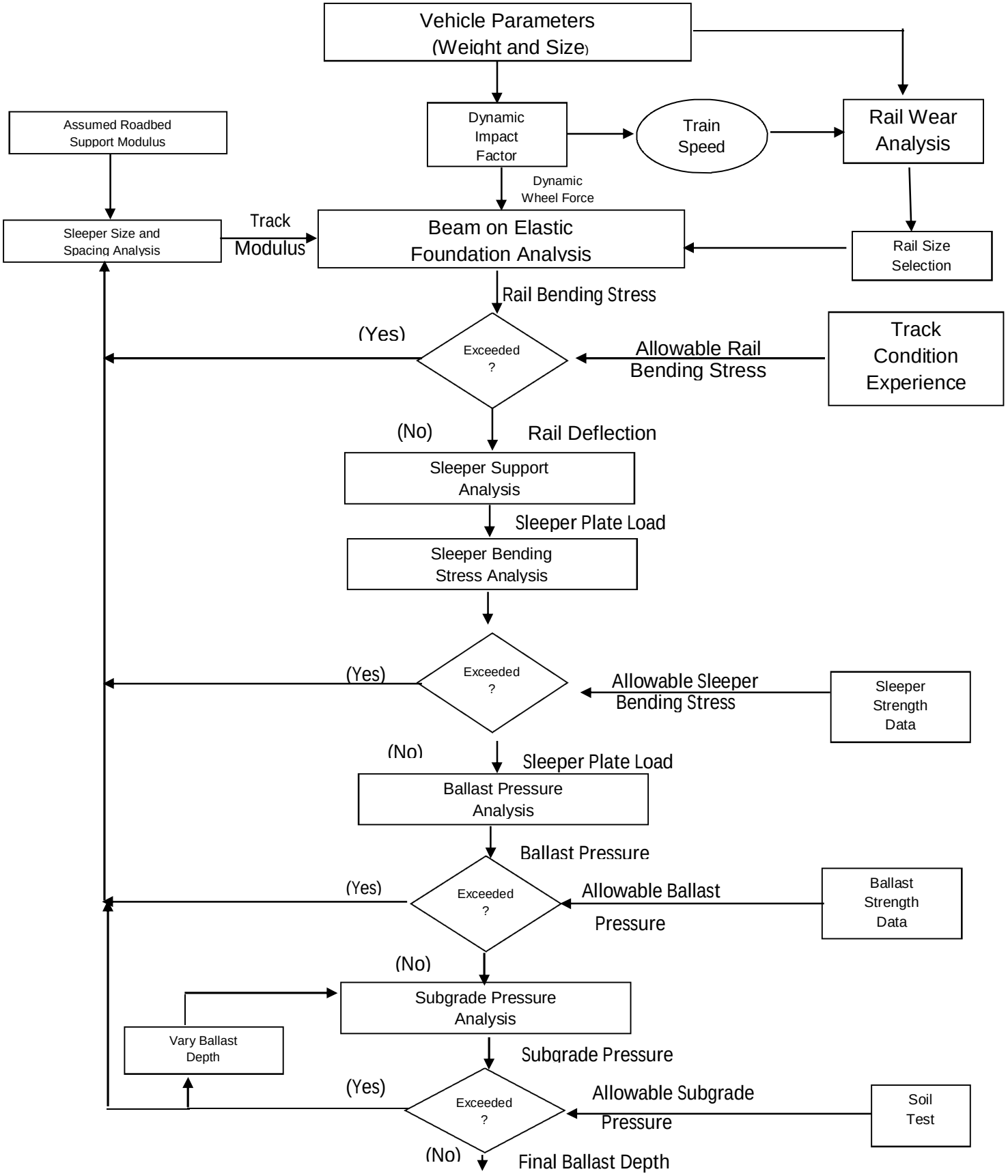


Figure 3.2: Flow chart for conventional ballasted track structure design [15]

### 3.2.2. Loading

Adopting the flow chart for conventional ballasted track structure design (figure 3.2)

Design Wheel Load

$$P^D = \emptyset P_S \qquad (3.1)$$

Where $P^D = design\ wheel\ load\ (kN)$

$P_S = static\ wheel\ load\ (kN)$

$\emptyset = dimesionless\ impact\ factor\ (> 1)$

This factor is a percentage increase over static vertical loads intended to estimate the dynamic effect of wheel and rail irregularities and is given as:

$$\emptyset = 1 + 5.21\frac{V}{D} \qquad \text{AREMA 2.11.2.2}$$

Where V= Design Speed (km/h)

D=Wheel Diameter (mm)

Hence

$$P_S = \frac{axle\ load}{2} = \frac{(25ton)(1000kg)(9.81m/s2)}{2} = 122.5kN$$

$$\emptyset = 1 + 5.21\frac{120km/h}{840} = 1.74$$

Design Wheel Load, $P^D = 1.74x122.5 = 213.5kN$

### 3.2.3. Beam on Elastic Foundation Rail Analysis

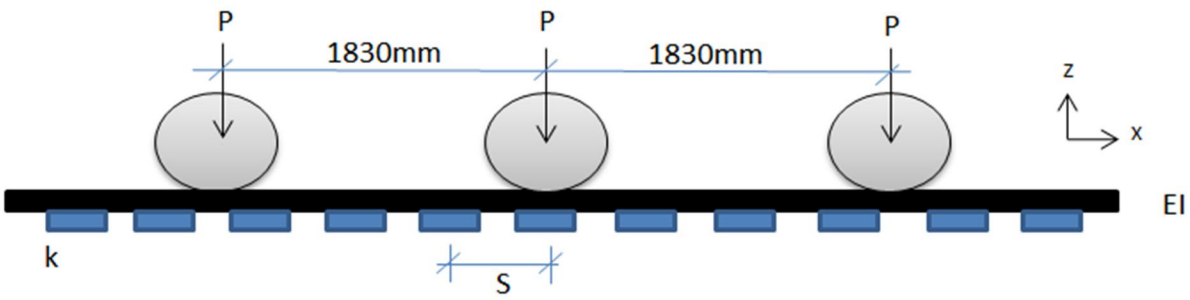

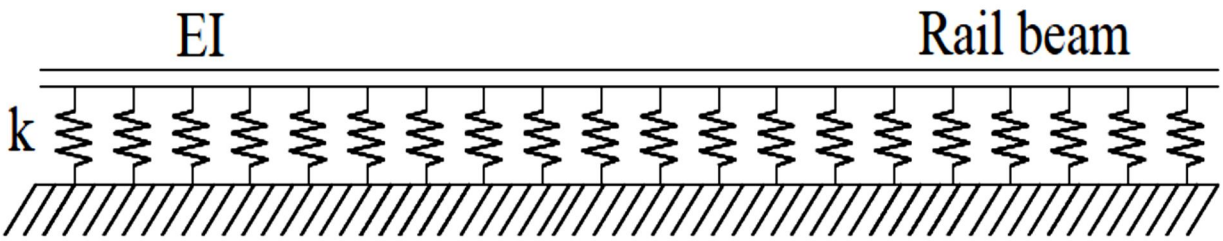


Figure 3.3: Schematic representation of beam on elastic foundation model of three axle bogie

- Rail profile selection

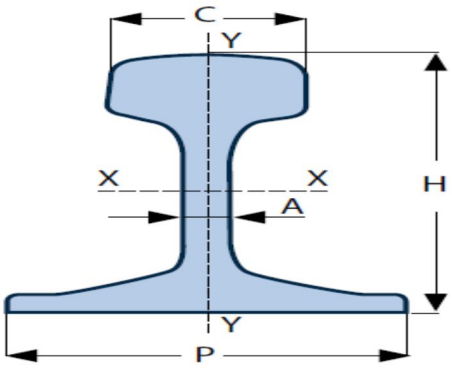


Adopting rail section of UIC54 continuously welded rail with the following section properties [18]:

Table 3.1: Adopted rail profile section properties

| Rail profile | UIC54 |
|---|---|
| Section weight Kg/m | 54.77 |
| Rail height mm (H) | 159.00 |
| Head width mm (C) | 70.00 |
| Web thickness mm (A) | 16.00 |
| Foot width mm (P) | 140.00 |
| Moment of inertia Ixx $cm^4$ | 2337.90 |
| Moment of inertia Iyy $cm^4$ | 419.20 |
| Section modulus of the head $mm^3$ | 278752.83 |
| Section modulus of the base $mm^3$ | 311180.62 |

For a single wheel load the corresponding equation for the calculation of rail bending moment and rail deflection are:

$$M(x) = \frac{P}{4\beta} e^{-\beta x}(\cos \beta x - \sin \beta x) \qquad y(x) = \frac{P\beta}{2k} e^{-\beta x}(\cos \beta x + \sin \beta x) \tag{3.2}$$

Where $P = design\ wheel\ load\ (kN)$

$k = track\ modulus\ (MPa)$

$\beta = characterstics\ length\ (mm^{-1})$

The characteristics length β is given by:

$$\beta = \sqrt[4]{\frac{k}{4EI}} \tag{3.3}$$

- Track modulus

Vertical track stiffness or vertical track modulus, k, represents the vertical response of the entire track system below the base of the rail including cross ties, fasteners, tie pads, ballast, and subgrade. Each of these components contributes to the overall track modulus, and it is important to utilize appropriate track components to maintain uniform stiffness while traversing all subgrades and structures.

The modulus of elasticity of rail support defined within the "beam on elastic foundation" theory. The track modulus is the load which causes unit vertical deflection in unit length of the rail.

For sleeper spacing of $S = 600mm$ and sleeper type-II, PRC Standard recommends the stiffness of rail support $D = 27.2kN/mm$

The track modulus $k$ is calculated as:

$$k = \frac{D}{S} = 45.33MPa$$

Thus

$$\beta = \sqrt[4]{\frac{45.33}{4*210000*2337.9}} = 0.0012mm^{-1}$$

But for this case the bogie has three axles as it can be seen in figure 3.1.hence the above equations are rewritten as:

$$M(x) = \frac{1}{4\beta}\sum P_i e^{-\beta x_i}\left(\cos \beta x_i - \sin \beta x_i\right)$$

$$y(x) = \frac{\beta}{2k}\sum P_i e^{-\beta x_i}\left(\cos \beta x_i + \sin \beta x_i\right)$$

Where $P_i = design\ wheel\ load\ (kN)$

$k = track\ modulus\ (MPa)$

$x = distance\ from\ the\ reference\ wheel\ (mm)$

The Max Moment occurs beneath the end wheels but Max Deflection occurs beneath the end wheels.

Thus

$$M_{max} = 37.36\ kNm$$

$$Y_{max} = 3.00\ mm$$

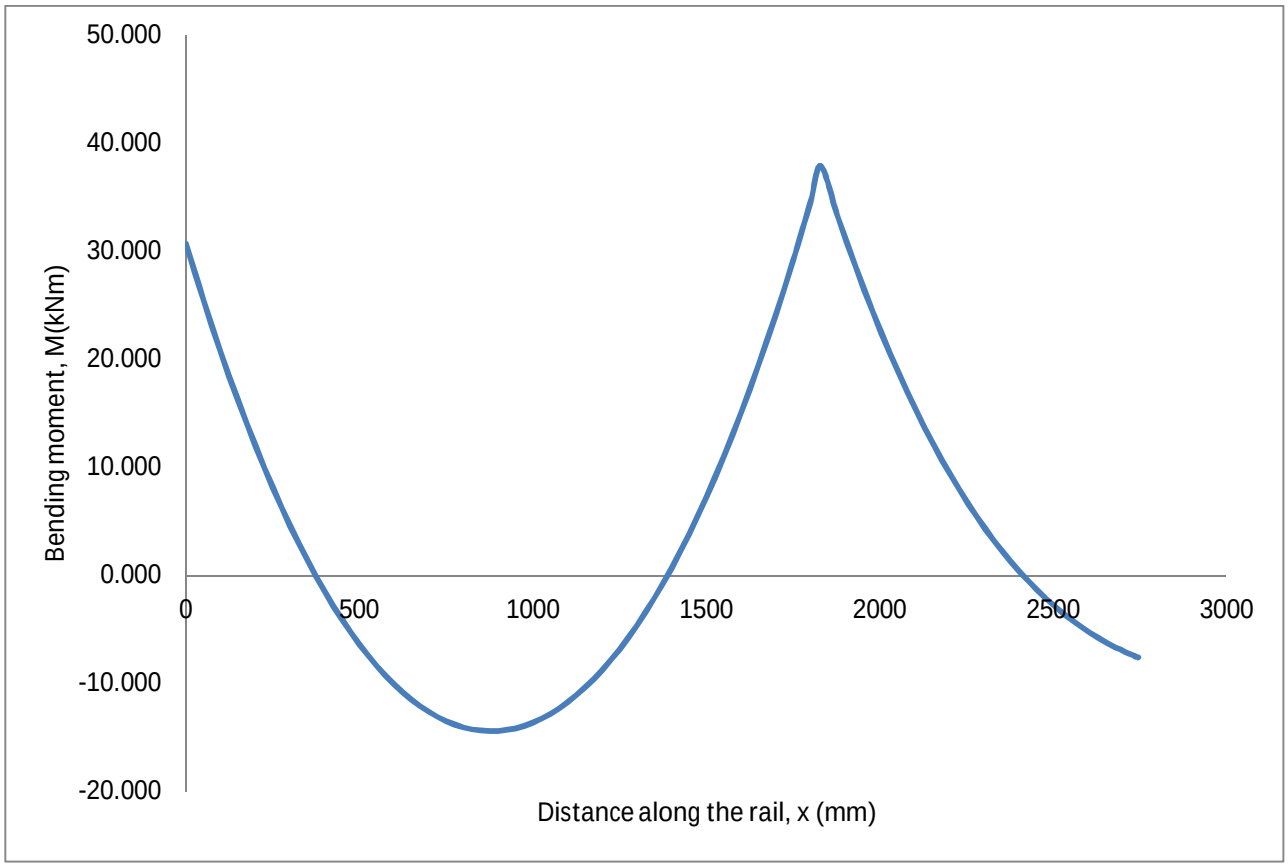


Figure 3.4: Bending moment diagram of beam on elastic foundation model

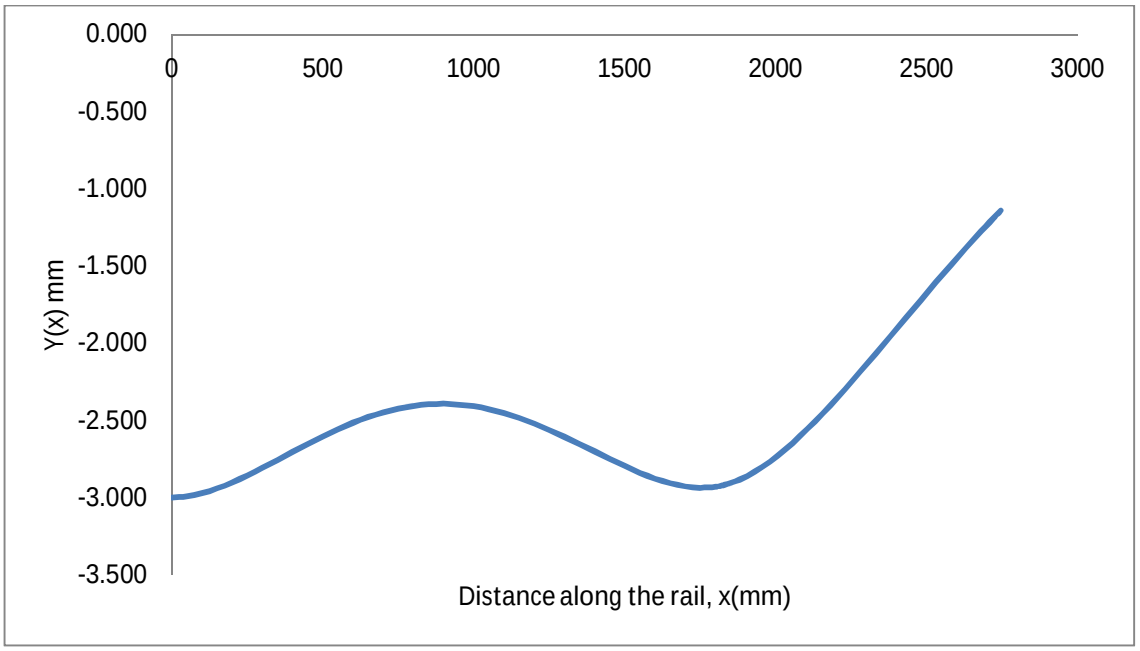


Figure 3.5: Deflection diagram of beam on elastic foundation model

i. Rail Bending Stress

The maximum rail stress at the center of the rail base $\sigma_b$ $(MPa)$ is readily calculated using simple applied mechanics, and can be stated as:

$$\sigma_b = \frac{M_m \cdot 10^6}{Z_b} \quad (3.4)$$

Where $M_m = maximum\ rail\ bending\ moment\ (kNm)$

$Z_b = section\ modulus\ of\ the\ rail\ relative\ to\ the\ rail\ base\ (mm^3)$

Thus $\sigma_b = \frac{37.36 * 10^6}{311180.62} =$ 120.06MPa

- Allowable Bending Stress in the Rail

The Association of American Railroads recommends that acceptable rail stress for continuous welded rail be established as:

$$\sigma_{all} = \frac{\sigma_y - \sigma_t}{(1 + A)(1 + B)(1 + C)(1 + D)}$$

| Reduction Factor | Severity Assumption |
|---|---|
| A, Lateral Bending | 20% |
| B, Track Condition | 25% |
| C, Rail Wear Corrosion | 15% |
| D, Unbalanced Elevation | 15% |
| $\sigma_t$, Temperature stress | 20,000 psi (138MPa) |

Table 3.2: Acceptable Rail Stress for Continuous Welded Rail (adopted from AREMA)

$\sigma_y = 74\ ksi\ (510\ MPa)$ AREMA table 4-2-1-4-1c

Thus,

$$\sigma_{all} = \frac{510 - 138}{(1 + 0.2)(1 + 0.25)(1 + 0.15)(1 + 0.15)} = 187.52\ MPa$$

$\sigma_b \ll \sigma_{all}$ $\ldots\ldots\ldots OK!$

ii. Wheel- Rail Contact Stress

Wheel-rail contact stresses mainly include rolling and shear stresses. The magnitude of these stresses is greatly dependent upon the geometry of ellipsoidal wheel-rail contact patch.

- rolling contact stress

Based on Hertz's theory, the following formula for the calculation of the mean value of the rolling contact stress is adopted:

$$\sigma_{mean} = \frac{P_s x 10^3}{2ax2b} \tag{3.5}$$

Where $P_s = vertical\ wheel\ load(kN)$

$2b = breadth\ of\ contact\ area\ (mm); Eisemann\ adopts\ the\ value\ of$

$2b = 12mm$

The contact length 2a (mm) is derived from Hertz's formula and can be calculated by

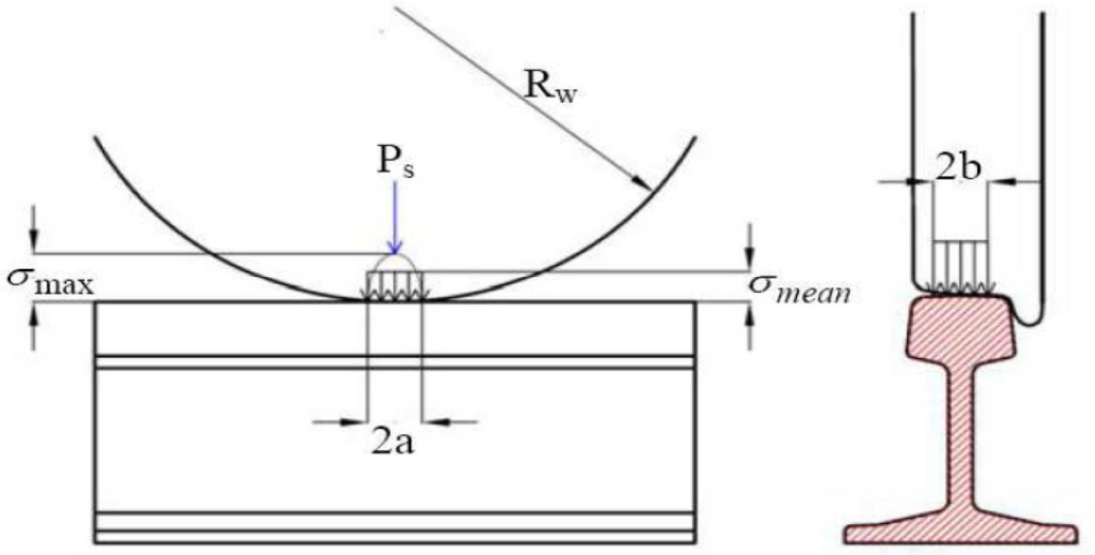


Figure 3.6: uniform distribution of wheel-rail contact stress

$$2a = 3.04x \left[\frac{P_s R_w x 10^3}{2b.E}\right]^{0.5} \tag{3.6}$$

Where $P_s = vertical\ wheel\ load(kN)$

$R_w = wheel\ radius\ (mm)$

E = youngs modulus of the rail steel (MPa)

Thus $2a = 3.04x\left[\frac{122.3x420x10^3}{12x210000}\right]^{0.5} = 13.72mm$

$$\sigma_{mean} = \frac{122.3x10^3}{13.72x12} = 743.55\ MPa$$

Considering required fatigue strength for rail steel, Eisenmann proposed the limit value for mean rolling contact stress as a percentage of the ultimate tensile strength of rail steel.

$$\sigma_{all} = 0.5\sigma_{ult}$$

$\sigma_{ult} \geq 1180\ MPa\ \ for\ standard\ high\ strength\ rail\ steel$ $\quad AREMA\ table$ 4-2-1-4-1c

Take $\sigma_{ult} = 1500MPa$

$$\sigma_{all} = 0.5x1500 = 750\ MPa > \sigma_{mean} = 743\ MPa \quad \ldots\ldots\ldots\ldots\ldots\ldots OK!$$

- Shear stress

Maximum shear stress value is simply interrelated to mean rolling contact stress values using the theory shear strain energy and is given by the following equation:

$$\tau_{max} = 0.3\sigma_{mean} \rightarrow \tau_{max} = 410\sqrt{\frac{P_S}{R_w}} \qquad (3.7)$$

Thus $\tau_{max} = 0.3x742.83 = 222.07\ MPa$

The subsequent criterion for the shear stress limit can be obtained as:

$$\tau_{all} = \frac{1}{\sqrt{3}}\sigma_{mean} \rightarrow \tau_{all} = 0.3\tau_{ult}$$

Thus

$$\tau_{all} = \frac{1}{\sqrt{3}} x742.83 = 429.29\ MPa > \tau_{max} = 222.80\ MPa \quad \ldots\ldots\ldots\ldots OK!$$

- Check the deflection

AREMA [10.2.2.4.] has proposed a limiting range for the magnitudes of vertical rail deflections. According to this recommendation, vertical rail deflections should be kept within the range of 3.175 to 6.35 millimeters.

$$3.175 < Y_{max} = 3.00\ mm < 6.35\ mm \quad \ldots\ldots\ldots\ldots\ldots\ldots\ldots\ldots\ldots\ldots\ldots\ldots OK!$$

- Rail Pad

The raid pad prevents rail-sleeper abrasion and the crushing of the sleeper under the rail foot. Rubber rail pads are normally designed to a specified load-deflection characteristic. The initial stiffness of the rail pad is designed to be low so that that their deformations under the springs toe loads is quite substantial. This ensures that the rail pad remains in intimate contact with the rail despite any vertical movements of the latter. When the wheel is over the pad, the latter's stiffness must be high to prevent large movements which can result in the metal spring becoming loose. Such a load-deflection characteristic can be obtained by introducing grooves in the rubber rail pads. Rubber pad or grooved rubber rail pad are made up of rubber or plastic to dampen the shocks of vibrations of a passing train.

AREMA recommendations: The fastening system and rail are assembled with a *5 mm* thick plain reference pad of HDPE or Rubber with a stiffness not less than 500 MN/m measured in accordance with EN 3146-4.complying with the following requirements:

- Minimize abrasion of the rail seat area, reduce impacts and vibration effects on the track structure and provide electrical insulation of the rail.

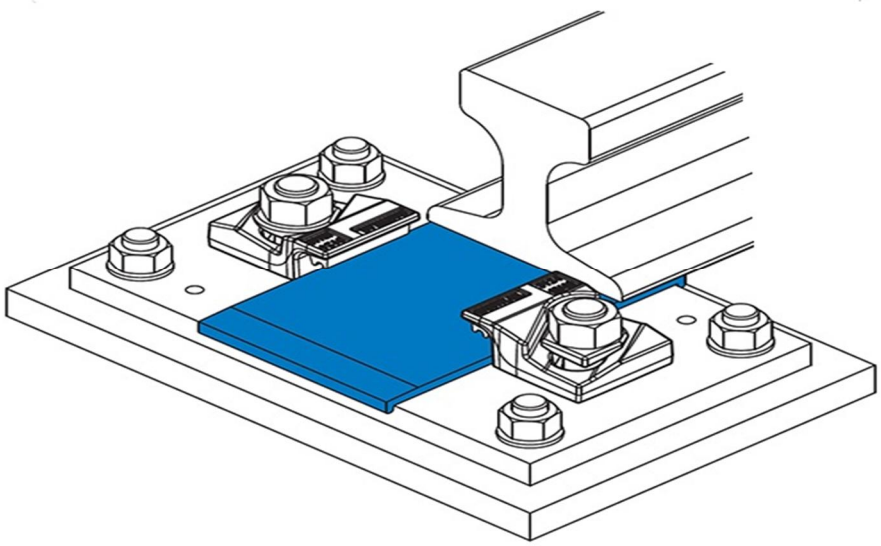

Figure 3.7: schematic of typical rail – fastening system

- Provide a positive means of preventing movement of the pad parallel to the rail and the pad with a width to extend around the shoulder to lock it in place.
- Manufactured from natural rubber or thermoplastics which provide the required chemical and physical properties to resist effects of temperature

### 3.2.4. Sleeper Stress Analysis

- Spacing

Tie spacing affects rail flexural stress, compressive stress on ballast and roadbed, lateral resistance of the track structure and the flexural stress in the ties themselves.

Sleeper spacing, $S = 600mm$[18]

- Concrete

Minimum 28 day design compressive strength of concrete is 7000psi (48MPa) reinforced with high tensile pre-stress wires [AREMA 4.2.2].

- Tie Dimensions and Weight

Weight: for ease of handling it is recommended that the weight of the tie not exceed approximately 800Ib (363 kg).

| | Min. Dimension (mm) | Max. Dimension (mm) |
|---|---|---|
| Length | 2440 | 2740 |
| Width<br>*top*<br>*bottom* | <br>150<br>200 | 330 |
| Depth | 150 | 250 |

AREMA 4.3.1

Therefore based on the above requirements a sleeper Type-II of dimensions shown below is selected:

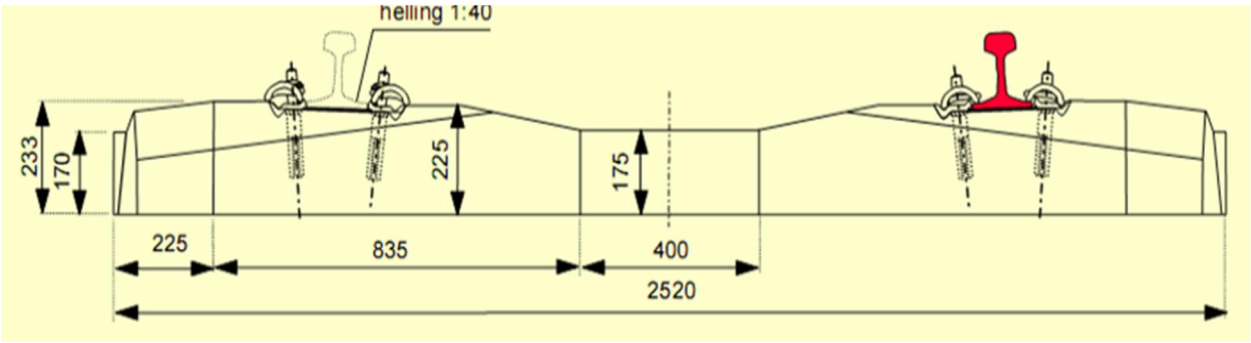


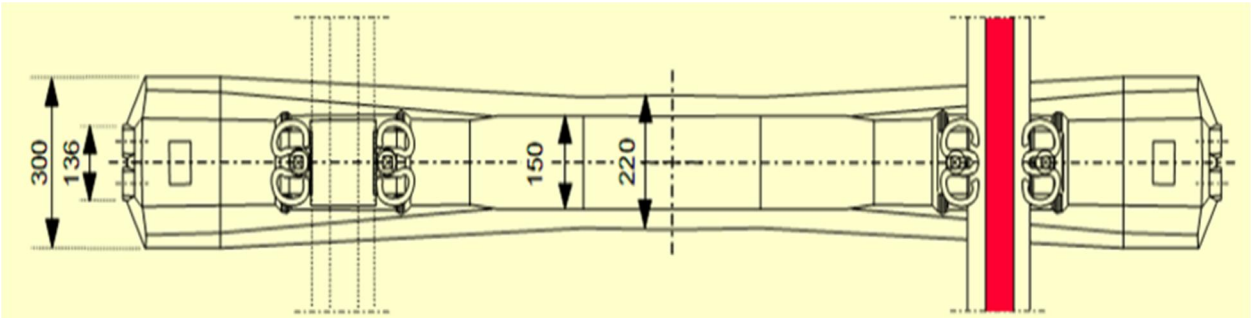


Table 3.3: selected sleeper dimensions

| parameters | units |
|---|---|
| Permissible axle load | 25t |
| Max. speed | 250 km/h |
| Concrete grade | C 50/60 |
| Concrete volume | Approx. 0.127$m^3$ |

| | |
|---|---|
| Weight | Approx. 312kg |
| Length (L) | 2520 mm |
| Width (W) | 300 mm |
| Sleeper height (H) | 233 mm |
| Height of center of rail base (h1) | 225 mm |
| Height sleeper center (h2) | 175 mm |
| Support surface (total) | 639.2 $cm^3$ |
| Standard application | Main track sleeper |

- estimation of vertical rail seat load, $q_r$

Wheel loads applied to the rail will be distributed by the rail to several ties. The distribution of load is dependent upon tie and axle spacing, ballast and subgrade reaction, and rail rigidity.

The percentage of wheel-to-rail load carried by an individual tie varies from location to location. A conservative estimate of the distribution is given in AREMA Figure 30-4-1.

Thus, for a tie spacing of 600mm

Percentage of axle load (distribution factor, DF) carried by a single tie = 50%

$$\rightarrow q_r = 0.5.P^D = 0.5X213.5 = 106.75\ kN$$

- Max. bending moment on the sleeper

AREMA (4.4.1) states required moment calculations are to be based on the geometry of the bottom surface of the tie subjected to uniform ballast pressure.

Therefore the assumed uniformly distributed load $w$ ($kN$/m) over the entire sleeper length $l$(m) is:

$$w = \frac{2q_r}{l}$$

$$\rightarrow \qquad w = \frac{2x106.75}{2.52} = 84.72kN/m$$

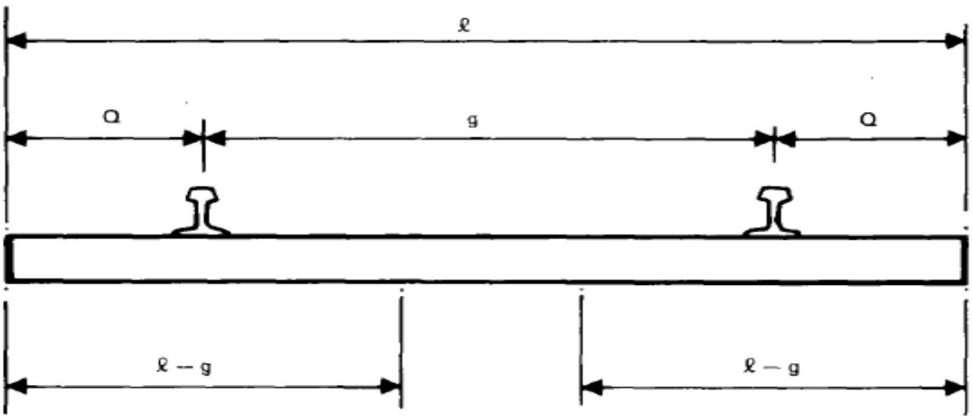


The maximum positive sleeper bending moment at the rail seat $M_r$ $(kNm)$ is given by:

$$M_r = \frac{w(l-g)^2}{8}$$

Where $l = total\ sleeper\ length\ (m), l = 1.5m$

$g = distance\ between\ rail\ centers\ (m)\ and$

$w = assumed\ uniformly\ distributed\ loads\ (kN/m)$

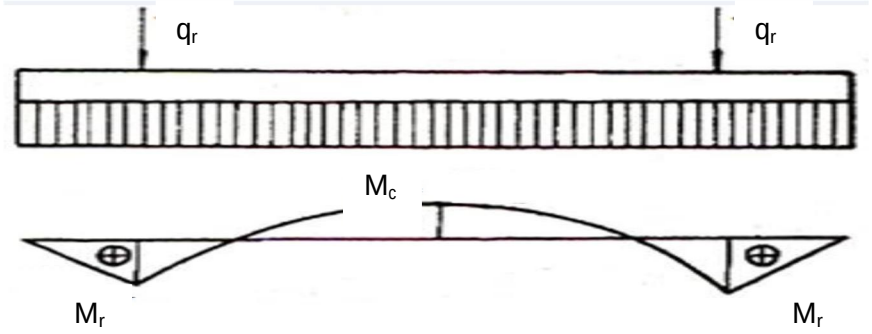


→ $$M_r = \frac{84.72(2.52-1.5)^2}{8} = 11.01\ kNm$$

The maximum negative sleeper bending moment at the center of the sleeper$M_C$ $(kNm)$ is given by:

$$M_c = \frac{wg^2}{8} - M_r \Rightarrow M_c = \frac{q_r(2g-l)}{4}$$

→ $M_c = \frac{84.72x1.5^2}{8} - 11.01 = 12.82kNm$

- Section properties of the sleeper

*Sleeper seat plan*

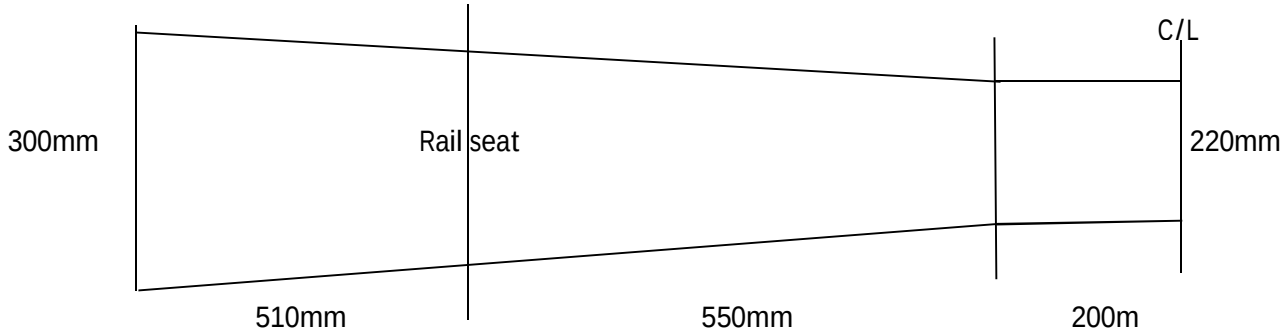


*Elevation*

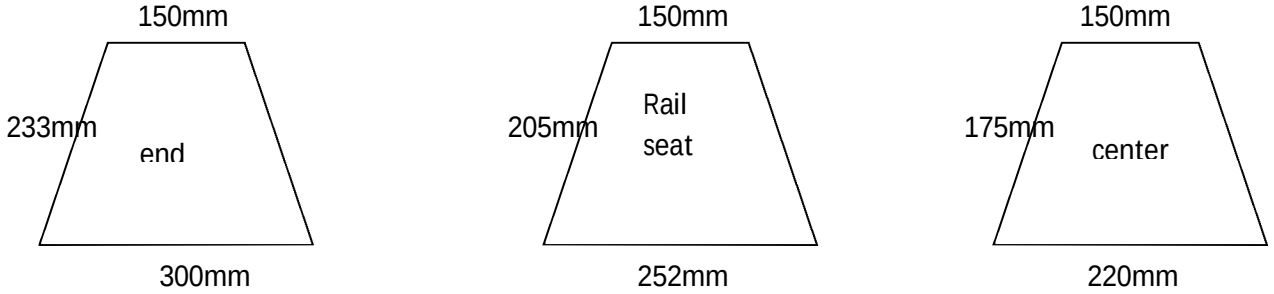


Plan

$A = 3145.6cm^2$

Elevation

***Rail seat***

$area, A = \left(\frac{15 + 25.2}{2}\right) * 20.5 = 412.05cm^2$

$center\ of\ gravity\ from\ bottom = \frac{20.5}{3}\left[\frac{2 * 15 + 25.2}{15 + 25.2}\right] = 9.38cm$

$Moment\ of\ inertia,\ \ I_x = \frac{(20.5)^3}{36}\left[\frac{15^2 + 25.2^2 + 4 * 15 * 25.2}{15 + 25.2}\right] = 14{,}120cm^4$

$section\ modulus$:

$$Z_b = \frac{I_x}{y_b} = \frac{14{,}120}{9.38} = 1505.3cm^3$$

$$Z_t = \frac{I_x}{y_t} = \frac{14{,}120}{11.12} = 1269.7cm^3$$

***Center***

$$area, A = \left(\frac{15 + 22}{2}\right) * 17.5 = 323.75cm^2$$

$$center\ of\ gravity\ from\ bottom = \frac{17.5}{3}\left[\frac{2 * 15 + 22}{15 + 22}\right] = 8.20cm$$

$$Moment\ of\ inertia,\ \ I_x = \frac{(17.5)^3}{36}\left[\frac{15^2 + 22^2 + 4 * 15 * 22}{15 + 22}\right] = 8{,}163.8cm^4$$

$section\ modulus$:

$$Z_b = \frac{I_x}{y_b} = \frac{8{,}163.8}{8.20} = 995.6cm^3$$

$$Z_t = \frac{I_x}{y_t} = \frac{8{,}163.8}{9.30} = 877.8cm^3$$

***End area***

$$area, A = \left(\frac{15 + 30}{2}\right) * 23.3 = 524.25cm^2$$

$$center\ of\ gravity\ from\ bottom = \frac{23.3}{3}\left[\frac{2 * 15 + 30}{15 + 30}\right] = 10.35cm$$

$$Moment\ of\ inertia,\ \ I_x = \frac{(23.3)^3}{36}\left[\frac{15^2 + 30^2 + 4 * 15 * 30}{15 + 30}\right] = 22{,}839cm^4$$

$section\ modulus$:

$$Z_b = \frac{I_x}{y_b} = \frac{22{,}839}{10.35} = 2206.6cm^3$$

$$Z_t = \frac{I_x}{y_t} = \frac{22{,}839}{12.95} = 1763.63cm^3$$

- Bending stress

***At Rail seat***

$$top = \frac{M_r}{Z_t} = \frac{11.01 * 10^6}{1269.7 * 10^3} = 8.67MPa$$

$$bottom = \frac{M_r}{Z_b} = \frac{11.01 * 10^6}{1505.3 * 10^3} = 7.31MPa$$

***At center***

$$top = \frac{M_c}{Z_t} = \frac{12.82 * 10^6}{877.8 * 10^3} = 14.6MPa$$

$$bottom = \frac{M_c}{Z_b} = \frac{12.82 * 10^6}{955.6 * 10^3} = 12.87MPa$$

- Pre-stress

Initial assumptions:

- ☞ High strength steel (strand)
- ☞ Initial pre-stressing is not more than 75% of breaking load
- ☞ 25% loss of pre-stressing loss due elastic shortening, creep of concrete, shrinkage of concrete and steel relaxation.
- ☞ Use $20\Phi_4$ wires
- ☞ Assume $f_s' = 1500MPa$
- ☞ Min. cover$= 40mm$

$$initial\ prestressing, \qquad p_i = 0.75 * 20 * \pi * \frac{4^2}{4} * 1500 = 377kN$$

Wire distribution at the center

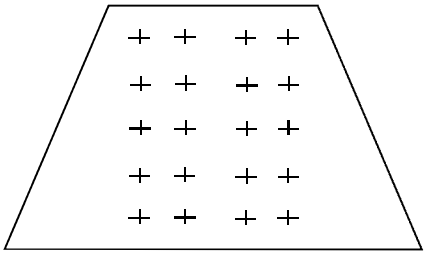

$center\ of\ gravity\ of\ the\ wires = 8.75cm$

$eccentricity\ of\ cables\ at\ the\ rail\ seat = 9.38 - 8.75 = 0.63cm$

$eccentricity\ of\ cables\ at\ the\ center = 8.20 - 8.75 = -0.55cm$

- Stress due to pre-stress

***At Rail seat***

$$top = \frac{p_i}{A} - \frac{p_i e}{Z_t} = \frac{377 * 10^3}{412.05 * 10^2} - \frac{(377 * 10^3)(6.3)}{1269.7 * 10^3} = 7.28MPa$$

$$bottom = \frac{p_i}{A} + \frac{p_i e}{Z_b} = \frac{377 * 10^3}{412.05 * 10^2} + \frac{(377 * 10^3)(6.3)}{1505.3 * 10^3} = 10.72MPa$$

***At center***

$$top = \frac{p_i}{A} - \frac{p_i e}{Z_t} = \frac{377 * 10^3}{323.75 * 10^2} - \frac{(377 * 10^3)(-5.5)}{877.8 * 10^3} = 15.20MPa$$

$$bottom = \frac{p_i}{A} + \frac{p_i e}{Z_b} = \frac{377 * 10^3}{323.75 * 10^2} + \frac{(377 * 10^3)(-5.5)}{995.6 * 10^3} = 9.56MPa$$

- Final stress

| | **Rail seat** | | **center** | |
|---|---|---|---|---|
| Due to | top | bottom | top | bottom |
| Bending | 8.67 | -7.31 | -14.60 | 12.87 |
| Pre-stress | 7.28 | 10.72 | 15.20 | 9.56 |
| resultant | ***15.95*** | ***3.41*** | ***0.60*** | ***22.43*** |

- Permissible stress

AREMA (17.16.2) states stresses in concrete at service load shall not exceed the following:

$$\begin{cases} under\ compression \leq 0.4f_c' = 0.4 * 60 = 24MPa \\ tension\ in\ the\ precompressed \geq 0 \end{cases}$$

Therefore comparing the permissible values with the resultant, the stress is within the limit!

### 3.2.5. Ballast Analysis

- Ballast pressure

AREMA 4.1.2.5.1.1 states tie-to-ballast pressure is not uniformly distributed across or along the bottom of a cross tie; an approximate calculation can be made of "average" pressure at the bottom of the tie. The average pressure at the tie bottom is equal to axle load, modified by distribution and impact factors, and divided by the bearing area of the tie:

$$average\ ballast\ pressure = \frac{q_r}{A}$$

$$where\ \ A = bearing\ area\ of\ cross\ tie\ (\frac{1}{3}\ of\ total\ base\ area)\ (mm^2)$$

$$q_r = rail\ seat\ load\ (N)$$

$$average\ ballast\ pressure, p_a = \frac{106.75 * 10^3}{314560} = 0.34MPa$$

The recommended ballast pressure should not exceed 85 psi (0.586 MPa) [AREMA 4.1.2.5.1.1] for high-quality, abrasion resistant ballast. If lower quality ballast materials are used, the ballast pressure should be reduced accordingly.

☞ Therefore the ballast pressure is within the limit!

- Ballast + sub ballast depth

In accordance of the UIC classification, the behavior of the subgrade may macroscopically be characterized by and classified as follows [19]:

- Low settlements and very good support of train loads. This subgrade is hereafter designated as $S_3$.
- Medium behavior in settlement and non-satisfactory support of loads. This subgrade is designated as $S_2$.
- Large settlements and non-satisfactory support of loads. This subgrade is designated as $S_1$.

- Extensive settlements and a very bad performance in withstanding loads. The quality of such a subgrade is designated as $S_0$.

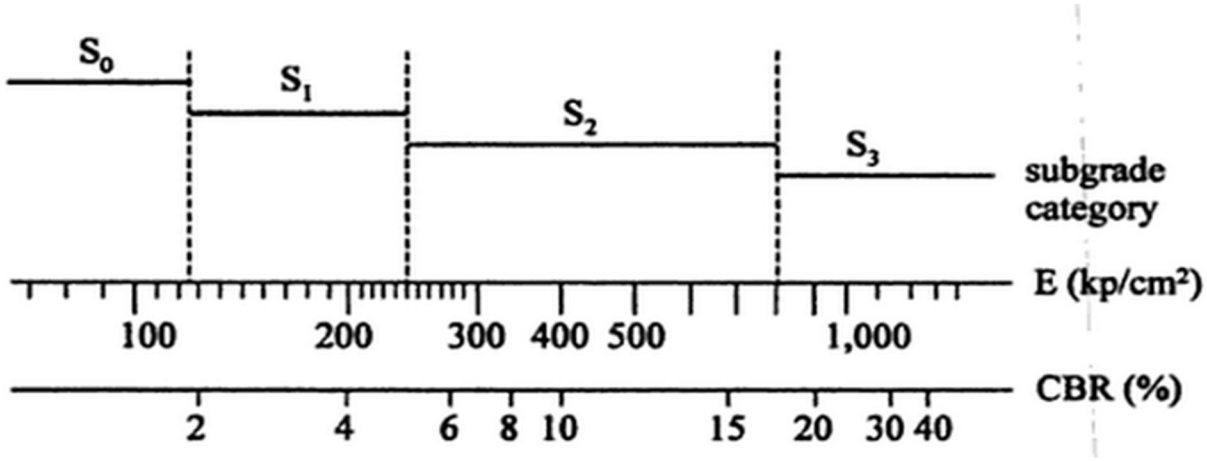


For ease of comparison two cases are considered:

a) Excellent subgrade: based on maximum allowable subgrade pressure recommended by AREMA with a pressure of $25psi$ $(0.172MPa)$ or CBR between 20% and 30%.
b) Poor subgrade: assume loose to medium dense sand; firm to stiff clays and silts; alluvial fills. assume allowable pressure of $6.94psi$ $(0.10MPa)$ $is\ adopted$

The distribution of loads to depth is approximately the same regardless of the granular material. Therefore the combined depth of sub-ballast and ballast is calculated as a single unit to develop the pressure on the subgrade. The most notable and most widely used empirical relationship is the equation recommended and developed by Talbot (1919). The maximum vertical pressure $\sigma_z$ (kPa) under the rail seat for any particular ballast depth is defined as:

$$\sigma_z = p_a \left[\frac{1}{5.9z^{1.25}}\right] \Rightarrow z_{min} = \left[\frac{p_a}{5.9\sigma_z}\right]^{\frac{4}{5}}$$

$where\ \ p_a = average\ uniform\ pressure\ between\ the\ sleeper\ and\ the\ ballast\ (kPa)$

$z = ballast\ depth\ (m)$

Thus for case a: excellent subgrade

$$z = \left[\frac{340}{5.9 * 172}\right]^{\frac{4}{5}} = 0.41m$$

For case b: poor subgrade

$$z = \left[\frac{340}{5.9 * 100}\right]^{\frac{4}{5}} = 0.64m$$

- Ballast Shoulder Width (BSW)

AREMA (2.1.1.5.2.2) a value for BSW (Ballast Section Shoulder Width) of not less than 12 inches (300mm) is recommended for Standard Gage construction of continuous welded rail in main track service.

- Side Slope (BSS)

AREMA (2.1.1.5.2.3) The Side Slope run component of the Ballast Section is proportioned to provide confining pressure to that part of the Ballast Section expected to transmit the vertical load from the bottom of the cross tie to the top of the sub-ballast. The BSS run component is measured in the plane of the top of the cross tie, and the rise component is measured perpendicular to the run component. A BSS value of 2:1 is commonly used.

- Sub-ballast Depth

AREMA (2.1.1.5.3) states a minimum value of 6 inches (152mm) compacted is considered necessary to perform the separation of layers and shielding of the roadbed from weather functions.

Material most commonly available for use as sub-ballast are those aggregates ordinarily specified and used in construction for highway bases and sub bases. These include crushed stone, natural or crushed gravels, natural or manufactured sands, crushed slag or a homogeneous mixture of these materials.

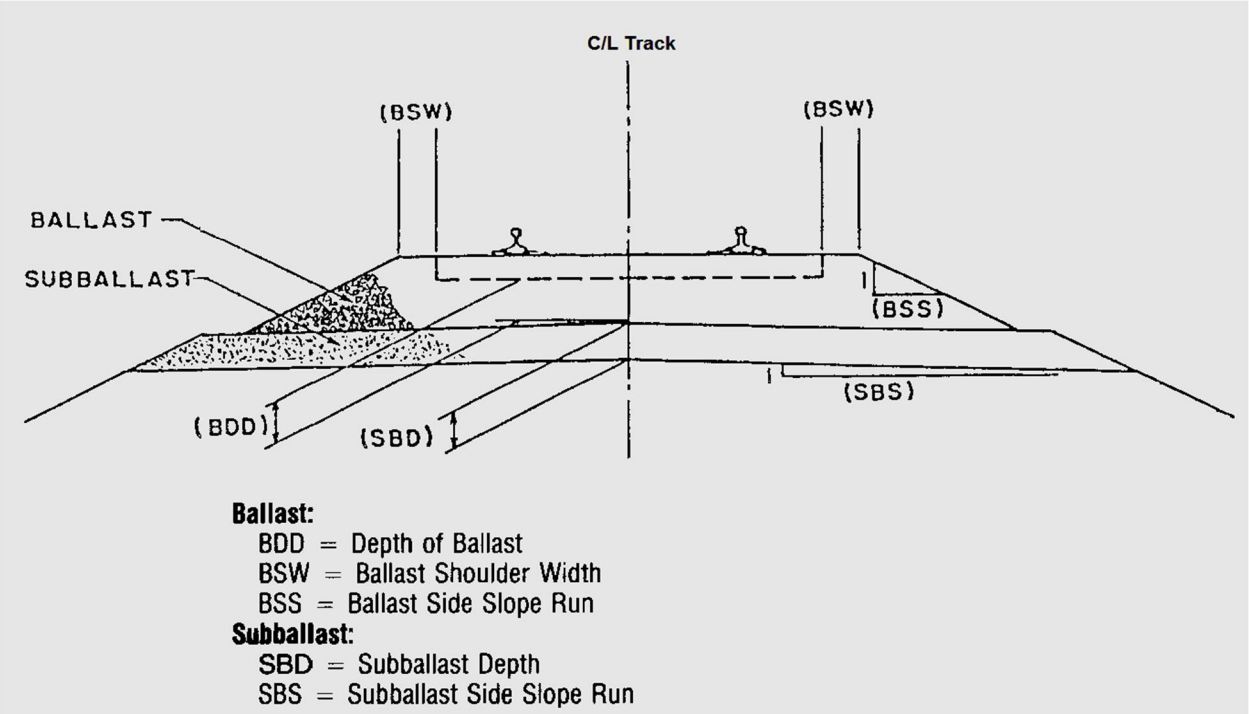


Figure 3.8: Typical Section of Track Substructure

- Side Slope (SBS)

AREMA (2.1.1.5.3.2) The Side Slope run component of the Sub-ballast Section is proportioned to provide drainage from the top of the roadbed construction. A value for SBS of not less than 24 or more than 40 is recommended. Sub-ballast materials having relatively lower permeability rates may use relatively higher SBS values.

- Ballast gradation

Ballast gradations should be graded uniformly from the top limit to the lower limit to provide proper density, uniform support, and elasticity and to reduce deformation of the ballast section from repeated track loadings.

AREMA (2.10.4) states Ballast for concrete tie installations must be limited to crushed granites, trap rocks or quartzite. A very important consideration is the selection of the proper gradation of the ballast material for concrete ties. The early concrete tie installations were placed on ballast

materials graded to the AREMA No. 4 (1½ inches- ¾ inch), resulting in good in track performance.

Therefore, crushed stone ballast bed in accordance with AREMA #4 (showing below) grading requirements will be used. Minimum depth of ballast for single track ballast is 300 cm.

| Size No. | Nominal square opening | Percent Passing | | | | | | | | | |
|---|---|---|---|---|---|---|---|---|---|---|---|
| | | 3'' | $2\frac{1}{2}''$ | 2'' | $1\frac{1}{2}''$ | 1'' | $\frac{3}{4}''$ | $\frac{1}{2}''$ | d'' | No.4 | No.8 |
| 4 | $1\frac{1}{2}'' - \frac{3}{4}''$ | - | - | 100 | 90-100 | 20-55 | 0-15 | - | 0-5 | - | - |

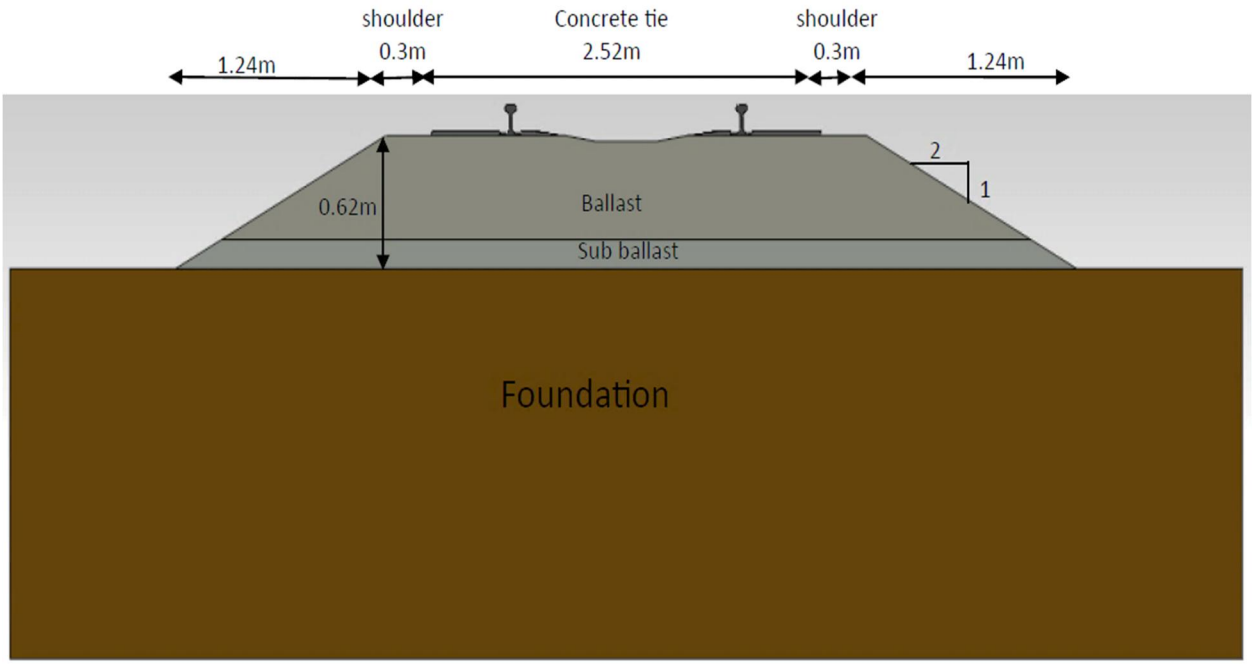


Figure 3.9: Geometry of Track Section (SolidWorks)

## 3.3. Finite element analysis

A series of four finite element analysis of ballasted railroad embankment were conducted: unreinforced ballast embankment used as control, ballast embankment reinforced with geocell and ballast embankment reinforced with geogrid at two different depths below the tie.

### 3.3.1. Assumptions

The following assumptions have been made throughout the analysis:

- The analysis is completely quasi-static and considers vertical track force only
- The effect of wind, curving and hunting of the bogies is excluded or lateral and longitudinal forces not incorporated.
- The rib and web of the geogrid is made same dimension and the thickness of geocell is made to be 2mm to provide load transfer characteristics.
- Ballast and sub-ballast are assumed to have the same material properties and for ease comparison the subgrade is made to be soft
- Foe ease of simplification symmetry of the line is considered

### 3.3.2. Symmetry

Due to the symmetry of the model in geometry, loading, materials and degree of freedom constraints half of the track along the center of railroad is considered.

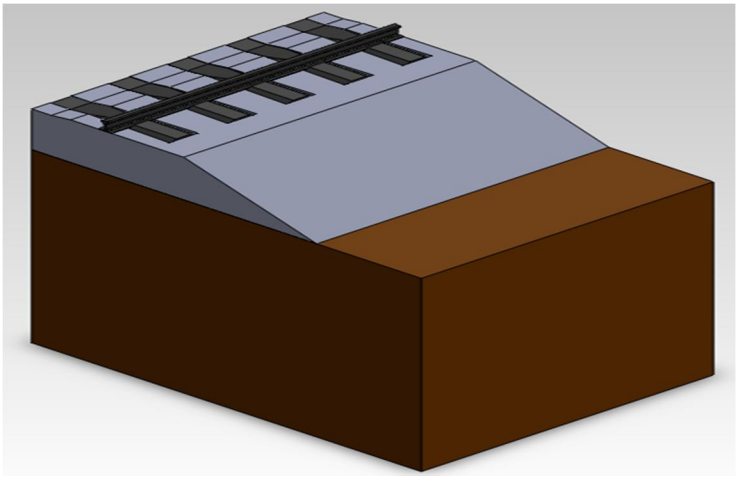

Figure 3.10: symmetry of the line Considered for FEA (SolidWorks)

### 3.3.3. Geometry and Cross-Section

The geometric modeling of the individual track components and the entire track with and without geosynthetics is modeled with a software package called SolidWorks.

The ballast embankment is 5.85 meters in width at the base, 3.12 meters at the crest, and 0.62 meters in height. The foundation dimension is limited to 3mx3mx8m (hxdxw) for ease of computation. The geometric detail of each track components and their models is described (figure 3.9):

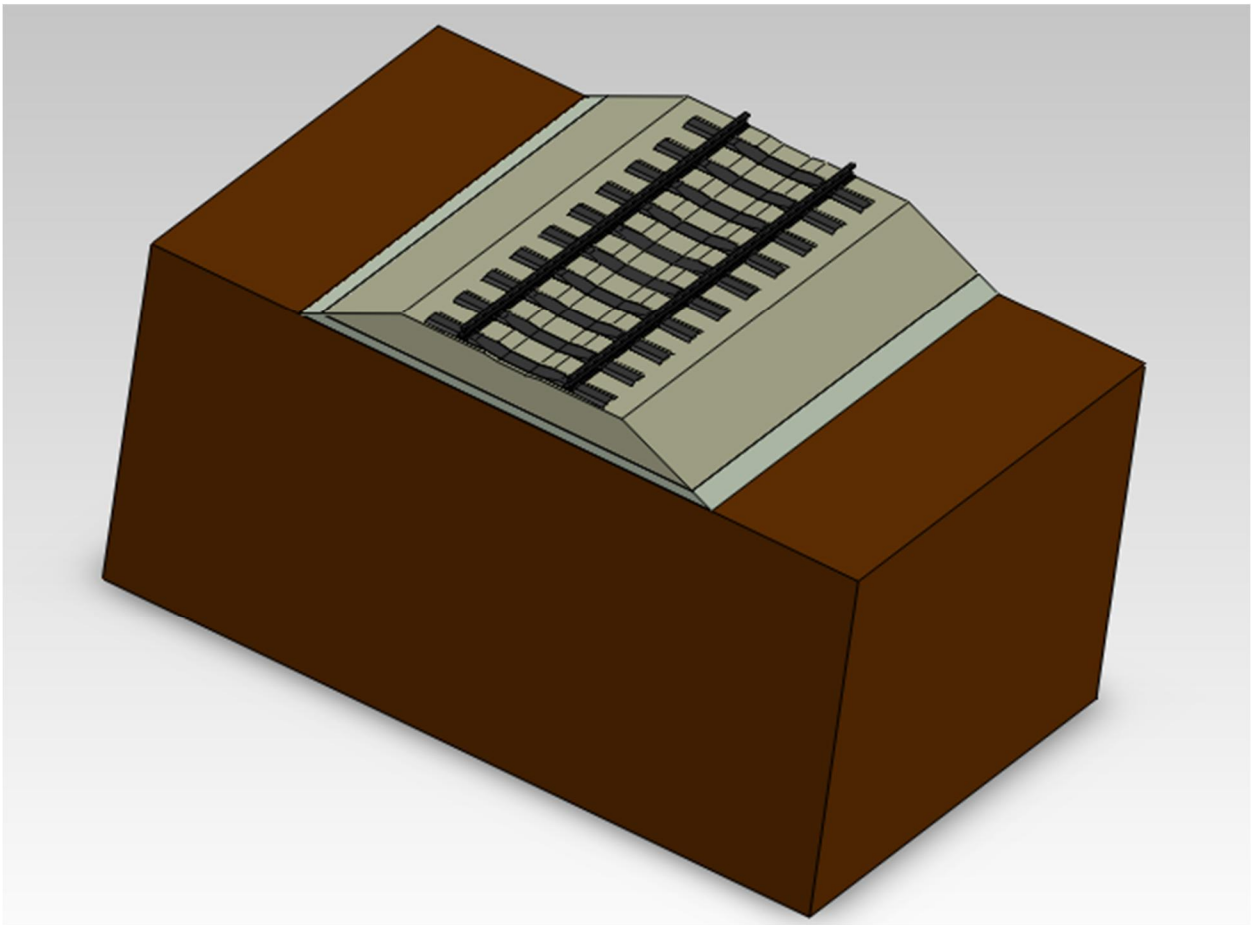

Figure 3.11: Railway track 3D model (SolidWorks)

i. Rail

The adopted rail profile is UIC54 [18]

| | |
|---|---|
| Rail profile | UIC54 |
| Section weight Kg/m | 54.77 |
| Rail height mm | 159.00 |
| Head width mm | 70.00 |
| Web thickness mm | 16.00 |
| Foot width mm | 140.00 |
| Moment of inertia Ixx $cm^4$ | 2337.90 |
| Moment of inertia Iyy $cm^4$ | 419.20 |
| Section modulus of the head $mm^3$ | 278752.83 |
| Section modulus of the base $mm^3$ | 311180.62 |

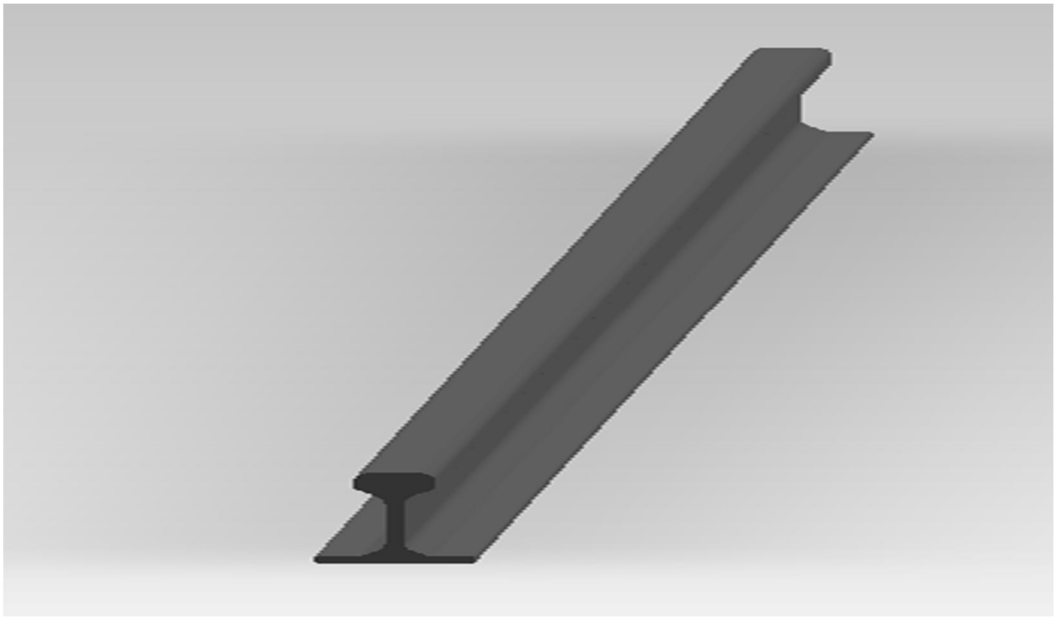

Figure 3.12: 3D model of rail profile UIC54 (SolidWorks)

ii. Rail Pad type-II [18]

The rail pad is modeled with the following dimensions:

$$Length, L = 240mm$$

$$Width, W = 140mm$$

$$Thickness, t = 5mm$$

iii. Sleeper

The sleeper is modeled with the following dimensions shown below (sleeper type B58) [18].

| parameters | Value |
|---|---|
| Concrete volume | Approx. 0.127$m^3$ |
| Length (L) | 2520 mm |
| Width (W) | 300 mm |
| Sleeper height (H) | 233 mm |
| Height of center of rail base (h1) | 225 mm |
| Height sleeper center (h2) | 175 mm |
| Support surface (total) | 639.2 $cm^3$ |

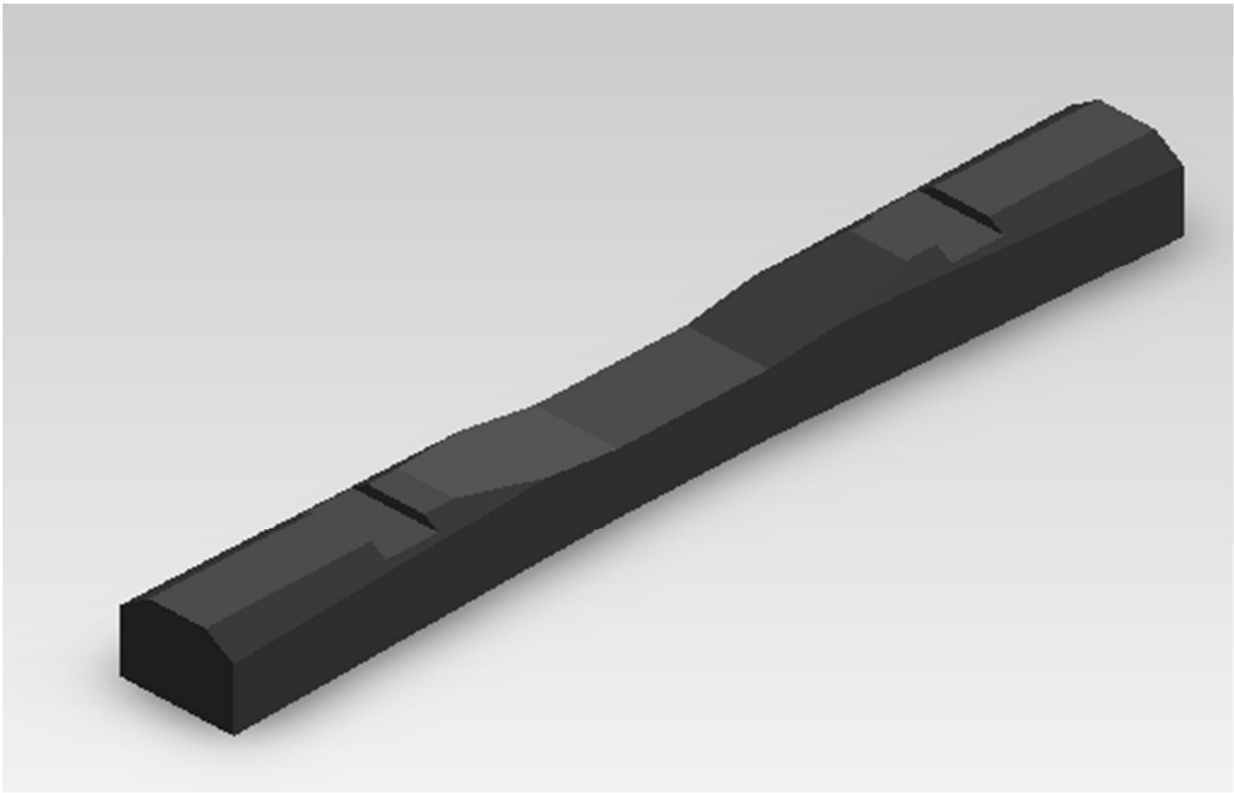

Figure 3.13: 3D model of pre-stressed concrete sleeper (SolidWorks)

iv. Geosynthetics

The dimensions of the geosynthetics are selected based on the recommendations stated in AREMA and based on tested dimensions from literatures.

a. Geocell

AREMA section 10.5 recommends the dimensions of the geocell to be as stated below:

Cell depth: The minimum cell depth for load support should be 8 inches (200 mm) and the surface of the geocells may be smooth or textured.

Infill Material: For structural applications, the infill material shall be a dry, granular cohesionless material, having filtering characteristics compatible with the subgrade below and the ballast section above. The material shall be a well-graded crushed stone with a maximum particle size of 1.5 inches (37.5 mm), with no greater than 10% passing the #200 sieve. The coarse fraction of the material shall have a Los Angeles Abrasion test wear of no greater than 50%.

Table 3.4: Polyethylene and Geocell Cellular Confinement System Properties [3]

| Property | Unit | Value | Test Method |
|---|---|---|---|
| Polyethylene Content | $lb/ft^3$ ($g/cm^3$) | 59.0 - 60.2 (0.945 - 0.965) | ASTM D1505 |
| Carbon Black | % | 1.5 - 2.0 | ASTM D4218 |
| Sheet Thickness | (mil) mm | 50 ±5% (1.25) | ASTM D3767 |
| Minimum ESCR[1] | Hr | 3000 | ASTM D1693 |
| Seam Peel Strength | lb (N) | 450 (2000) | USACOE Tech Report GL-86-19, Appendix A |
| Cell Area (Maximum) | $in^2$ ($cm^2$) | 44.8 (289)<br>71.3 (460)<br>187.0 (1206) | Load Support and Severe Slope Protection Applications<br>Load Support, Slope and Channel Protection, Earth Retention Applications<br>Channel Protection and Earth Retention Applications |
| Seam Hang Strength-Test | A 4" (102 mm) wide seam sample shall support a 160 lb (72.5 kg) load for 7 days minimum in a temperature controlled environment undergoing a temperature change on a 1 hour cycle from ambient[2] room to 130°F (54°C). | | |
| Alternative Seam Hang Strength-Test | A 4" (102 mm) wide seam sample shall support a 160 lb (72.5 kg) load for 30 days minimum in an ambient[2] room temperature environment. | | |
| [1] ESCR - Environmental Stress Crack Resistance<br>[2] Ambient room temperature is 74°F ±4° (23°C ±2°) | | | |

[13] Performed series of 6 large-scale model tests of ballasted railroad embankments were conducted in the laboratory. The ballast embankment model had a square base and top of widths 152 cm (after a slight truncation) and 61 cm, respectively. The height was 55 cm, such that the slope angle was 44.3°. Both monotonic and cyclic loading was applied on ballast embankments that were unreinforced (control tests), with a single layer of geocell placed at mid-height, or with two layers of geocell. Based on the model test, geocell of a polymer alloy called Novel Polymeric Alloy (NPA) and of height 15 cm, a diamond shaped pocket size that was 22.5 cm by 22.5 cm and a wall thickness of 0.1 cm showed a good performance. [3] Also States the geocell would have to be placed in the ballast/subballast layer at a minimum of 25 centimeters below the ties in order to avoid construction damage and stress concentrations from heavy axle loads from trains.

Therefore based on the above AREMA requirements and test results, the following dimensions of geocell are utilized for the analysis of ballast reinforced with Geocell:

| **Property** | **Unit** | **Value** | **Remark** |
|---|---|---|---|
| Sheet thickness | mm | 1.25 | |
| Cell Area | $cm^2$ | 460 | For Load Support |
| Cell Width (Cell Length) | cm | 22 (22) | Square cell |
| Cell depth | cm | 20 | |
| Geocell Location | cm | 25 | Below the tie bottom |
| Expanded Length | m | | |
| Width | m | | |

b. Geogrid

AREMA section 10.6 recommends the dimensions of the geogrid to be as stated below:

***Aperture size:*** When reinforcing sub-ballast layers, it is recommended that the aperture size of the geogrid does not exceed the average ($D_{50}$) particle size of the fill material being used. For ballast layers however, research has shown that the use of a larger aperture geogrid (greater than 1.7 inches (43 mm) almost always leads to optimum performance, irrespective of the particle size of the ballast (see Table 3.5).

Table 3.5: Physical Properties for Geogrids used in Track Stabilization [3]

| Property | Test Method | Units | Minimum Value (Sub-ballast reinforcement) | Minimum Value (Ballast reinforcement) |
|---|---|---|---|---|
| Aperture size (min. - max.) | Direct measurement | Inches (mm) | 0.70 - 1.60 (17.8 - 40.6) | 1.70 - 2.50 (43.2 x 63.5) |
| Open area | Direct measurement | % | 70 | 75 |
| Rib thickness | ASTM D1777 | Inches (mm) | 0.05 (1.27) | 0.05 (1.27) |
| Junction thickness | ASTM D1777 | Inches (mm) | 0.16 (4.0) | 0.17 (4.4) |
| Aperture stability modulus @ 20cm-kg | US Army Corps of Engineers | lb-ft/deg (kg-cm/deg) | 0.470 (6.5) | 0.419 (5.8) |
| Flexural rigidity (Machine direction) | ASTM D1388 | (lb-ft) (mg-cm) | 0.0542 (750,000) | 0.0325 (450,000) |
| Tensile modulus @ 2% strain (machine x cross machine direction) | ASTM D6637-01 | lb/ft (kN/m) | 18,500 x 30,000 (270 x 437) | 19,000 x 32,500 (277 x 474) |
| Junction strength | GRI GG2-87 | lb/ft (kN/m) | 1080 (15.7) | 956 (13.9) |
| Junction efficiency | GRI GG2-87 | % | 90 | 90 |
| Carbon black | ASTM 4218 | % | 0.5 | 0.5 |

[20] Tested five types of geogrids which are 50 mm x 50 mm, 40 mm x 40 mm, 30 mm x 30 mm square aperture size geogrids, hexagonal and crosswise aperture size geogrids were investigated. While the 50 mm x 50 mm square aperture size geogrid showed approximately 7.5-10 kN/m$^2$ Pullout stress value, the 30 mm x 30 mm square and the 40 mm x 40 mm square aperture size geogrids indicated 3 - 4.5 kN/m$^2$ stress and after this point, they were ruptured.

Table 3.6: Stress and internal friction angle values of each geogrid [20]

| Geogrid Aperture Type | Shear stress (kN/m²) | Internal friction angle (°) |
|---|---|---|
| 50 mm x 50 mm, Square | 8.32 | 14.85 |
| 40 mm x 40 mm, Square | 3.1 | 5.62 |
| 30 mm x 30 mm, Square | 4.23 | 7.66 |
| Hexagonal | 8.54 | 15.23 |
| Crosswise | 6.94 | 12.46 |

Therefore based on the above AREMA requirements and test results, the following dimensions of geocell are utilized for the analysis of ballast reinforced with Geogrid:

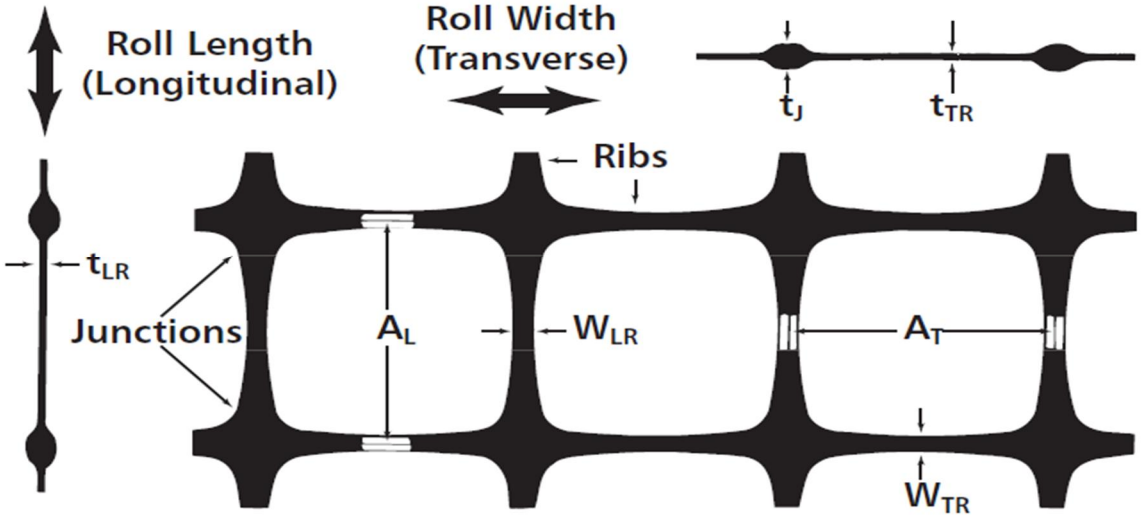


| **Property** | **Unit** | **Value** | **Remark** |
|---|---|---|---|
| Aperture Size, $A_L$x$A_T$ | mm | 50 | Biaxial Geogrid** |
| Open Area | % | 75 | |
| Rib Thickness, $t_{TR}$ | mm | 1.27 | |
| Junction Thickness, $t_J$ | mm | 4.4 | |
| Rib Width, $W_{TR}$/$W_{LR}$ | mm | 4.0 | |
| Roll Length | m | 30-50 | |
| Roll Width | m | 3.8-4.0 | |
| **Biaxial geogrids were manufactured by stretching the punched sheet of polypropylene in two orthogonal directions. This process resulted in a product with high tensile strength and modulus in two perpendicular directions. | | | |

Therefore based on the above geometric parameters, ballast embankmnet reinforced with geocell and geogrid are modeled with SolidWorks as shown in Figure 3.14 and Figure 3.15.

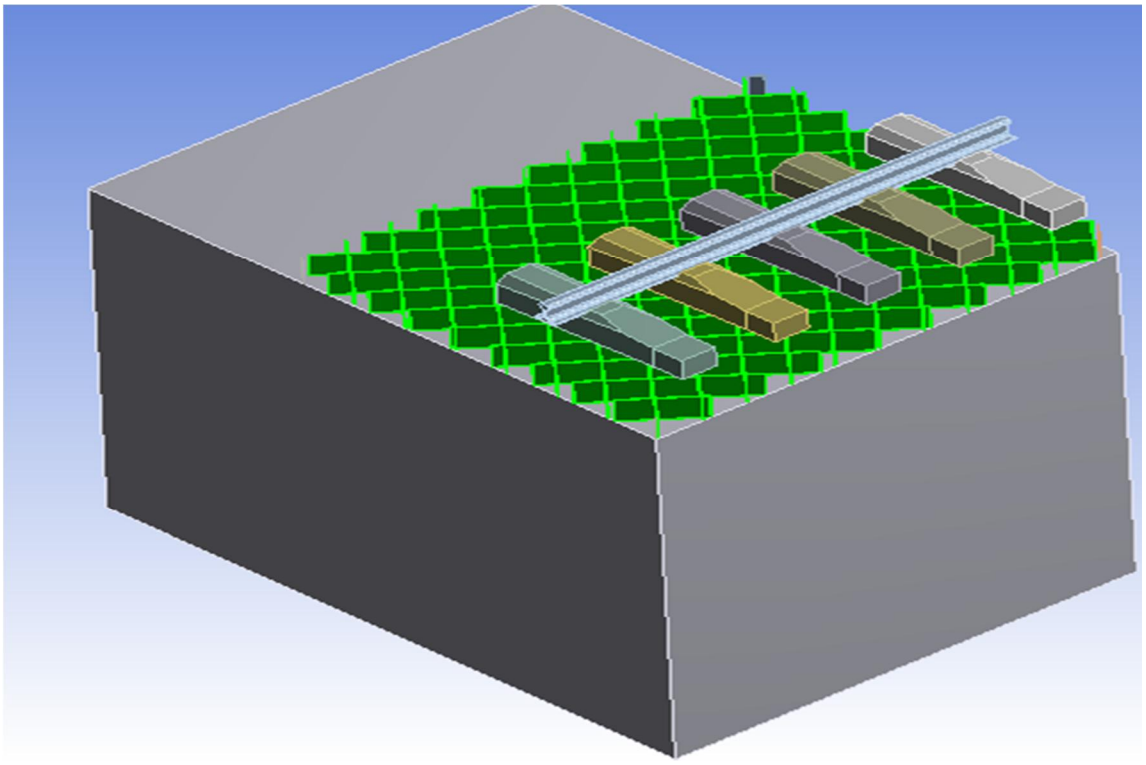

Figure 3.14: Railway geometry without geocell (ballast removed for illustration), SolidWorks

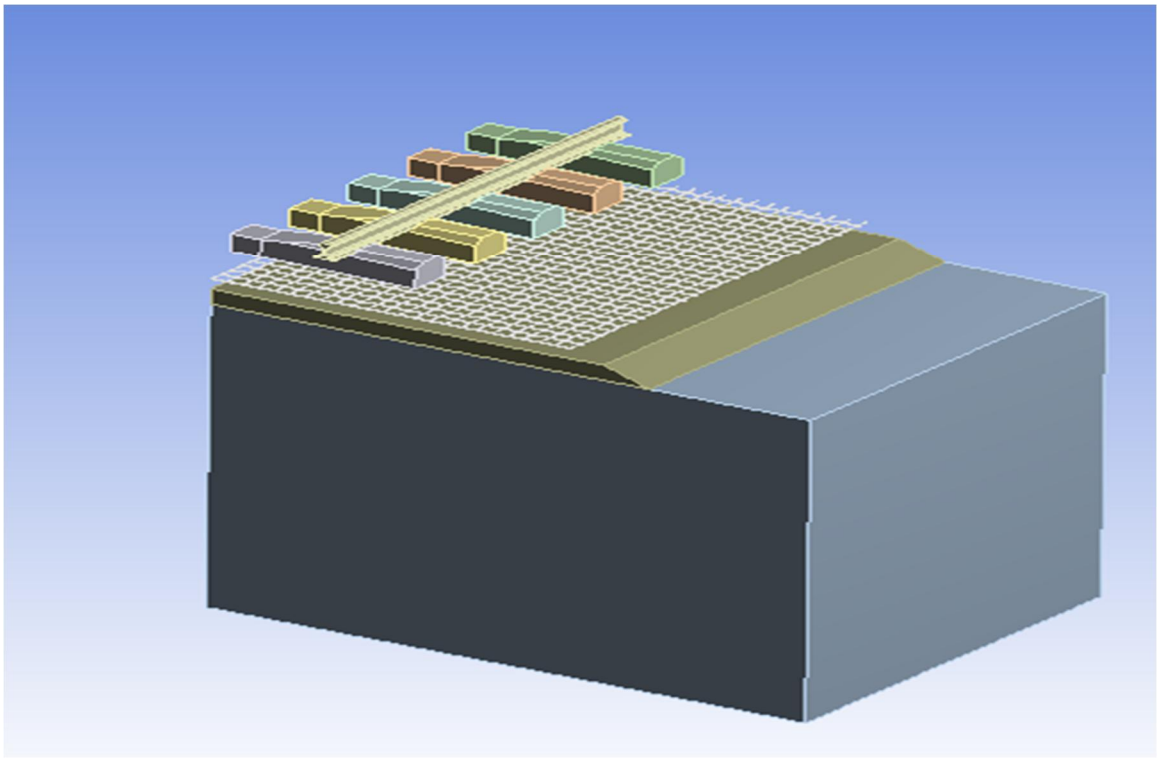

Figure 3.15: Railway geometry without geogrid (ballast removed for illustration), SolidWorks

### 3.3.4. Idealization of Three-Dimensional Railway Substructure

Due to the computational requirements of running a larger or more refined mesh, the width of the plane-strain slice was limited to 3m meters in thickness; that is, enough width to have five ties with the full thickness of ballast infill in between each. The boundary effects were generally considered small due to the symmetry. The FE simulation is modeled with five ties that is slightly more conservative as USACE railroad design manual recommends [1].

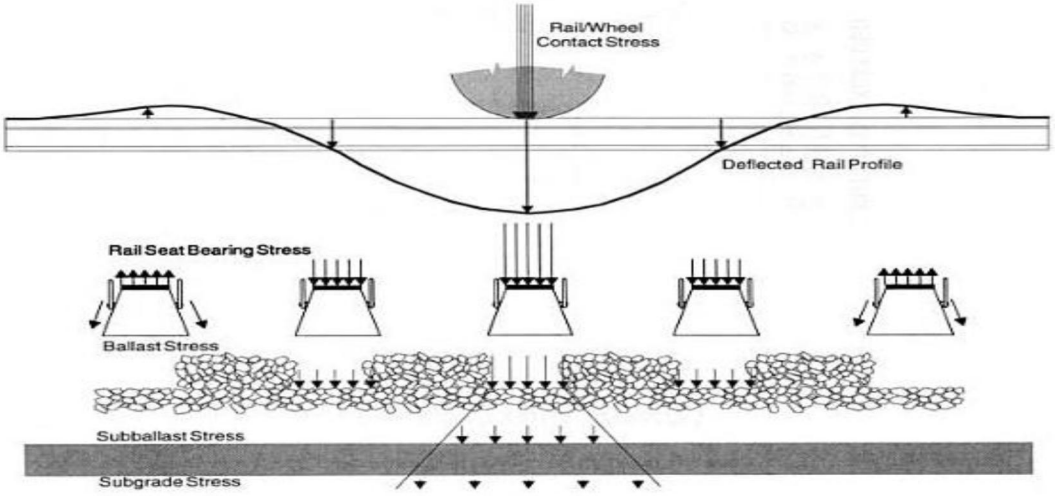


Figure 3.16: Rail deflection and stress distribution profile [1]

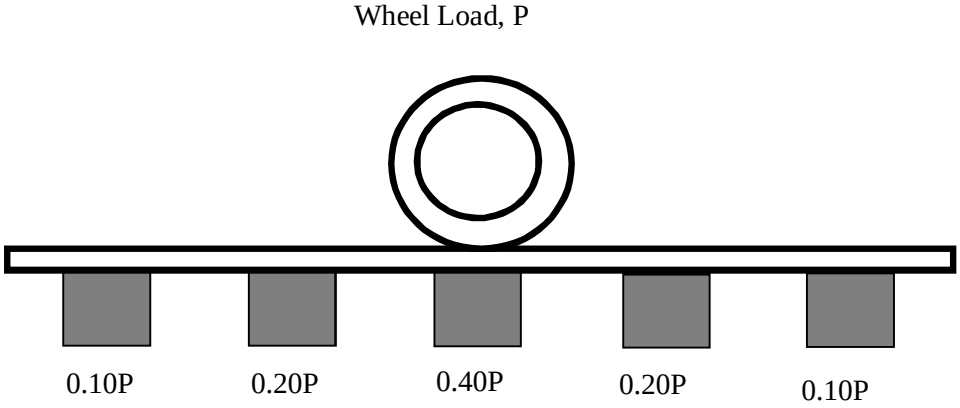


Figure 3.17: Assumed ballast-tie reaction from wheel load

### 3.3.5. Elements

The behaviors of elements that characterize each track components used in the FEA are described below:

*Rail*: The element is a linear, quadratic, or cubic two-node beam element. The element includes stress stiffness terms, by default, in any analysis with large deflection. The provided stress stiffness terms enable the elements to analyze flexural, lateral, and torsional stability problems. Elasticity, plasticity, creep and other nonlinear material models are supported. A cross-section associated with this element type can be a built-up section referencing more than one material. Added mass, hydrodynamic added mass and loading, and buoyant loading are available. Thus for this purpose element beam161 is selected from ANSYS element library.

*Ballast, Rail pad and Geosynthetics*: the element defined by eight nodes having three degrees of freedom at each node: translations in the nodal x, y, and z directions. The element has plasticity, hyperelasticity, stress stiffening, creep, large deflection, and large strain capabilities. It also has mixed formulation capability for simulating deformations of nearly incompressible elastoplastic materials, and fully incompressible hyperelastic materials. Thus for this purpose element Solid65 is selected from ANSYS element library.

*Sleeper*: the element used for the 3-D modeling of solids with or without reinforcing bars (rebar). The solid is capable of cracking in tension and crushing in compression. In concrete applications, for example, the solid capability of the element may be used to model the concrete while the rebar capability is available for modeling reinforcement behavior. Thus for this purpose element Solid164 is selected from ANSYS element library.

### 3.3.6. Meshing

#### 3.3.6.1. Unreinforced

The unreinforced model consisted of 18782 elements and 48129 nodes (Figure 3.8). Greatly coarser meshes provided lower, more conservative settlements. This implies that the element size would comply with the grain sizes of the ballast commonly used according to standard AREMA gradation specifications.

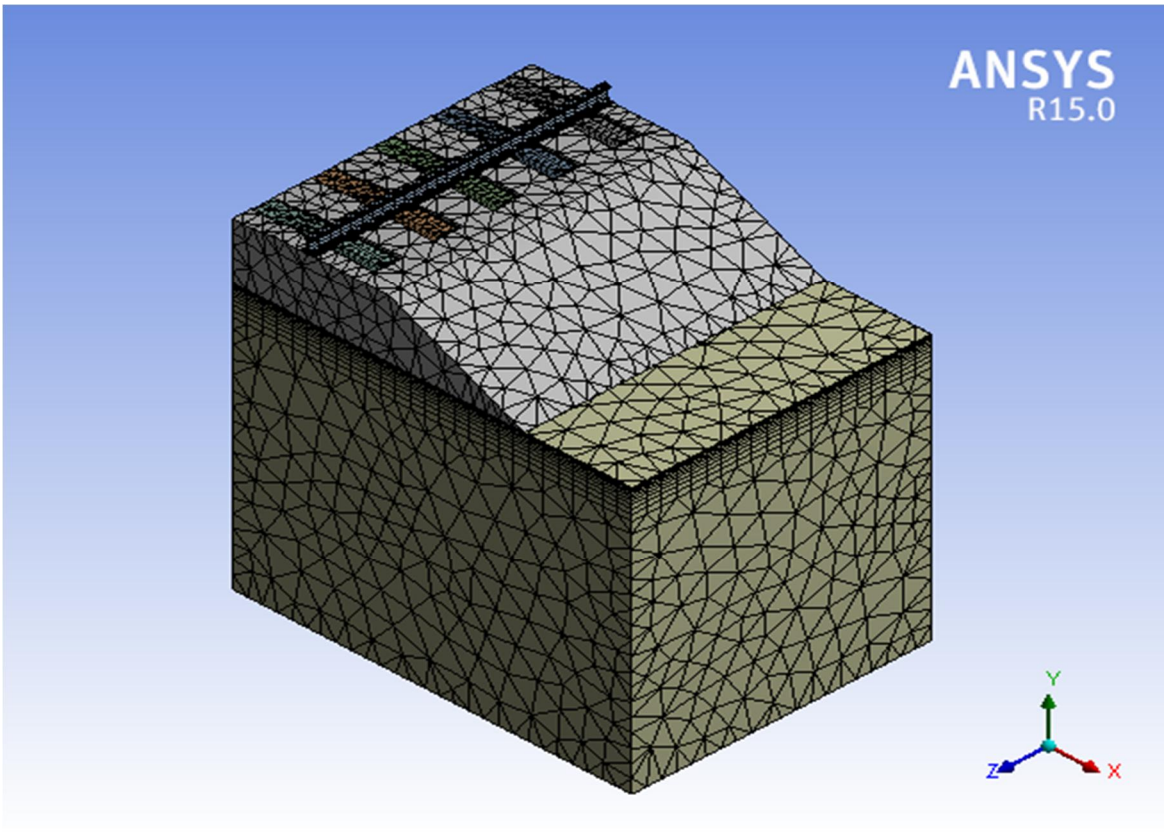


Figure 3.18: Mesh of ballasted railway track and foundation, ANSYS

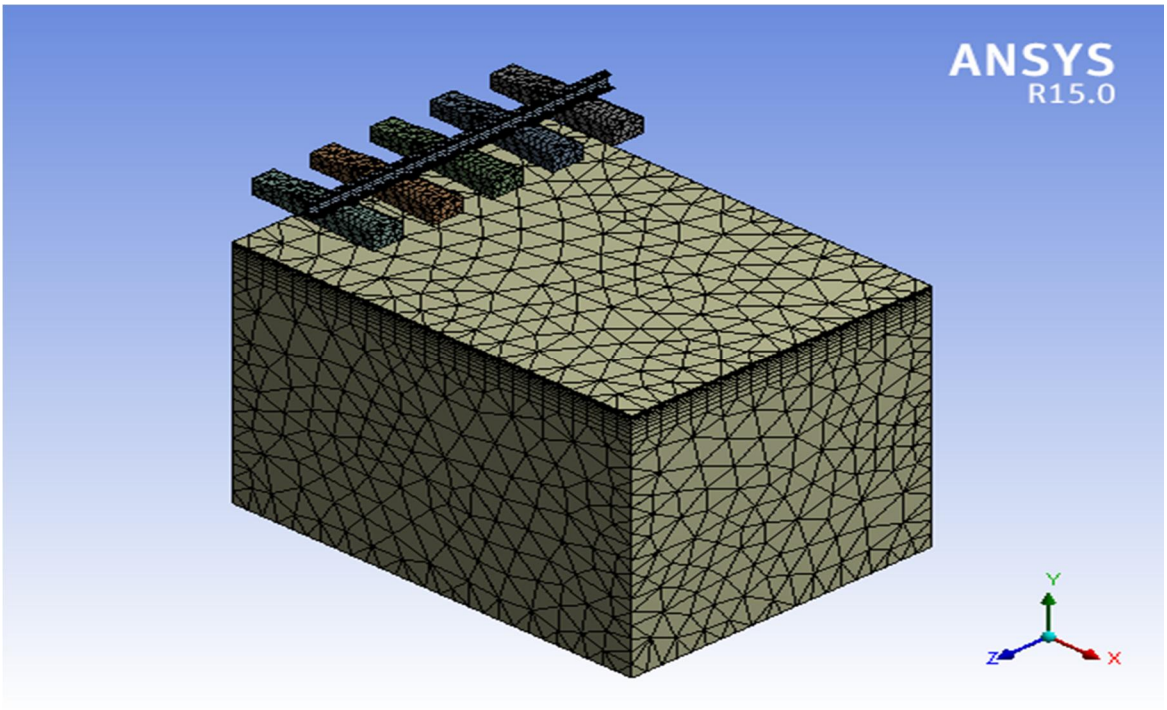


Figure 3.19: Mesh of rail, sleeper and foundation (ballast removed for illustration), ANSYS

### 3.3.6.2. Reinforced with Geocell

The geocell reinforced model consisted of 62364 elements and 148808 nodes. The large number of nodes and elements is because of more refinement is used around the geocell.

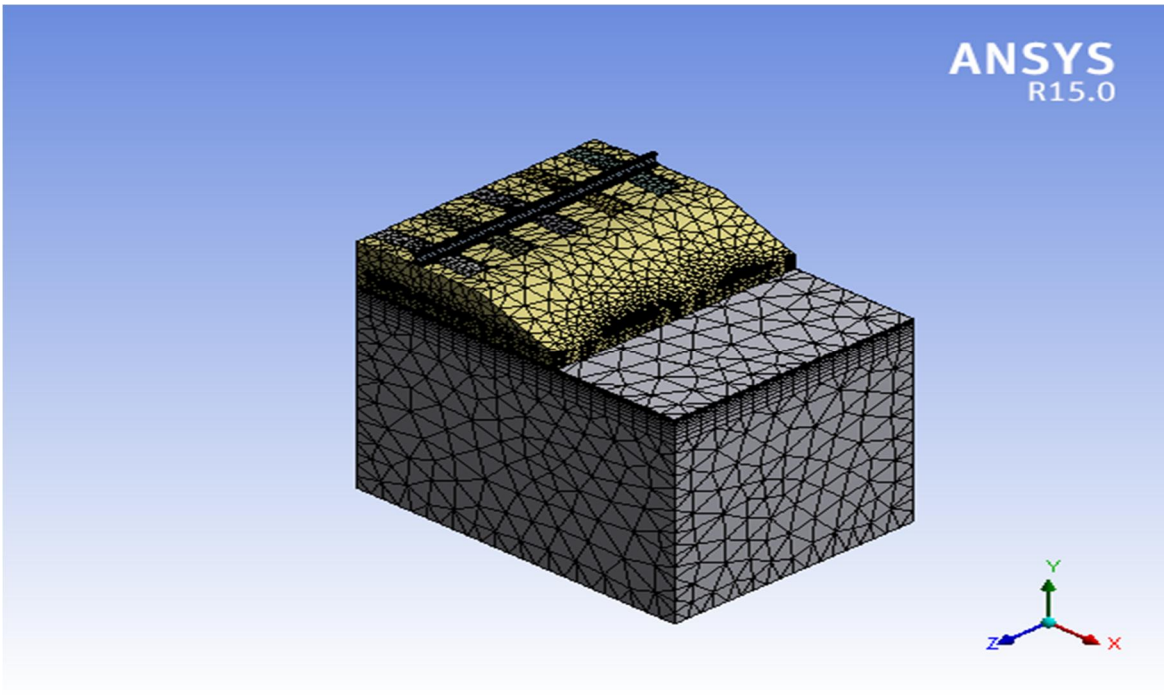


Figure 3.20: Mesh of ballasted railway track reinforced with geocell and foundation, ANSYS

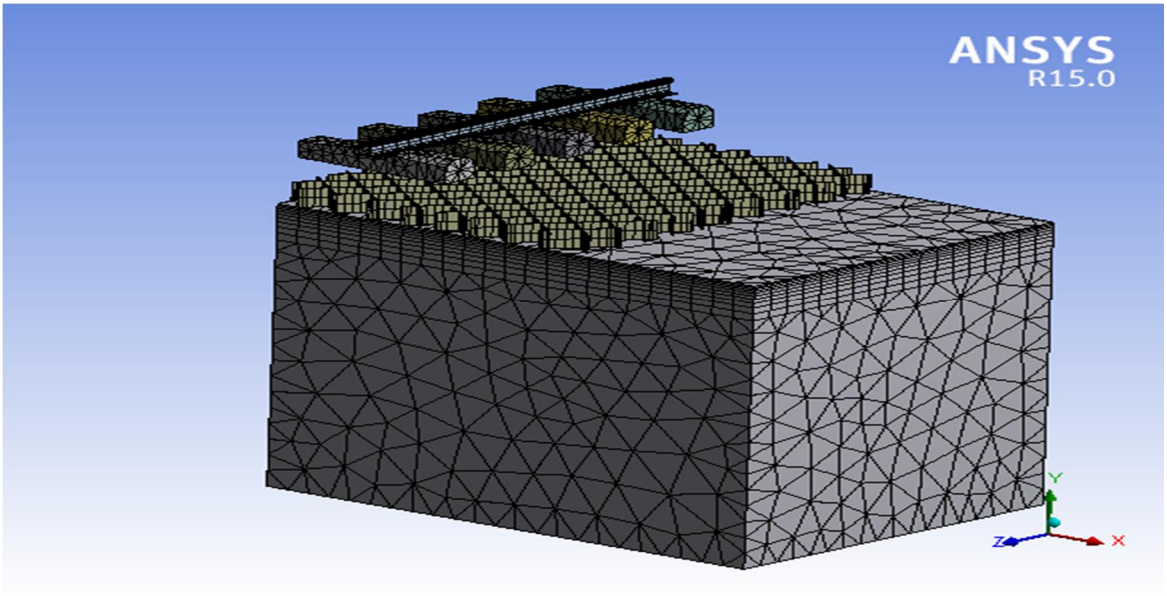


Figure 3.21: Mesh of rail, sleeper, geocell and foundation (ballast removed for illustration), ANSYS

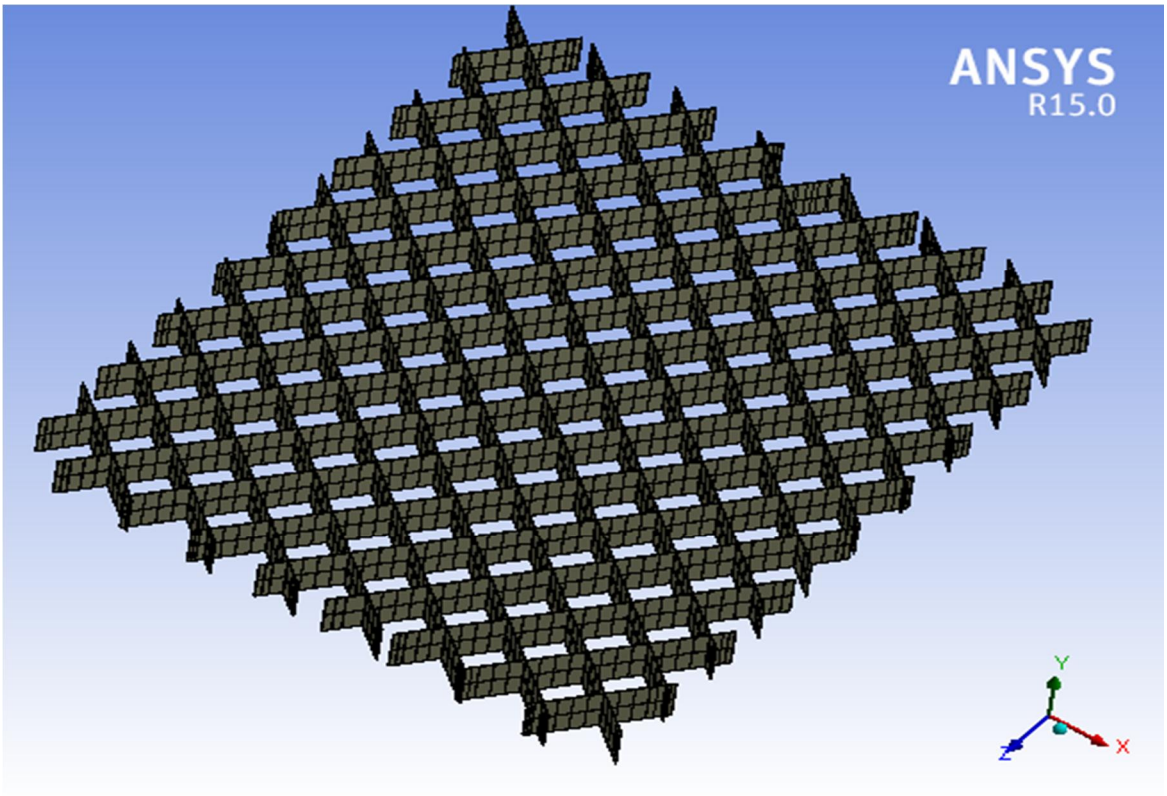


Figure 3.22: Mesh of embedded geocell, ANSYS

### 3.3.6.3. Reinforced with Geogrid

- At a depth of 300 mm below tie bottom

The geogrid reinforced model consisted of 182693 elements and 361604 nodes.

- At a depth of 200 mm below tie bottom

The geogrid reinforced model consisted of170325 elements and 341191 nodes.

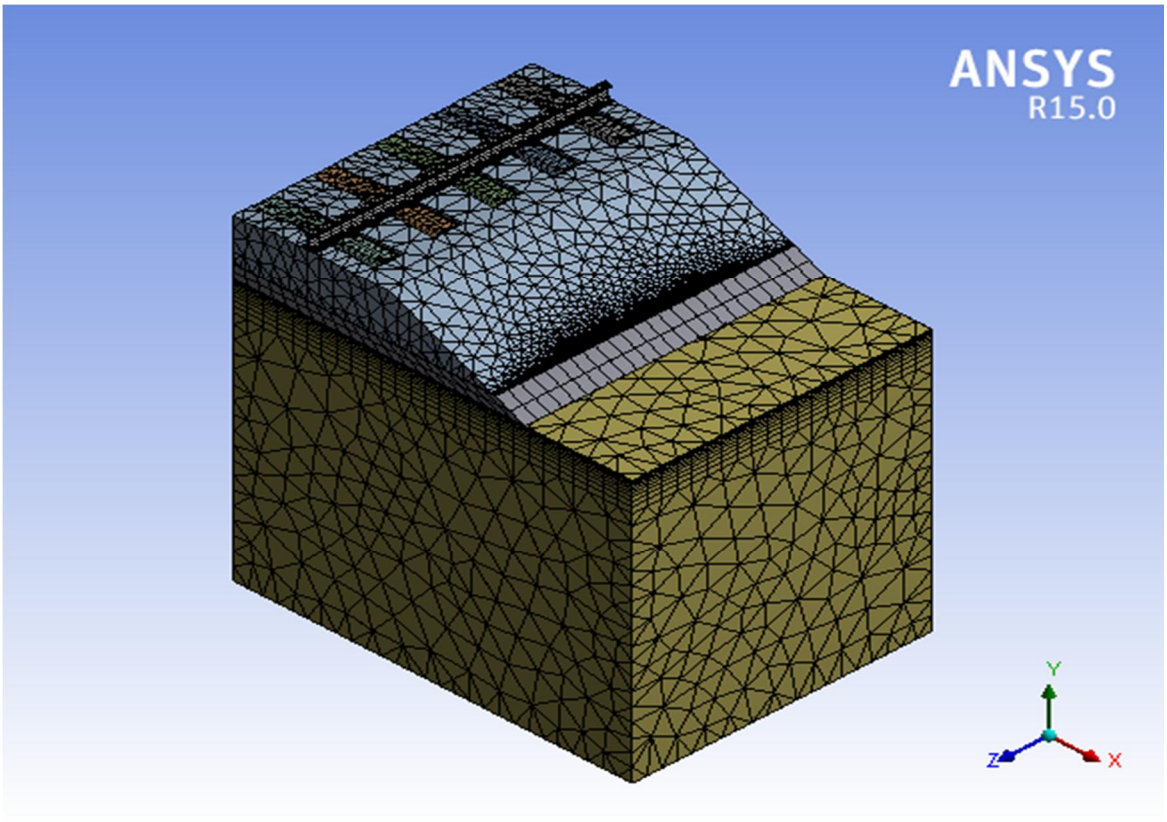


Figure 3.23: Mesh of ballasted railway track reinforced with geogrid and foundation, ANSYS

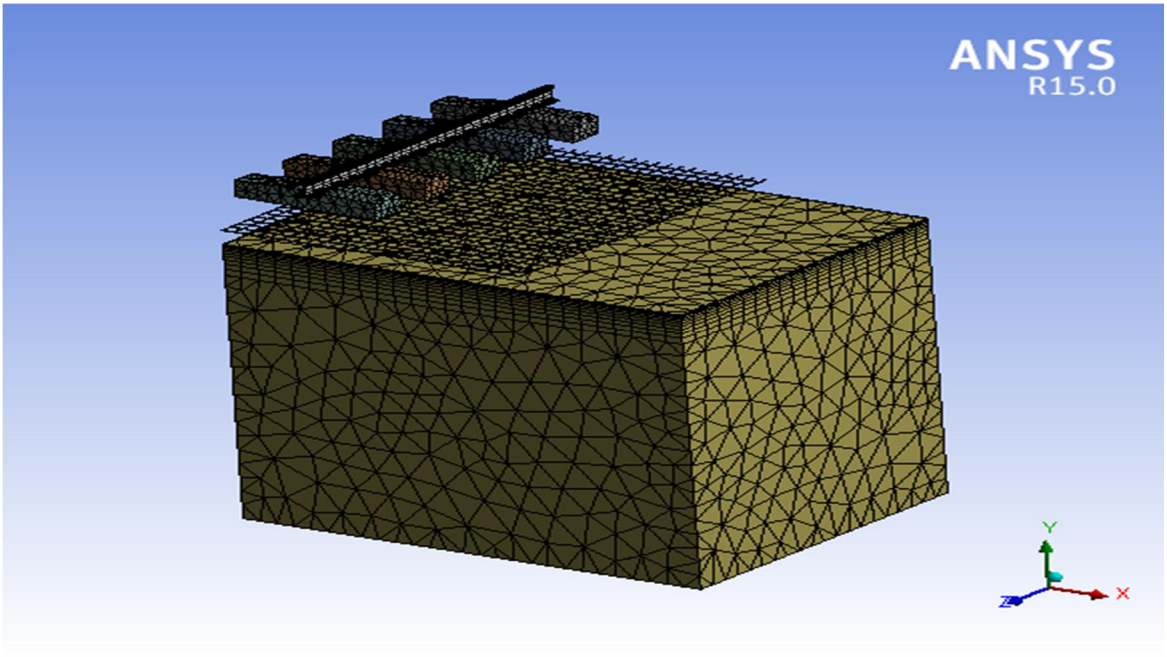


Figure 3.24: Mesh of rail, sleeper, geogrid and foundation (ballast removed for illustration), ANSYS

### 3.3.7. Contact

Planar interface elements were assigned to the surfaces including the inside, outside, top and bottom of each track component.

Physical contacting bodies do not interpenetrate. Therefore, the program was set to establish a relationship between the two surfaces to prevent them from passing through each other in the analysis.

For nonlinear solid body contact of faces, Pure Penalty or Augmented Lagrange formulations can be used. And in this analysis Augmented Lagrange is used. Where for a $F_{normal}$, there is a stiffness $k_{normal}$. The higher the contact stiffness, the lower the penetration $x_{penetration}$, as shown in the figure below:

$$F_{normal} = k_{normal} x_{penetration}$$

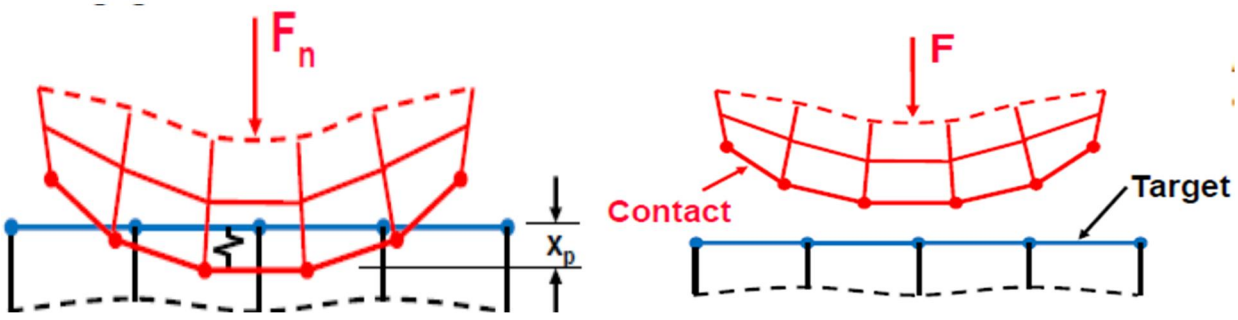


### 3.3.8. Boundary Conditions

The plane slice of half of the ballasted railroad embankment and foundation was assigned several boundary conditions meant to reduce boundary effects, take advantage of symmetry; the vertical planes under the centerline of the railroad and along the outer edge of the foundation were constrained from displacing laterally in the Z-direction (Figure 3.25). The same constraint was affixed to the Z-X planes to prevent lateral displacement in the X-direction. The base of the model was restricted from any displacement.

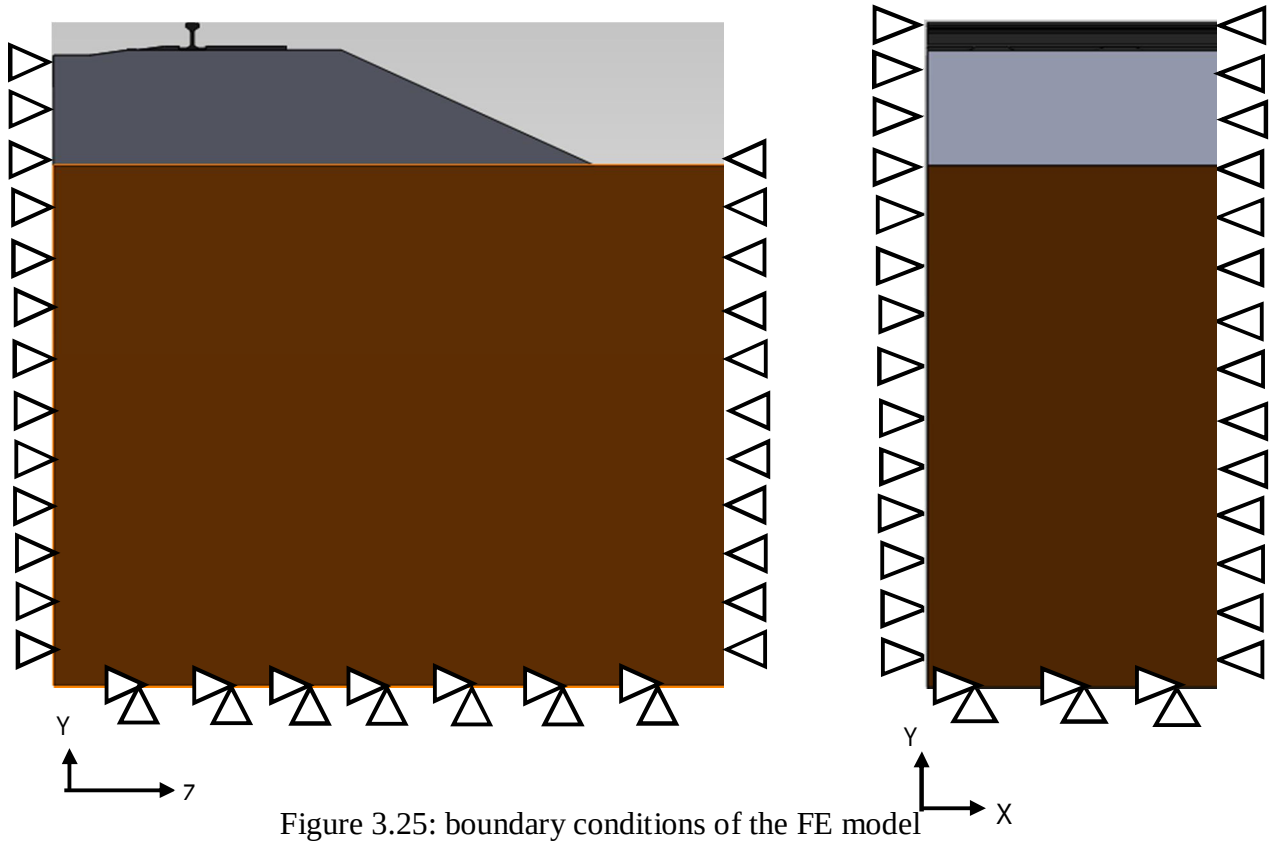


Figure 3.25: boundary conditions of the FE model

### 3.3.9. Analysis

The general Quasi-Static analysis involving both linear and nonlinear effects is performed to analyze static behavior such as deflection due to a static load. A criterion for the analysis to be possible is that it is comprised of including the dynamic effect. A static step uses time increments, not in a manner of dynamic steps but rather as a fraction of the applied load. The default time period is 1.0 units of time, representing 100% of the applied load.

### 3.3.10. Material Properties

The material properties used for FEA listed here under are from manuals, manufacturer's specifications and actual design specification of Addis Ababa/Sebeta-Djibouti railway project.

Rail: UIC54 [18]

| profile | UIC54 | | |
|---|---|---|---|
| **property** | **Unit** | **Value** | **Remark** |
| Mass Density, ρ | $kg/m^3$ | 7729 | |
| Elastic Modulus, E | GPa | 206 | |
| Poisons Ratio, υ | - | 0.3 | |
| Tensile Strength, $R_m$ | MPa | >1180 | Standard High Strength Steel |
| Elongation at Rapture, in 2 inches | % | ≥10 | |

Rail pad: Type-II fastener [18]

| **Property** | **Unit** | **Value** | **Remark** |
|---|---|---|---|
| material | | | High Density Polyethylene, HDPE |
| Density | $g/cm^3$ | 0.95 | |
| Elastic Modulus, E | GPa | 0.8 | |
| Poisons Ratio, υ | - | 0.46 | |
| Tensile Strength | MPa | 19 | |
| Elongation | % | 150 | |
| Insulation Resistance | Ω | $3.5x10^{10}$ | |
| Hardness | A | 98 | |
| Stiffness | N/m | $6.5x10^7$ | |
| Damping | Ns/m | $7.5x10^4$ | |

Sleeper: Type-II S58 concrete sleeper [18]

| **Property** | **Unit** | **Value** | **Remark** |
|---|---|---|---|
| Concrete Grade | MPa | 50/60 | |
| Mass Density, ρ | $kg/m^3$ | 2300 | |
| Weight | kg | Approx. 312 | |
| Elastic Modulus, E | GPa | 36 | |
| Poisons Ratio, υ | - | 0.3 | |
| Unit Weight, $\gamma$ | $kg/m^3$ | 2400 | |

Ballast, Sub-Ballast and Subgrade

| **Property** | **Unit** | **Ballast[3]** | **Sub Ballast[3]** | **Subgrade[18]** | **Remark** |
|---|---|---|---|---|---|
| | | **Value** | | | |
| Mass Density, ρ | $kg/m^3$ | 1800 | 1800 | 1600 | |
| Elastic Modulus, E | MPa | 170 | 170 | 30 | |
| Poisons Ratio, υ | - | 0.3 | 0.3 | 0.25 | |

*[18] The subgrade is assumed to be relatively soft to exhibit the effect of geosynthetics reinforcement and this is the type of Subgrade that exists at the chainages DK0+500, DK0+540, DK0+600, DK5+320, DK5+800, DK79+513 and DK79+900 along the route of Addis/Sebeta-Djibouti railway project.*

Geogrid and Geocell

| **Property** | **Unit** | **Geogrid[21]** | **Geocell[22]** | **Remark** |
|---|---|---|---|---|
| | | **Value** | | |
| Mass Density, ρ | $g/cm^3$ | ≥0.94 | ≥0.94 | |
| Elastic Modulus, E | GPa | 70 | 2.10 | |
| Poisons Ratio, υ | - | 0.35 | 0.35 | |
| Ultimate Elongation (min) | % | 500 | - | |
| Tensile Strength | MPa | 24 | >23 | |
| Seam Peel Strength | N | - | 2000 | |
| Flexural rigidity (Machine direction) | Mg-cm | 750,000 | - | |
| Junction strength | KN/m | 15.7 | - | |

### 3.3.11. Loading

The wheel load chosen for the geometry was very conservative in order to demonstrate track behavior under the worst conditions possible. That is, the load corresponds to two wheels, Therefore, the equivalent axle load of 427 kN, placed on a small area at the top center of the steel rail railroad track to represent approximate point-loading of a wheel on a rail. The loading is applied above the central tie in the 3 meter-wide, plane-strain slice as it provides the most conservative representation by distributing the loads over a slightly smaller group of ties as stated in 3.3.2

## 3.4. Discussion of Results

The results from the finite element modeling in ANSYS are presented. The purpose of the modeling is to investigate some of important parameters of the railway track.

Four static analyses have been carried out:-

- Unreinforced ballast embankment,
- ballast embankment reinforced with geocell
- ballast embankment reinforced geogrid at a depth of 200mm below the tie and
- ballast embankment reinforced geogrid at a depth of 300mm.below the tie

Three parameters are analyzed:-

- track settlement
- subgrade stress and
- subgrade stress-strain

The analysis results for track settlement, subgrade stress and subgrade stress and strains are presented here under.

**(i) Unreinforced ballast embankment**

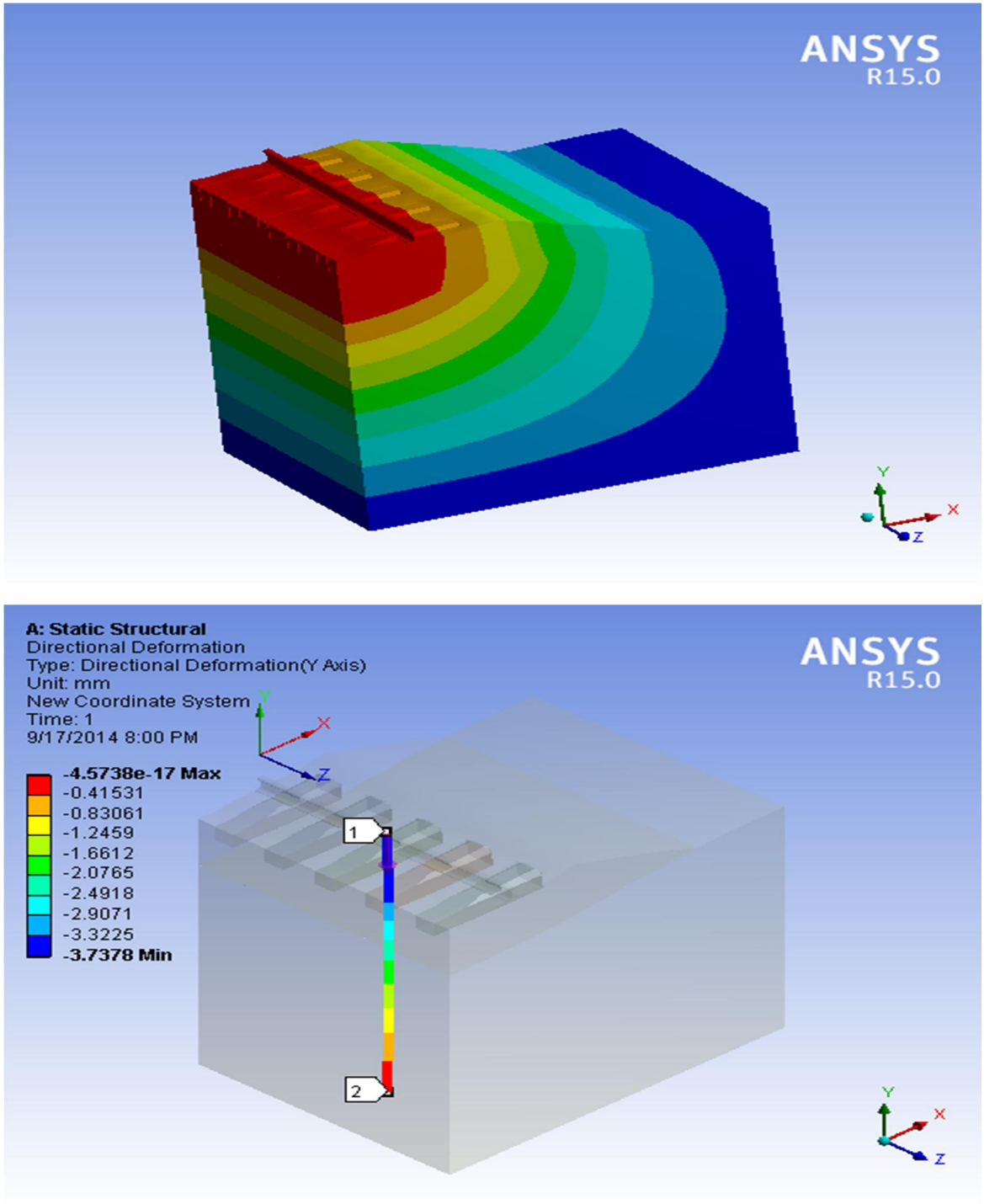


Figure 3.26: deformation/settlement of unreinforced ballast embankment (path 1_2 represents the location of maximum deformation at the track center), ANSYS

Figure 3.26 illustrates the analysis output from ANSYS for unreinforced ballast embankment settlement versus depth of the track. Path 1_2 represents location of maximum deformation which is in line with the point of wheel load application. As can be seen from this figure; the deformation is 3.73 mm at the point of load application and gradually decreases to zero.

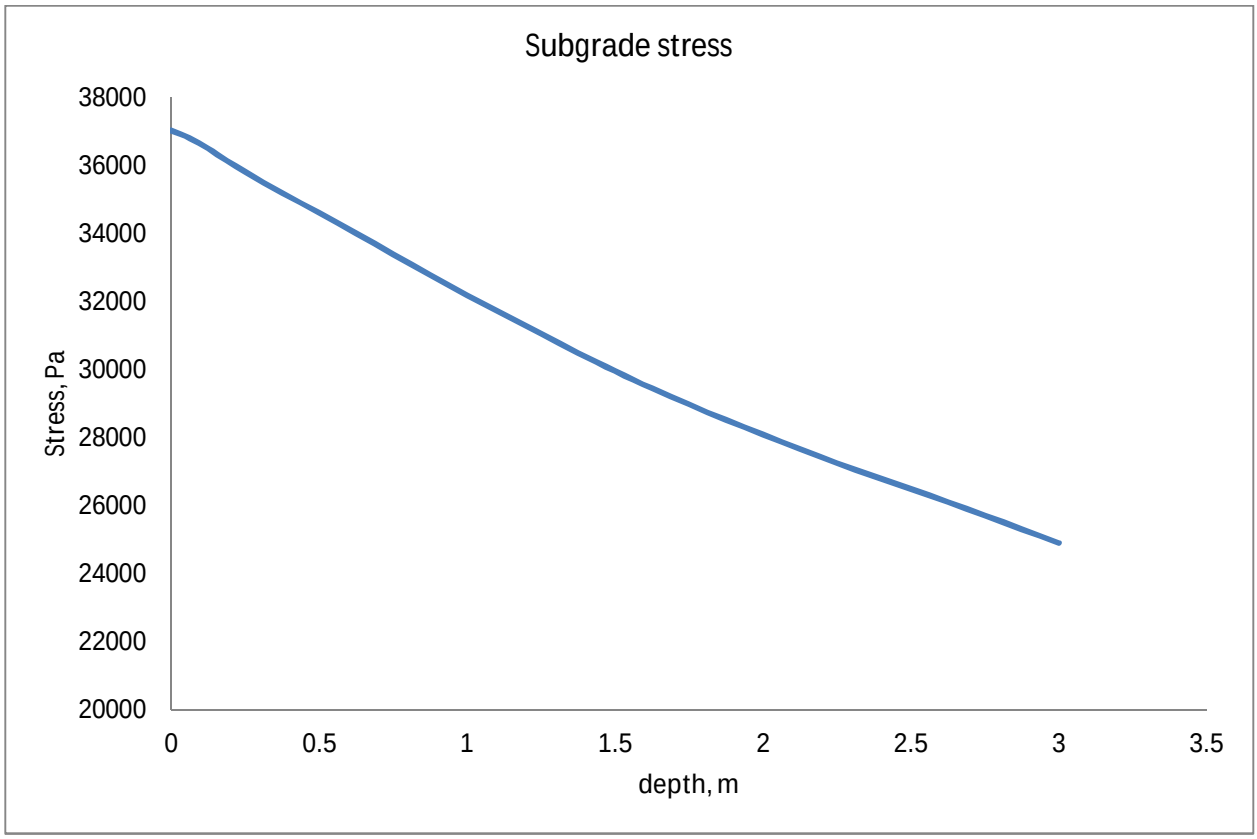


Figure 3.27: subgrade stress versus track depth of unreinforced ballast (below the bottom of the central tie), ANSYS

Figure 3.27 shows the analysis output from ANSYS for unreinforced ballast embankment subgrade stress (load transmitted underneath the tie) and as a function of depth of the track. As can be seen from this figure; the subgrade stress is 37.04 kPa at the ballast-subgrade interface and gradually decreases to 24.90 kPa at a depth of 3 m below the bottom of the ballast.

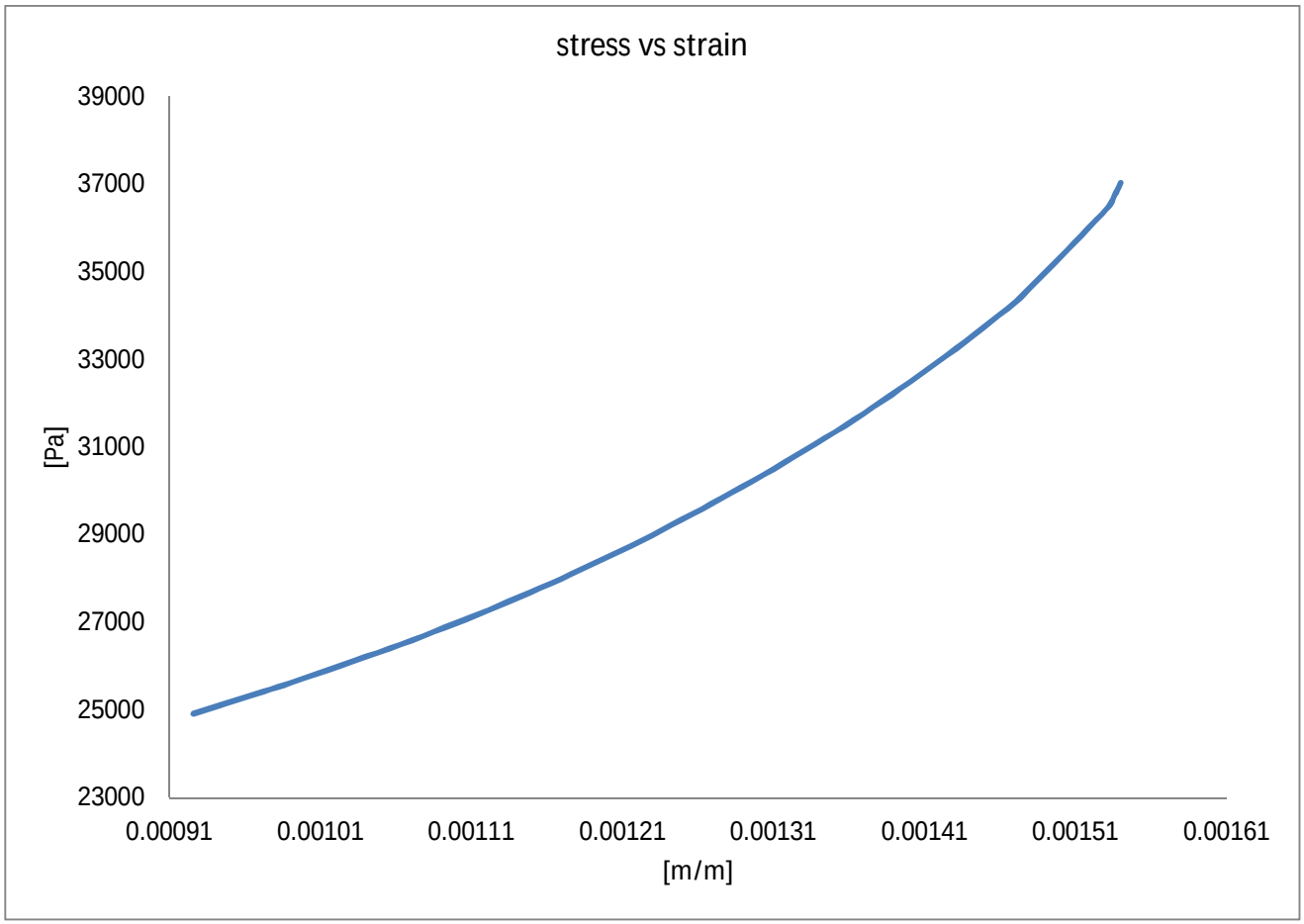


Figure 3.28: subgrade stress versus strain of unreinforced ballast, ANSYS

Under a static loading, Figure 3.28 shows the analysis output from ANSYS for unreinforced ballast embankment subgrade stress (underneath the ties) as a function of the subgrade strain. As can be seen from this figure; the subgrade stress and strain is 37.04 kPa and 0.00154 m/m respectively at the ballast-subgrade interface, and gradually decreases to 24.90 kPa and 0.00092 m/m at a depth of 3 m below the bottom of the ballast.

**(ii) ballast embankment reinforced with geocell**

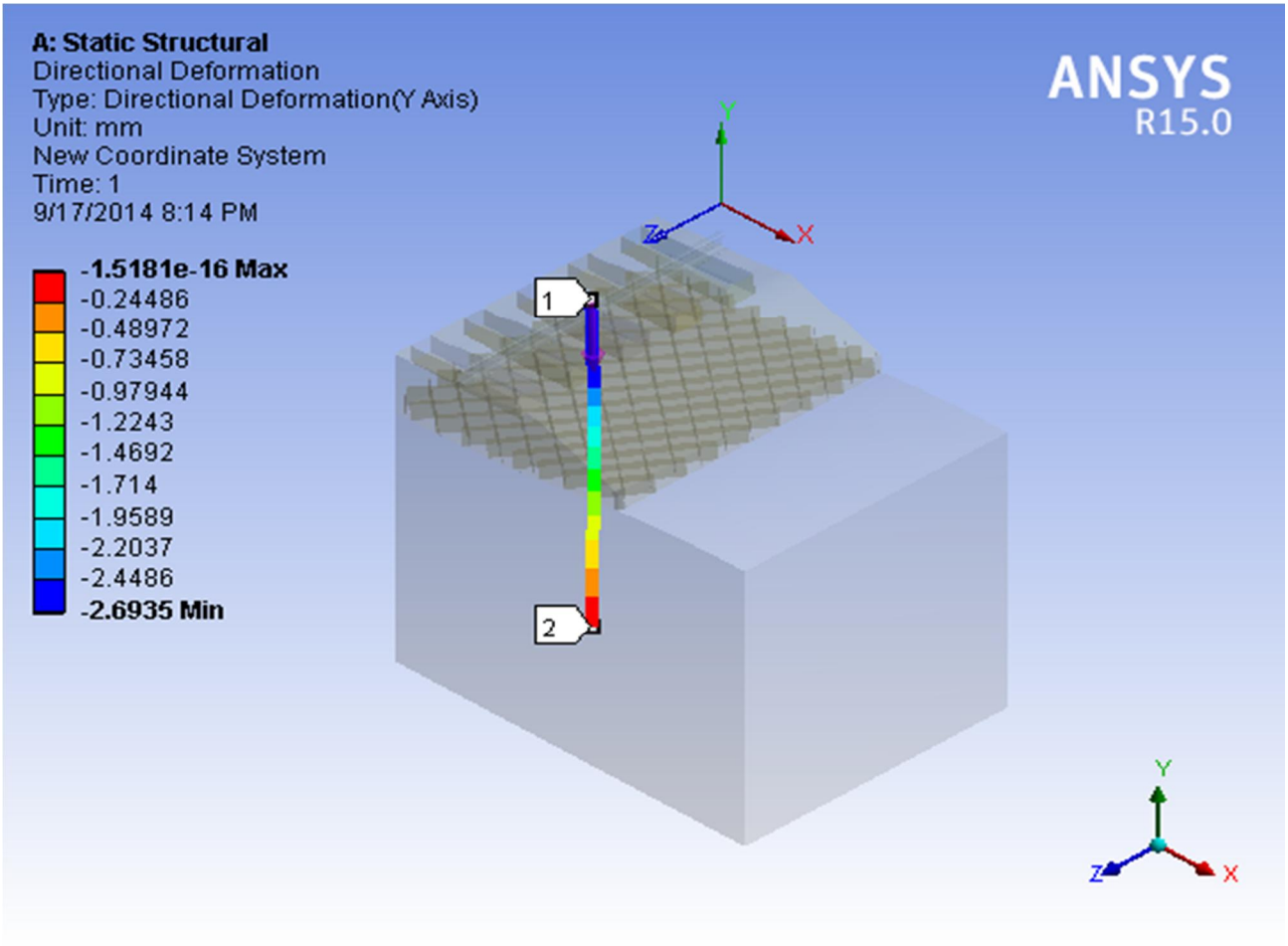


Figure 3.29: deformation/ track settlement of geocell reinforced ballast embankment (path 1_2 represents the location of maximum deformation at the track center), ANSYS

Figure 3.29 illustrates the analysis output from ANSYS for geocell reinforced ballast embankment settlement versus depth of the track. Path 1_2 represents location of maximum deformation at the track center which is in line with the point of wheel load application. As can be seen from this figure; the deformation is 2.69 mm at the point of load application and gradually decreases to zero.

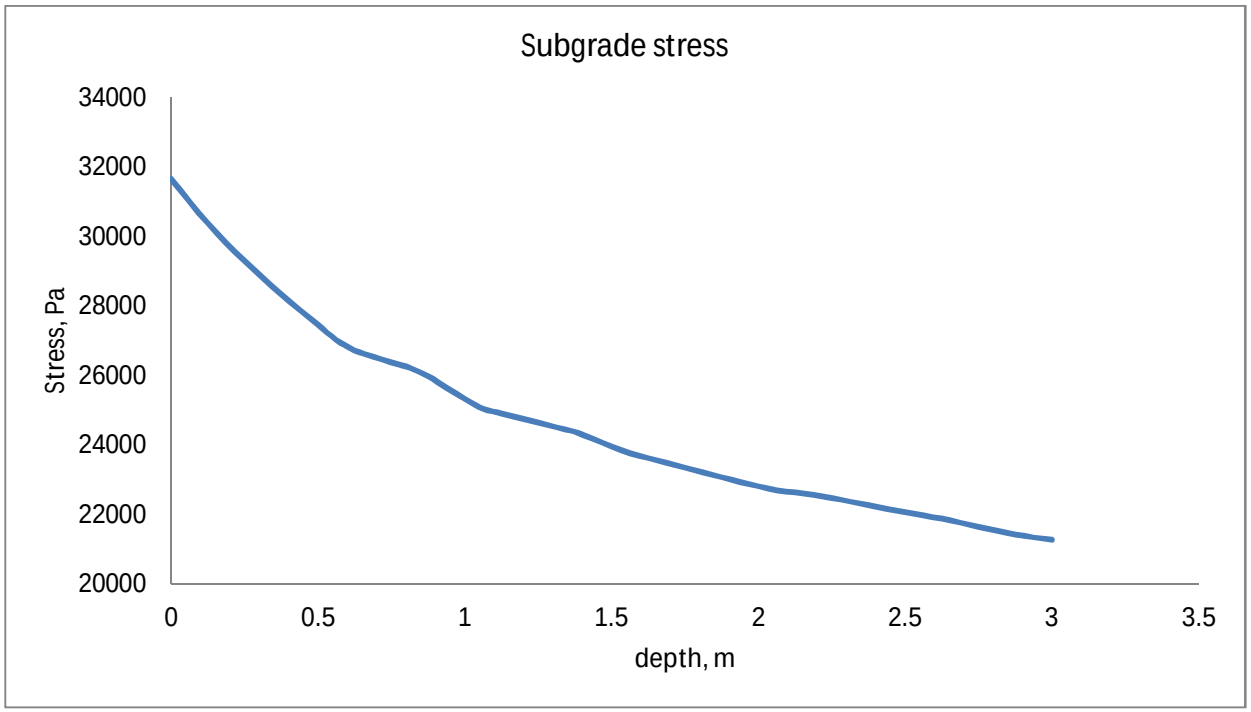


Figure 3.30: subgrade stress versus track depth of geocell reinforced ballast (below the bottom of the central tie), ANSYS

Figure 3.30 shows the analysis output from ANSYS for geocell reinforced ballast embankment subgrade stress (load transmitted underneath the tie) and as a function of depth of the track. As can be seen from this figure; the subgrade stress is 31.67 kPa at the ballast-subgrade interface and gradually decreases to 21.27 kPa at a depth of 3m below the bottom of the ballast.

Figure 3.31 below illustrates the analysis output from ANSYS for geocell reinforced ballast embankment subgrade stress (underneath the ties) as a function of the subgrade strain. As can be seen from this figure; the subgrade stress and strain is 31.67 kPa and 0.000945 m/m respectively at the ballast-subgrade interface, and gradually decreases to 21.27 kPa and 0.000591 m/m at a depth of 3 m below the bottom of the ballast.

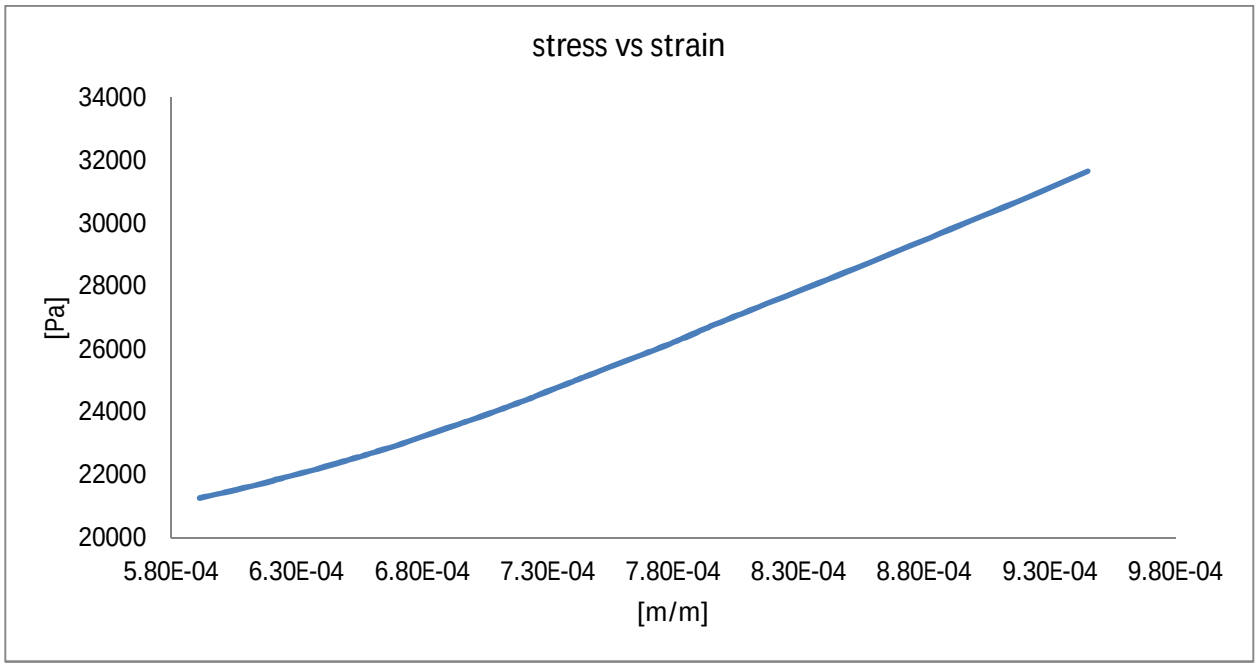


Figure 3.31: subgrade stress versus strain of geocell reinforced ballast (below the bottom of the central tie), ANSYS

**(iii) Reinforced with Geogrid at a depth of 200mm and 300mm below tie**

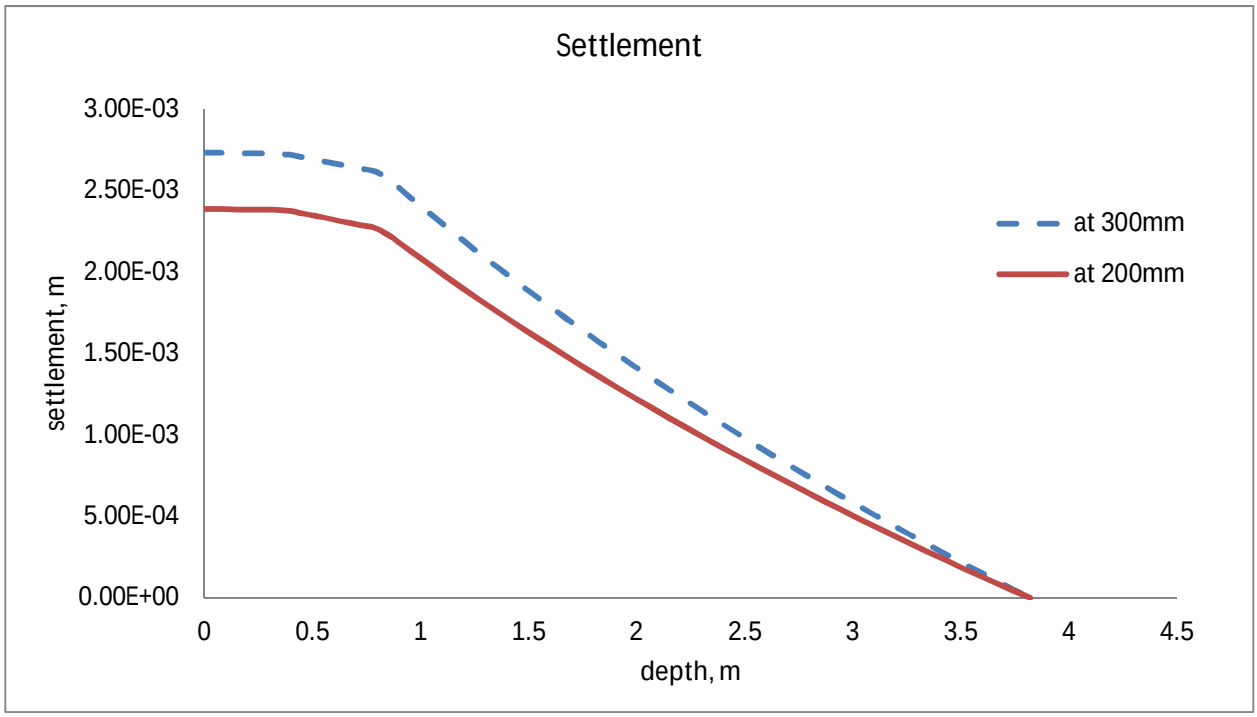


Figure 3.32: track settlement of geogrid reinforced ballast embankment, ANSYS

Figure 3.32 illustrates the analysis output from ANSYS for geogrid reinforced ballast embankment settlement versus depth of the track. The solid line represents ballast embankment reinforced with geogrid at a depth of 200 mm below the tie while the dotted line represents geogrid reinforcement at a depth of 300 mm below the tie. As can be seen from this figure; the deformation is 2.38 mm and 2.73 mm at the point of load application for ballast embankment reinforced with geogrid at 200 mm and 300 mm below the tie respectively and gradually decreases to zero.

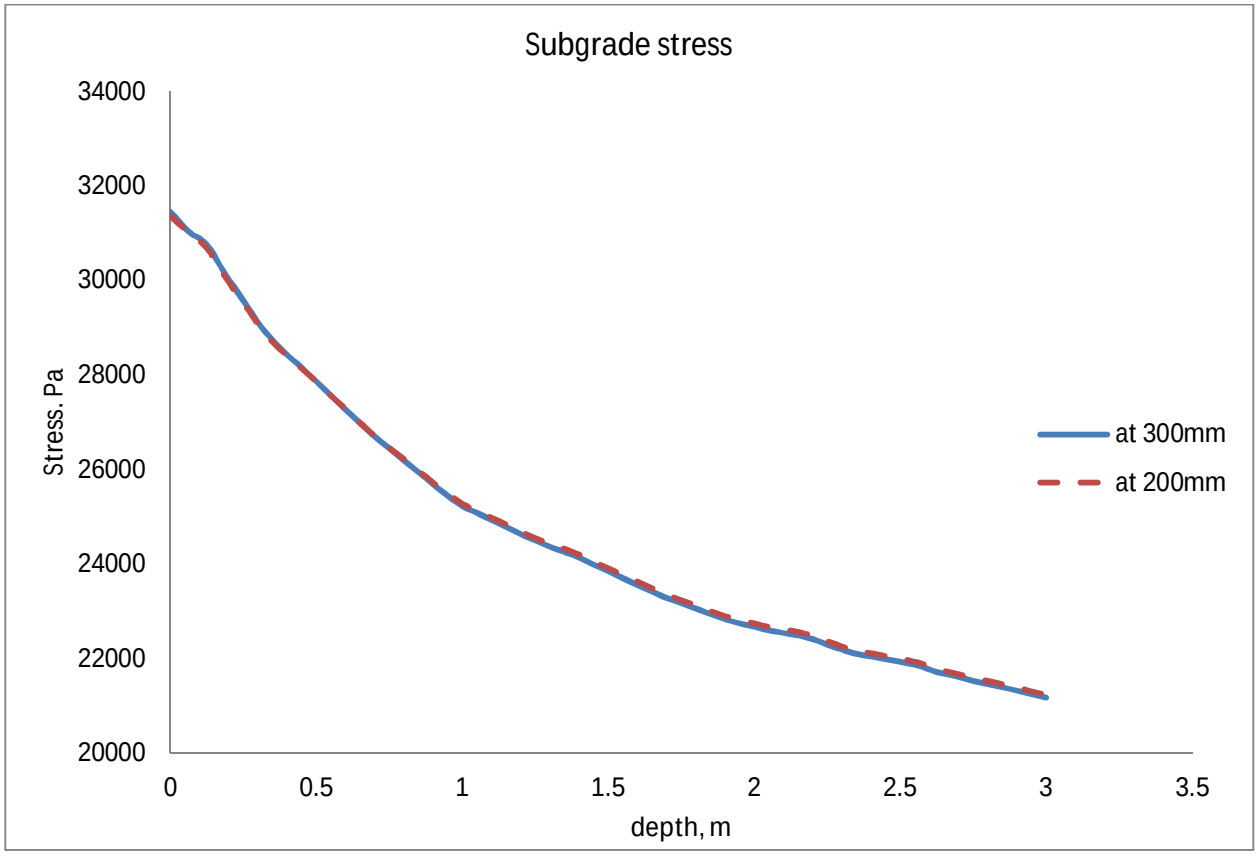


Figure 3.33: subgrade stress versus track depth of geogrid reinforced ballast, ANSYS

Figure 3.33 shows the analysis output from ANSYS for gegrid reinforced ballast embankment subgrade stress (load transmitted underneath the tie) and as a function of depth of the track. The solid line represents ballast embankment reinforced with geogrid at a depth of 300 mm below the tie while the dotted line represents geogrid reinforcement at a depth of 200 mm below the tie As can be seen from this figure; the subgrade stress is 31.38 kPa and 31.47 kPa at the ballast-

subgrade interface for ballast embankment reinforced with geogrid at 200 mm and 300 mm below the tie respectively and gradually decreases to 21.34 kPa at a depth of 3m below the bottom of the ballast.

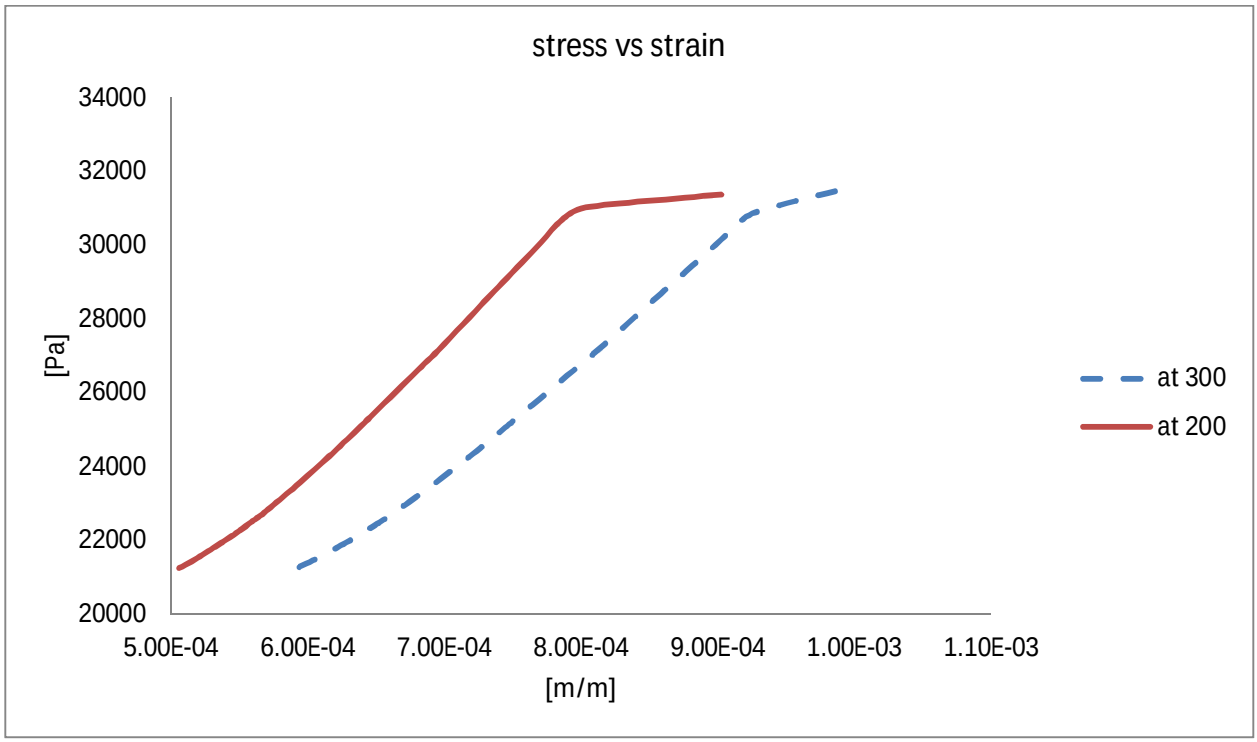


Figure 3.34: subgrade stress versus strain of geocell reinforced ballast, ANSYS

Figure 3.34 below illustrates the analysis output from ANSYS for geogrid reinforced ballast embankment subgrade stress (underneath the ties) as a function of the subgrade strain. The solid line represents ballast embankment reinforced with geogrid at a depth of 200 mm below the tie while the dotted line represents geogrid reinforcement at a depth of 300 mm below the tie As can be seen from this figure; the subgrade stress and strain is 31.638 kPa and 0.000902 m/m and 31.47 kPa and 0.000986 m/m for ballast embankment reinforced with geogrid at 200 mm and 300 mm below the tie respectively at the ballast-subgrade interface, and gradually decreases to 21.51 kPa and 0.000519 m/m and 21.54 kPa and 0.000608 m/m at a depth of 3 m below the bottom of the ballast respectively.

# CHAPTER FOUR

# 4. PARAMETRIC STUDY

A series of simulations were performed on the railway geometry in order to determine some of the selected important parameters. During the simulation, track settlement, subgrade stress, and subgrade stress-strain of ballast embankment were observed. And a comparison is made between unreinforced ballasted track and those of tracks reinforced with Geocell and Geogrid.

## 4.1. Unreinforced versus Reinforced with Geocell

- Track Settlement

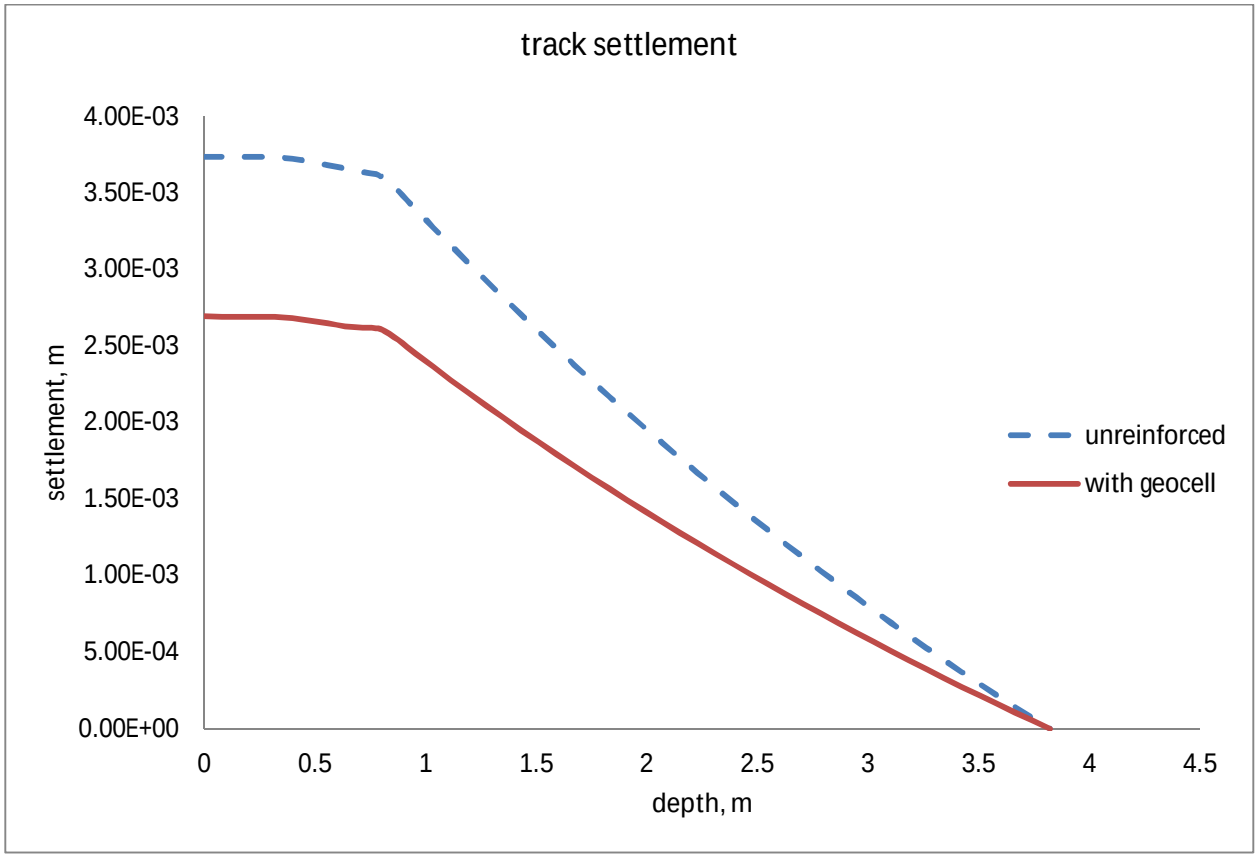


Figure 4.1: track settlement of unreinforced and geocell reinforced ballast embankment

Figure 4.1 shows the settlement of the track with depth, the use of geocell confinement reduced the vertical track settlement as shown in the figure. The confinement mechanism of the geocell

was effective in preventing excessive settlement by providing a relatively rigid mattress, reducing the track settlement by about 28% (from 3.73mm to 2.69mm).

- Subgrade Stress

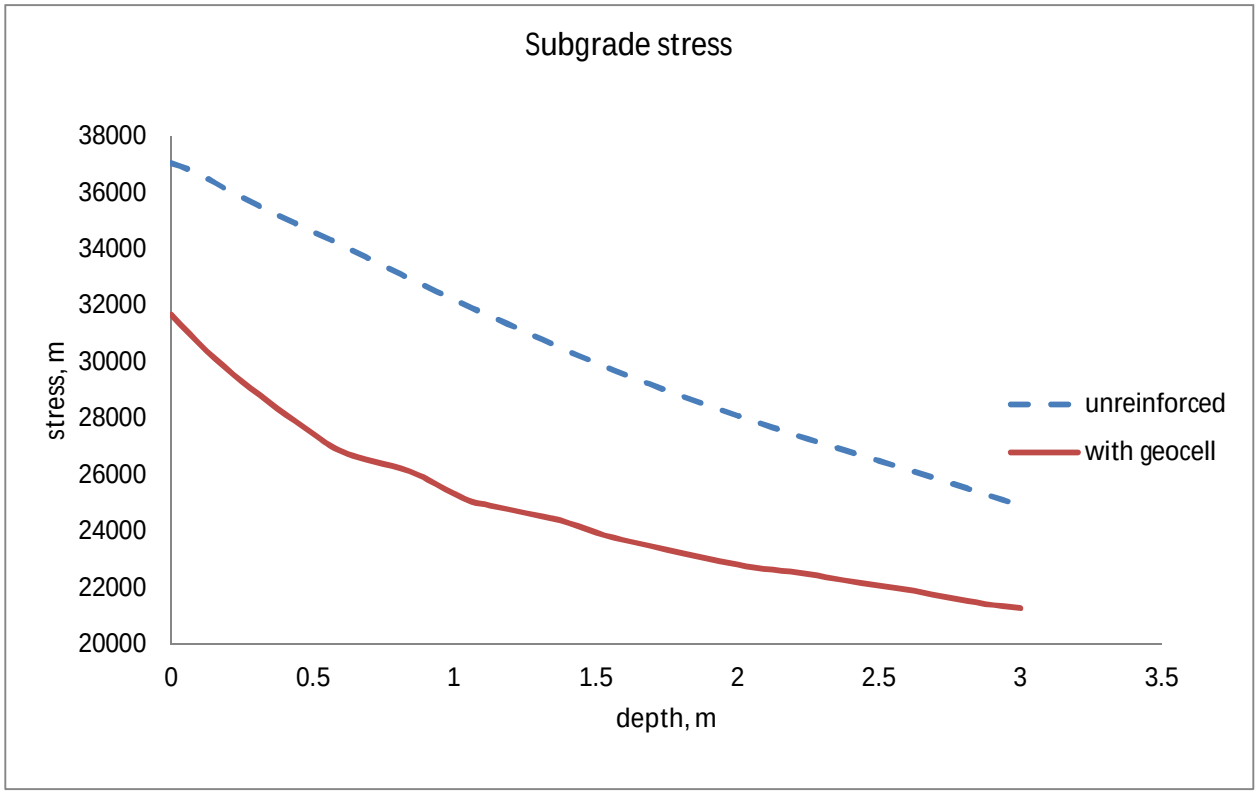


Figure 4.2: subgrade stress of unreinforced and geocell reinforced ballast embankment

One great advantage of the geocell was its redistribution of stress over a wider area. The peak stress was reduced by approximately 14.5% when using geocell as shown in figure 4.2. The distribution of the rail loads over a wider area is also advantageous as it mobilizes more of the subgrade's strength and resistance, unlike the singular peak loads that induce shear when no reinforcement is present. Not only did use of geocell distribute the stress more evenly; it reduced the magnitude of the subgrade stresses when placed over a very compressible foundation or in an embankment consisting of weak ballast.

- Subgrade Stress-Strain

The stress-strain curve for the subgrade is shown below (figure 4.3) and as it shown from the figure the intrusion of geocell gave an added performance in reducing the stress as well the strain and makes the stress-strain more linear hence this will help to reduce differential settlement.

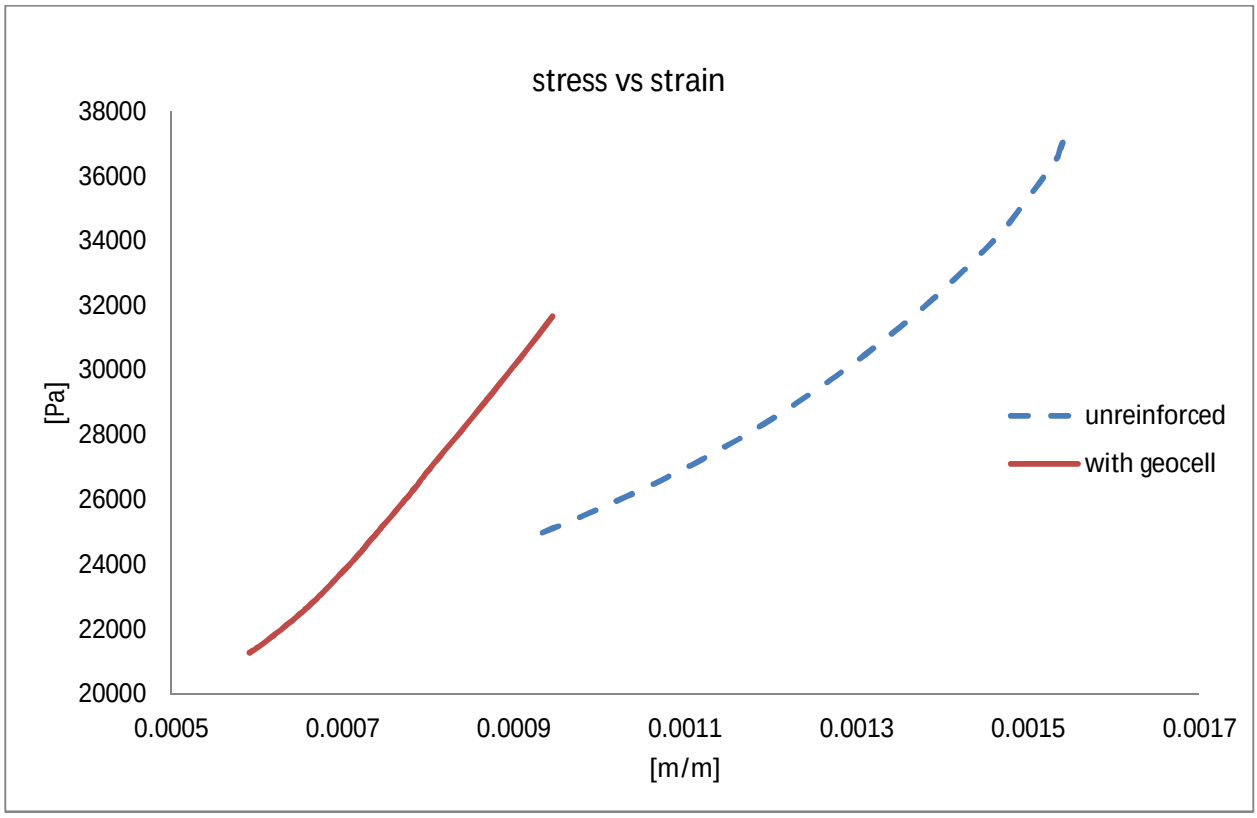


Figure 4.3: subgrade stress-strain of unreinforced and geocell reinforced ballast embankment

Table 4.1: Summary of finite element analysis for ballast reinforced with geocell

| **Parameters** | **Unreinforced** | **Reinforced with Geocell** | **% Reduction** |
|---|---|---|---|
| Settlement (mm) | 3.73 | 2.69 | 28 |
| Subgrade Stress (Pa) | 37048 | 31677 | 14.5 |

## 4.2. Unreinforced versus Reinforced with Geogrid

- Track Settlement

The use of geogrid reinforcement reduced the vertical track settlement, The reinforcement mechanism (aggregate particles partially penetrate and interlock within the apertures of the geogrid) of the geogrid was effective in preventing excessive settlement by providing a relatively rigid mat, reducing the track settlement by about 27% (from 3.73mm to 2.73mm) when the geogrid is placed at a depth of 300mm below tie (at the ballast – sub ballast interface) and 35% (from 3.73mm to 2.38mm) when the geogrid is placed at a depth of 200mm below the tie (with in the ballast) as shown in figure 4.4..it is observed that placing the geogrid with in the ballast provide good performance of the ballast as stated in the literature part.

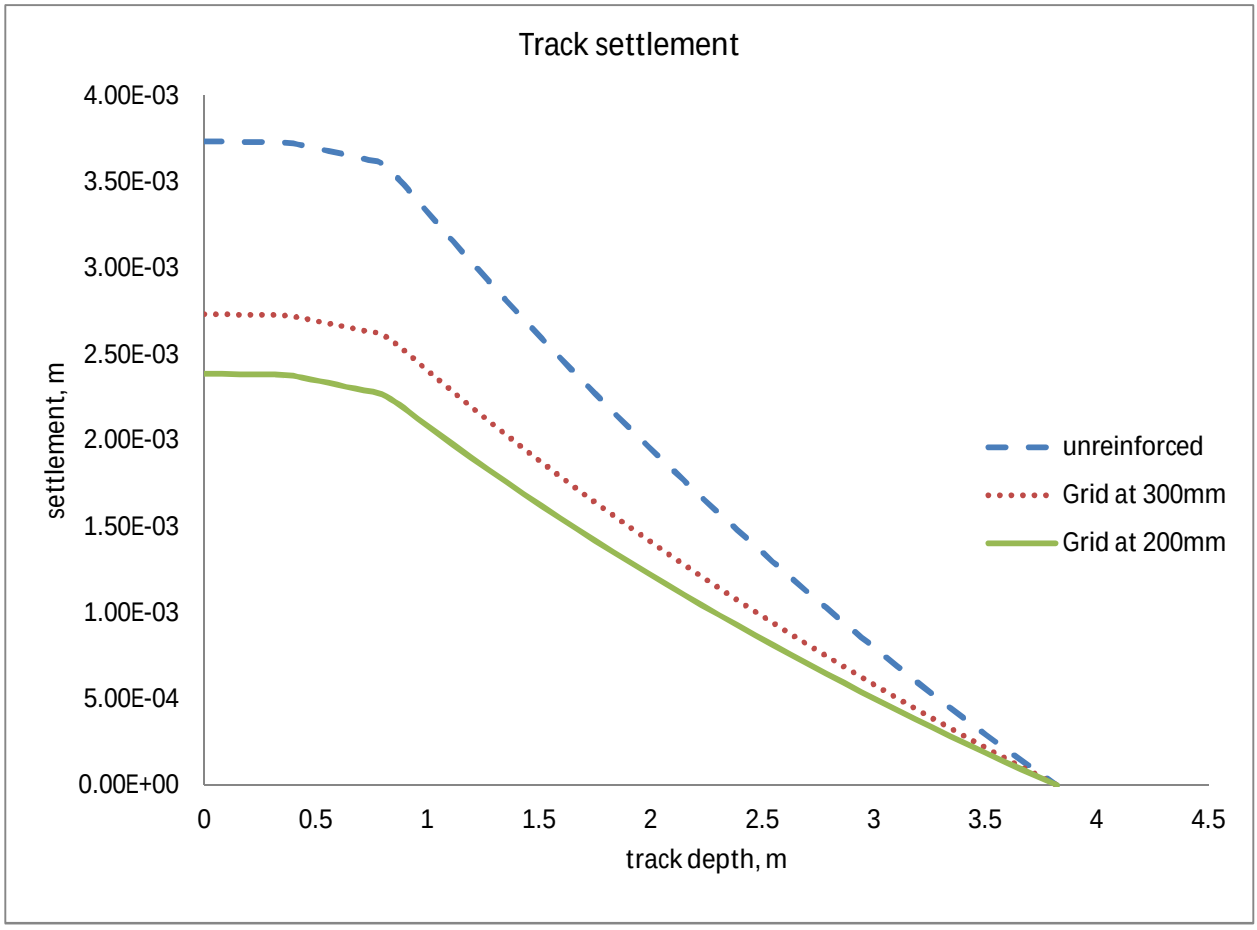


Figure 4.4: track settlement of unreinforced and geogrid reinforced ballast embankment

- Subgrade Stress

Confinement of ballast with geogrids results in an increase in the lateral stress within the aggregate, thereby increasing its stiffness this reduces the stress transferred to the subgrade. The peak stress was reduced by approximately 15% when using geogrid placed at a depth of 300mm below the tie and 15.04% when using geogrid placed at a depth of 200mm below the tie as shown in figure 4.5. With this regard the two different locations have the same effect in reducing the stress. Geogrids also distribute the stress more evenly; it reduced the magnitude of the subgrade stresses when placed over a very compressible foundation or in an embankment consisting of weak ballast.

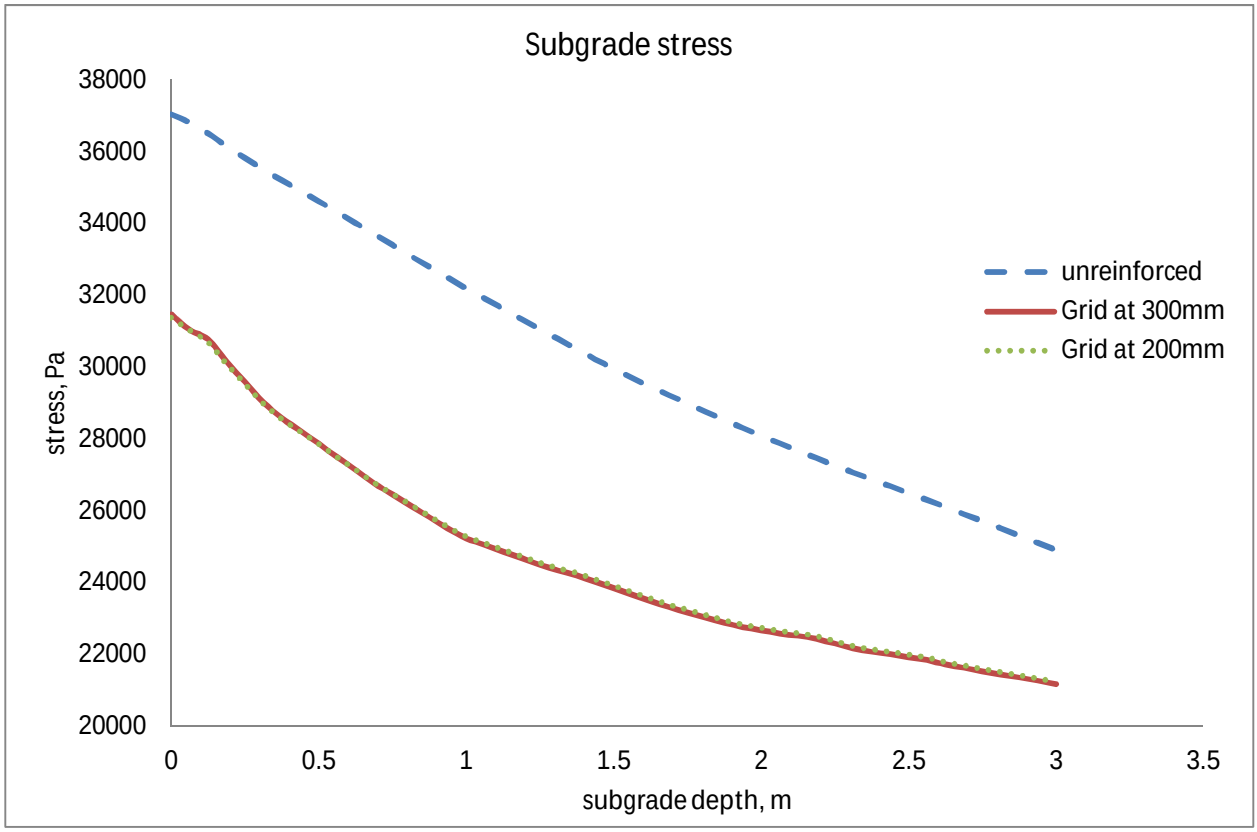


Figure 4.5: subgrade stress of reinforced and geogrid reinforced ballast embankment

- Subgrade Stress-Strain

The stress-strain curve for the subgrade is shown below (figure 4.7) and as it shown from the figure the intrusion of geogrid gave an added performance in reducing the stress as well the strain. And makes the stress-strain more linear hence this will help to reduce differential settlement.

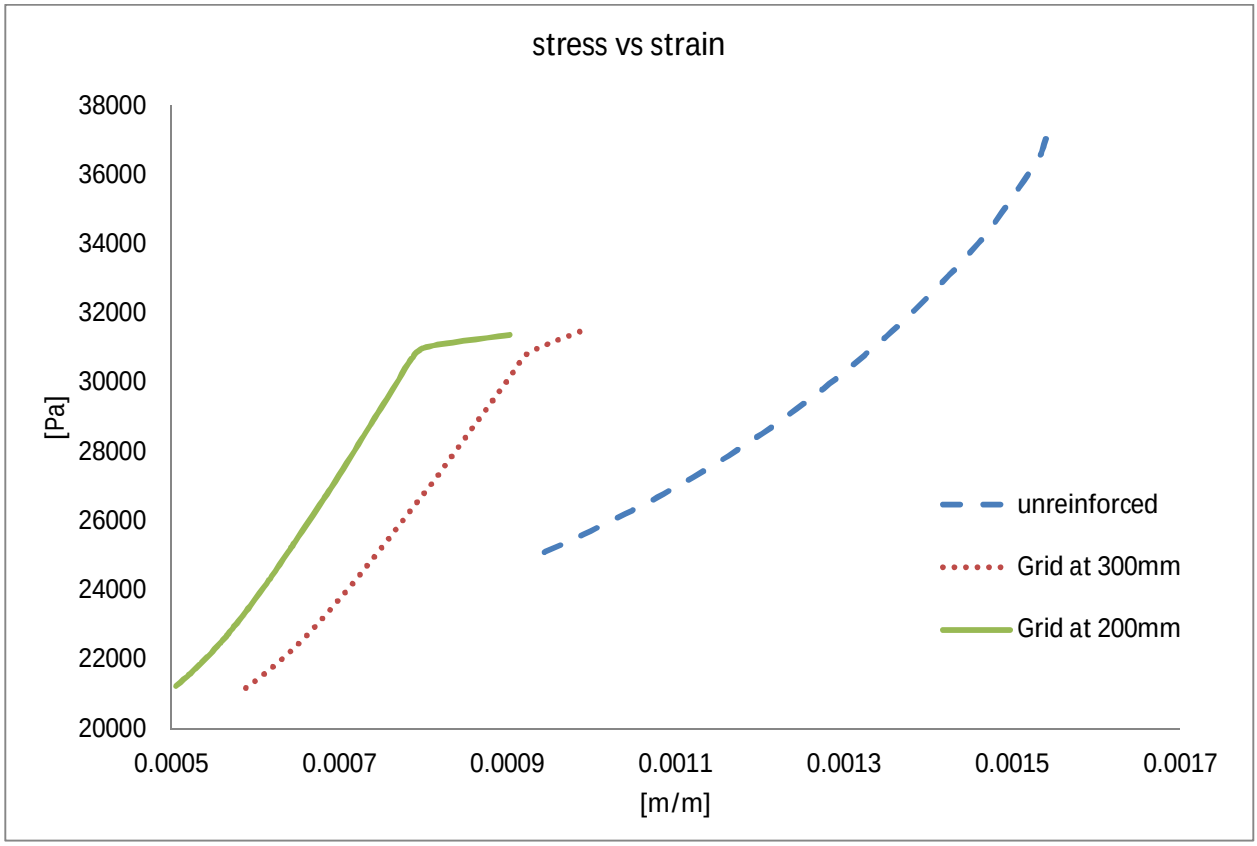


Figure 4.6: subgrade stress-strain of unreinforced and geogrid reinforced ballast embankment

Table 4.2: Summary of finite element analysis for ballast reinforced with geogrid

| **Parameters** | **Unreinforced** | **Reinforced with Geogrid @ 300mm below tie** | **% Reduction** | **Reinforced with Geogrid @ 200mm below tie** | **% Reduction** |
|---|---|---|---|---|---|
| Settlement (mm) | 3.73 | 2.73 | 27 | 2.38 | 35 |
| Subgrade Stress (Pa) | 37048 | 31475 | 15 | 31384 | 15.04 |

# CHAPTER FIVE

# 5. CONCLUSIONS AND RECOMMENDATIONS

The objective of this thesis was to study the performance of a ballasted railroad substructure by incorporating geocell and geogrid to the ballast. Ballasted track unreinforced, reinforced with geocell and geogrid based on three dimensional finite element methods have been modeled and analyzed .a comparison is made between reinforced and unreinforced section of the track. Results are presented below. Suggestions for future study also have been proposed.

## 5.1. Conclusions

The conclusions that can be drawn from this research are:

- The confinement of the ballast using geocell was quite effective in reducing vertical deformations up to 28%; the three dimensional confinement of the geocell minimizes the movement of the aggregates hence it reduced the track settlement. This is promising when considering the possibility for using weaker ballast materials like recycled ballast or well-graded particles, or allow for longer maintenance cycles when the ballast loses shear strength due to degradation.

- Due to beam effect of the geocell a uniform subgrade stress distribution is obtained. In addition to being more uniform, the magnitudes of stresses were reduced significantly (15%) and hence mobilizing more of the subgrade's shear strength and preventing shear failure. Also due to added performance by geocell, placing a weak ballast embankment reinforced with geocell on soft subgrade results in economical approach.

- The use of the geocell more likely contributes resistance to spreading above, below and within the cell through frictional resistance and of the composite mattress. This is a promising solution when weaker ballast materials are used due to added shear strength.

- The reinforcement of the ballast using geogrid was also quite effective in reducing vertical deformations and a better result can be obtained when placing the geogrid within

the ballast at a depth of 200mm below the tie instead of placing at the ballast-sub ballast interface as most literatures suggest and shown on the analysis. Due to the reduced depth of geogrid unlike that of geocell the confinement of the grid is reduced, hence using fresh and good quality ballast gives good performance.

- Due to interlock effect of the geogrid and the ballast a uniform subgrade stress distribution is obtained. In addition to being more uniform, the magnitudes of stresses were reduced significantly (15%). The reduction of the stress when the geogrid is placed within the ballast or at the ballast- sub ballast interface is nearly the same, this could give preference freedom for the placement of the geogrid to avoid construction damage as well stress concentration meaning extended life for the geogrid as well the ballast performance.

Generally, the use of geocell or geogrid have a direct benefit of extending the maintenance cycles (period between ballast cleaning and replacement operation), increase the effective bearing capacity of underlying subgrade especially applying on soft soils, increase the stiffness and strength of ballast and reduce settlement, cost effective alternative when using weaker ballast

The preference weather geocell or geogrid to be used depends primarily by the quality of the ballast. For weak ballast it is preferable to use geocell instead of geogrid due to its depth which will confine the weak ballast and increase the shear strength and hence reduce subgrade stress. as well lateral spreading. However geogrids requires specific good quality ballast since they cannot reinforce fine grained or weak ballast as there is no interlocking mechanism for degraded ballast.

## 5.2. Recommendations

- The implications of the finite element analysis were promising, but using further justification by a laboratory testing of the prototype of the track is essential. This will help in demonstrating the various benefits provided by the geocell-ballast and goegrid-ballast composite to improve the ballast performance and to characterize the materials of

the track components effectively. These tests could also include full-scale railway geometry and loading patterns representative of exact train wheel passes.

- FEM analysis provides a useful way to simulate the behavior of ballast. The initial simulations using a nonlinear elastic material model and a Drucker-Prager material model show the potential of FEM to build a rigorous scientific analysis, which gives a reliable simulation of stress condition but considers the soil as continuum and describes the soil by point wise mathematical expressions. Discrete Element Method (DEM) is a numerical method used to compute the stress and displacements in a volume containing a large number of particles as grains of sand, the granular material is modeled as an assembly of rigid particles and the interaction between each particle is explicitly considered. Therefore, it is better to use DEM for more confined results.

- The use of multiple layer goegrid reinforcement require due consideration and should be analyzed considering economy as well.

- Lateral displacement analysis requires lateral model, lateral force analysis and a complex interaction of finite element method (FEM) modeling with a programming language therefore considering this to the future is critical.

- Optimization of the aperture size of the geogrid and the grain size needs a thorough investigation since the principles of reinforcement of the geogrid lies on the interlock of the geogrid and the ballast. For this reason more a detail study is required.

- An economic analysis should be done on using geocell, geogrid or with other methods of ballast performance improvement like using chemical binders, ballast mat or on frequency of ballast cleaning and replacement.

# References:

[1] Waters, S. &. (1994). *Geotechnology and Substructure Management.*

[2] F.Bonett, C. (1996). *Practical Railway Management.* Imperial Collage Press.

[3] *American Railway Engineering and Maintenance of Way Association (AREMA).* (2010).

[4] Dahalberg, T. *Railway Track Dynamics.*

[5] Shi, X. (2009). *Pridiction of Permanenet Deformation in Railway Track.*

[6] Tzanakakis, K. *Railway Track and Its Long Term Behavior: A Handbook for Railway Track of High Quality.*

[7] Chen, C. *Descrete Element Modeling of Geogrid-Reinforced Railway Ballast and Track Transition Zones.*

[8] Kwan, C. C. *Geogrid Reinforcement of Railway Ballast.*

[9] Bailey, B. J. *Investigation into the Source and Progression of Railway Track Ballast Layer Fouling Material.*

[10] Kassa, P. E. (2013). *Lecture Note.*

[11] Sd Karimullah Hussaini1, B. I. *Performance of Geosynthetically-Reinforced Rail Ballast in Direct Shear Condition.*

[12] Ling, H. L. (2012). *Numerical Modeling of Behavior of Railway Ballast Structure with Geocell Confinement.*

[13] Das, B. M. *Use of Geogrid in Subgrade-Ballast System of Railroads Subjected to Cyclic Loading for Reducing Maintenanace.* Sacramento, USA: Emeritus California State University.USA

[14] Elsveld, C. *Modern Railway Track.* Delft University of Technology.

[15] BHP, N. *Railway Track Design: A Review of Current Practice.* Melbourne Research Laboratories.

[16] (ERC), E. R. *Rolling Stocks Specifications.* Addis Ababa: Operation and Service Division, Equipment Supply and Technical Service Department.

[17] (ERC), E. R. (April 2012). *Techno-Economic Feasibility Study Volume 1: Addis Ababa/Sebeta - Djibouti Railway Railway Project.* Addis Ababa.

[18] (ERC), E. R. (2011). *Baic Design Report: Addis-Ababa/Sebeta - Djibouti Railway Project, Sebeta-Adama-Meiso Section.* Addis Ababa.

[19] V.A.Profilidis. (2006). *Railway Management and Engineering.*

[20] T. Kütük-Sert, M. V. *The Shape Analysis of Geogrids with Different Aperture Structure Used for Road Subgrade Reinforcement.*

[21] *Geotech Data.* Retrieved August 8, 2014, from http://www.geotechdata.info/parameter/soil-young's-modulus.html

[22] *Alibaba*. Retrieved August 8, 2014, from http://www.alibaba.com/showroom/high-tensile-strength-geocell.html